

LOCKHEED MARTIN ENERGY RESEARCH LIBRARIES



3 4456 0515868 2

CENTRAL RESEARCH LIBRARY
DOCUMENT COLLECTION

154

ORNL-3978
Special

THE MOLECULAR ANATOMY OF CELLS AND TISSUES
(The MAN Program)
ANNUAL REPORT
FOR PERIOD JULY 1, 1965, TO JUNE 30, 1966

CENTRAL RESEARCH LIBRARY
DOCUMENT COLLECTION
LIBRARY LOAN COPY
DO NOT TRANSFER TO ANOTHER PERSON
If you wish someone else to see this
document, send in name with document
and the library will arrange a loan.



OAK RIDGE NATIONAL LABORATORY
operated by
UNION CARBIDE CORPORATION
for the
U.S. ATOMIC ENERGY COMMISSION

LEGAL NOTICE

This report was prepared as an account of Government sponsored work. Neither the United States, nor the Commission, nor any person acting on behalf of the Commission:

- A. Makes any warranty or representation, expressed or implied, with respect to the accuracy, completeness, or usefulness of the information contained in this report, or that the use of any information, apparatus, method, or process disclosed in this report may not infringe privately owned rights; or
- B. Assumes any liabilities with respect to the use of, or for damages resulting from the use of any information, apparatus, method, or process disclosed in this report.

As used in the above, "person acting on behalf of the Commission" includes any employee or contractor of the Commission, or employee of such contractor, to the extent that such employee or contractor of the Commission, or employee of such contractor prepares, disseminates, or provides access to, any information pursuant to his employment or contract with the Commission, or his employment with such contractor.

ORNL-3978
Special

Contract No. W-7405-eng-26

BIOLOGY DIVISION

THE MOLECULAR ANATOMY OF CELLS AND TISSUES

(The MAN Program)

Cosponsored by the National Cancer Institute
and the U. S. Atomic Energy Commission

ANNUAL REPORT

For Period July 1, 1965, to June 30, 1966

N. G. Anderson
Program Coordinator

NOTICE

This document contains information of a preliminary nature and was prepared primarily for internal use. It is subject to revision or correction and, therefore, does not represent a final report. Quotations from, or reference to, this report must not be made in open literature without written permission from individual authors.

NOVEMBER 1966

OAK RIDGE NATIONAL LABORATORY
Oak Ridge, Tennessee
operated by
UNION CARBIDE CORPORATION
for the
U. S. ATOMIC ENERGY COMMISSION

LOCKHEED MARTIN ENERGY RESEARCH LIBRARIES

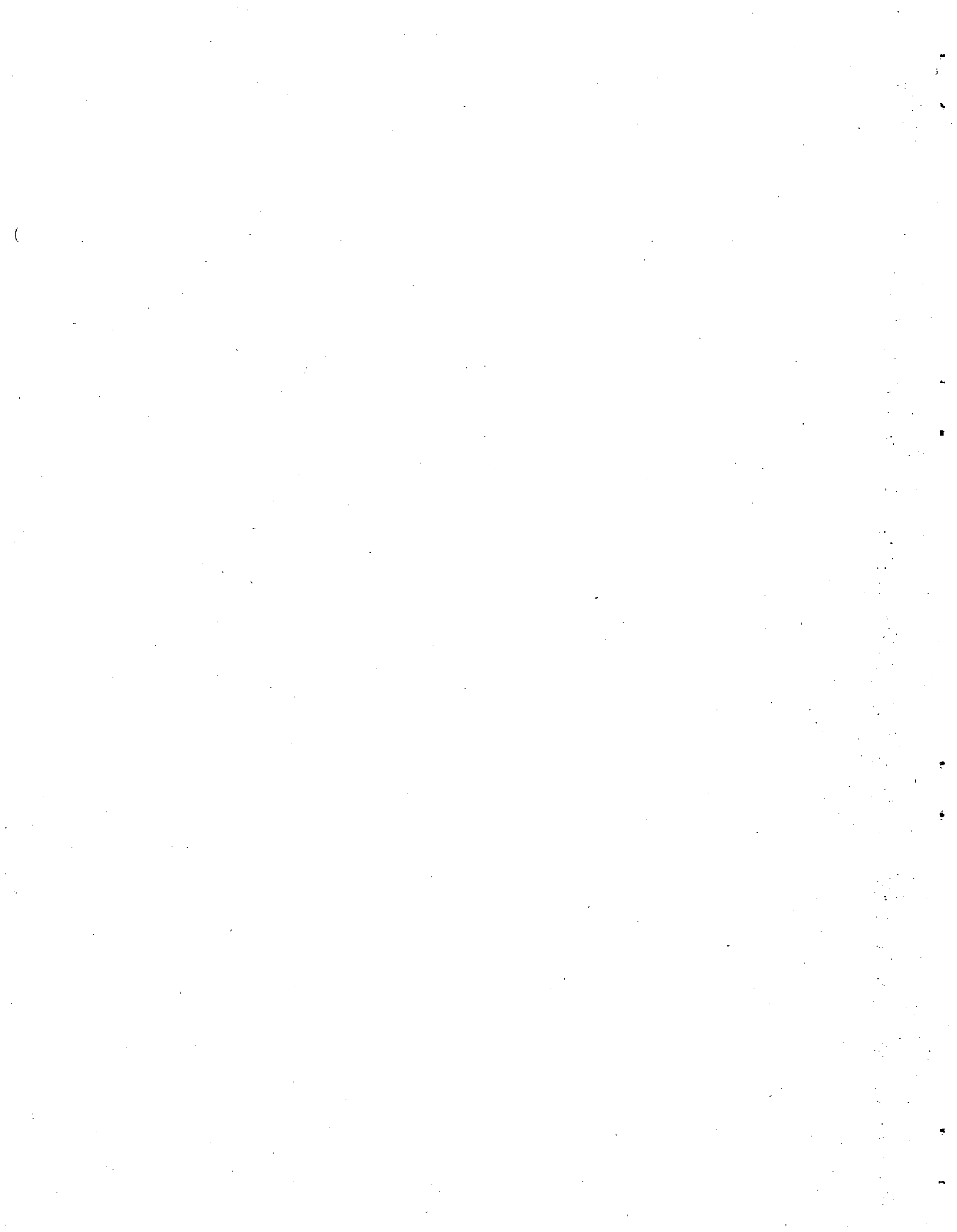


3 4456 0515868 2



Contents

ABSTRACT	v
1. INTRODUCTION	1
2. THE B-SERIES ZONAL CENTRIFUGE ROTORS	7
N. G. Anderson, D. A. Waters, G. B. Cline, C. E. Nunley, and C. T. Rankin, Jr. – Design and Evaluation of B-XIV and B-XV Rotors	7
Elizabeth L. Rutenberg – Calculation of Radius as a Function of Volume for the B-XIV and B-XV Rotors	19
C. E. Nunley – Improvements to B-Series Rotor Systems	25
3. CONTINUOUS-FLOW CENTRIFUGES FOR LARGE-SCALE VIRUS ISOLATION	30
G. B. Cline, R. F. Gibson, D. A. Waters, and N. G. Anderson – The K-I Zonal Rotor	30
N. G. Anderson and D. A. Waters – The K-II Zonal Rotor	33
4. ADVANCED ROTOR CONCEPTS	36
H. P. Barringer – High-Speed Drive Systems	36
E. C. Denny – Magnetically Suspended Rotor Systems	43
5. EXPERIMENTAL SEPARATIONS	52
J. R. Corbett – The Purification of Lysosomes	52
E. L. Candler, W. W. Harris, and N. G. Anderson – The S- ρ Separation of Human-Breast-Tumor Particles	55
G. B. Cline and W. W. Harris – Water Analysis in the Zonal Centrifuge	56
6. DEVELOPMENT OF AUTOMATED CHROMATOGRAPHIC SYSTEMS	60
J. G. Green and N. G. Anderson – The Assay of Sugars in Human Urine with the Prototype Carbohydrate Analyzer	60
C. D. Scott – Chromatographic Separation of UV-Absorbing Components of Human Urine	64
J. G. Green and G. L. Whitson – Changes in Soluble Carbohydrates of Synchronized <i>Tetrahymena</i>	69
R. H. Stevens – Flame-Ionization Analyzer for the Determination of Carbon in Liquid Streams or Solid Samples	72
J. G. Green, R. H. Stevens, and N. G. Anderson – Automated Carbohydrate Analyzer: Status of a Laboratory Model	75
7. SUPPORTING STUDIES	81
E. J. Barber, L. L. McCauley, P. F. Shorten, and J. F. Simmons – Physical Properties of Potassium Citrate Solutions	81
L. L. McCauley, R. H. Stevens, and W. M. Swartout – Dialysis Studies	83
N. G. Anderson and N. Cho – Density-Indicator Beads	88
W. S. Dritt – Stress-Corrosion Tests in Sodium Perchlorate	88



Abstract

The Molecular Anatomy (MAN) Program is concerned with the development of tools for the dissection and analysis, down to the molecular level, of cells and tissues. The following questions are asked: If available separation methods are extended to the limits of experimental resolution, would they resolve the complex mixture that is the cell? Given a complete molecular scan of cell contents in health and in disease, would differences due to an underlying malfunction be evident? What specific systems remain to be developed before a reasonably complete description of the molecular anatomy of a cell may be written? This report analyzes some aspects of these questions, describes analytical systems being developed under the program, and presents results of various bio-separations.

Two new zonal centrifuge rotors, B-XIV and B-XV, are described in detail, together with studies on the application of these rotors to particle isolation. Both rotors allow large-volume rate-zonal and isopycnic-zonal centrifugation to be done in conventional preparative ultracentrifuges. In addition, a computer method has been developed for calculating the radial distance from the center of the rotor for a specific volume, and improvements have been made to other B Series rotors.

A series of rotors is being designed and tested for large-scale virus isolation and other purposes by use of the continuous-flow principle. The prototype K-I rotor operates in the conventional air-driven Sharples machine. The large-volume (<10

liters/hr) K-II rotor is the first of several rotors that are being designed to do specific tasks. Direct motor drive or an air turbine will probably be the most economical method of spinning a production model of the K-II rotor.

Advanced concepts, such as high-speed drive systems and magnetically suspended rotors, are being explored. Materials requirements are stringent for systems in these categories because of extremely high g forces.

From experimental separations with several rotors, results with a number of materials are reported: lysosomes, human breast tumors, and natural waters.

High-performance chromatographic systems are being modified and refined. A laboratory model of an automated carbohydrate analyzer is described, together with results of experiments in following changes in soluble carbohydrates of synchronized *Tetrahymena* and in assaying sugars of human urine. Ultraviolet-absorbing components of urine were chromatographically separated with a modified nucleotide analyzer.

From a group of supporting studies, the following is reported: (1) physical properties of potassium citrate solutions, (2) design and testing of dialysis equipment and density indicator beads, (3) stress and corrosion tests in sodium perchlorate, and (4) determination of carbon in liquid streams or solid samples with a flame-ionization analyzer.

This program is cosponsored by the National Cancer Institute and the U.S. Atomic Energy Commission.



1. Introduction

N. G. Anderson

THE MAN PROGRAM

The Molecular Anatomy (MAN) Program deals with the analyses of cells, the perfection of methods for cell fractionation, and the isolation of separable molecular constituents of living systems. The anatomical viewpoint was chosen because description of physical units, in quantitative terms if possible, is fundamental to a scientific discipline. Early in the history of biomedical sciences, anatomical description generally preceded the understanding of the function of normal body components, of changes that produced diseases, and of therapy. As techniques were refined, structures, diseases, and treatments were studied first at the gross, then at the microscopic level. Today, at the molecular level, the techniques requisite for molecular dissection are still in an undeveloped state, and, therefore, descriptions of disease at this level are incomplete.

A classical example of another anatomical approach at the molecular level is the study of human blood plasma. From an enzymological viewpoint, serum proteins are a relatively uninteresting mixture. Fortunately, fractionation of them by purely physical methods was undertaken, and a wealth of information was obtained. Now we know that for nearly every major blood protein there is a disease-associated alteration. Little is known about cytoplasmic proteins, but it is very likely that disease-associated changes will be discovered for a high percentage of them.

Although work on cell constituents has proceeded empirically, it is important to raise and discuss the question, "Is the separation and characterization of all or nearly all the constituents of cells within the realm of possibility, given existing techniques and separation principles?" Stated in more

practical terms, with the best separation systems which we can devise or foresee, will the "lists" or "scans" cover all unique molecular species found in cells? The problem is central to attempts to find biochemical differences associated with disease (especially cancer) or with differentiation in biological systems.

The MAN Program was formally proposed in 1961 to investigate this problem,¹ and the portion undertaken as a joint NIH-AEC effort to develop zonal centrifuges (1962-1965) was summarized recently in a monograph.² Program emphasis now centers around the development of a spectrum of techniques that are required for the complete description of the molecular anatomy of cells. The basic premise, that new tools for the molecular dissection of cells can be developed, given suitable basic science and engineering support, appears to be borne out in practice, particularly here at the Oak Ridge National Laboratory. In this sense the development of zonal centrifuges demonstrated the feasibility of the MAN Program.

The hierarchical disassembly of cells requires techniques or systems capable of dealing with four subsets of particles: multimolecular subcellular components, macromolecules, mesomolecules, and (less distinctly separated) micromolecules. The first class of subcellular particles includes the multimolecular substructures seen in the light or electron microscope (nuclei, chromosomes, mitochondria, membrane fragments or vesicles derived from the endoplasmic reticulum, polysomes, ribo-

¹N. G. Anderson, The Cell Fractionation Project, ORNL Advanced Technology Seminar, No. 6, Jan. 25, 1961.

²N. G. Anderson, ed., *The Development of Zonal Centrifuges and Ancillary Systems for Tissue Fractionation and Analysis*, ed. by N. G. Anderson, Mono. 21, J. Natl. Cancer Inst. Mono. Ser., 1966.

somes, chloroplasts, lysosomes, secretory granules, cilia, viruses, and multimolecular substructures derived from these). The centrifuges described in this and previous reports were largely developed for the separation of particles of this class. During this report period, work on centrifuge development has proceeded along three lines. The first is the development of new centrifugal separation methods, the second is the development and engineering necessary to translate new concepts into experimental systems, and the third is the application of the experimental systems to biological problems.

To proceed meaningfully with the analysis of cells, certain problems must be faced. The first problem concerns the choice of cells. The availability of materials, such as tissues from laboratory animals, early determined our choice of cells. However, the ultimate objective remains the fractionation of human cells. Only these truly justify the effort. For this reason, preliminary studies on large-scale tissue cultures of human cells are being undertaken. The second problem, which has received the most attention thus far in this laboratory, concerns the fractionation of cells into their formed subcellular constituents. New rotor systems continue to be developed to solve this problem. Automated analytical systems are receiving attention in a continuing effort to investigate macromolecules and micromolecular constituents of cells and cell organelles.

NEW SEPARATION CONCEPTS

The basic concepts for advanced methods of separating cellular particles — rate-zonal, isopycnic-zonal, $S-\rho$, and continuous-flow-with-banding centrifugation — antedate the joint NIH-AEC zonal centrifuge development program. Although these techniques are valuable, it is important to develop new centrifugation concepts that are applicable to an even wider variety of separation problems.

Particle Immobilization During Chemical Dissection

Whole cells or subcellular particles may be banded isopycnicly in a density gradient containing enzymes, detergents, and other chemicals. These solubilizing agents could be distributed

uniformly through the gradient or, alternatively, be introduced as a narrow zone at the banding level of the sample or as an overlay that sediments or diffuses into the particle band. As the sample is disrupted, released subcellular constituents, such as viruses, nucleic acid, and glycogen, begin to move through the gradient and may be fractionated on the basis of sedimentation rate or banding density.

Particle Dissection by Sedimentation Through Reagents Immobilized in a Density Gradient

A variety of substances of low and intermediate molecular weight may be stabilized as zones in a density gradient. During the sedimentation of cells or large subcellular constituents through the gradient, these reagents do not move appreciably. Thus, a sample may be centrifuged through these zones, leaving behind small particles removed by reagents in the zones. The sequential removal of globulins and histones by sedimentation of nuclei through a gradient of increasing ionic strength and acidity is an example of this type of particle dissection. The method may also be used to fractionate membranes or ribosomes (by detergent or salt gradients) into their constituent macromolecules.

Gradient Resolubilization

During the precipitation of proteins, the approach to equilibrium between the dissolved and the precipitated or crystallized phases is extremely slow. Equilibrium is approached much more rapidly if a precipitated protein is added to a solution, especially when the protein is added in the form of very small floccules. A centrifugal method that uses these properties has been devised. It was observed (author's unpublished data, 1956) that protein precipitated at the top of an alcohol-water gradient will sediment in a centrifugal field until it reaches a level where it can dissolve. If the field is not too high, the protein will remain at the level where it dissolves. In the gradient-resolubilization technique (Fig. 1), the precipitating reagent and the flocculated sample are run into the rotor together. During centrifugation, the precipitate sediments into the immobilized

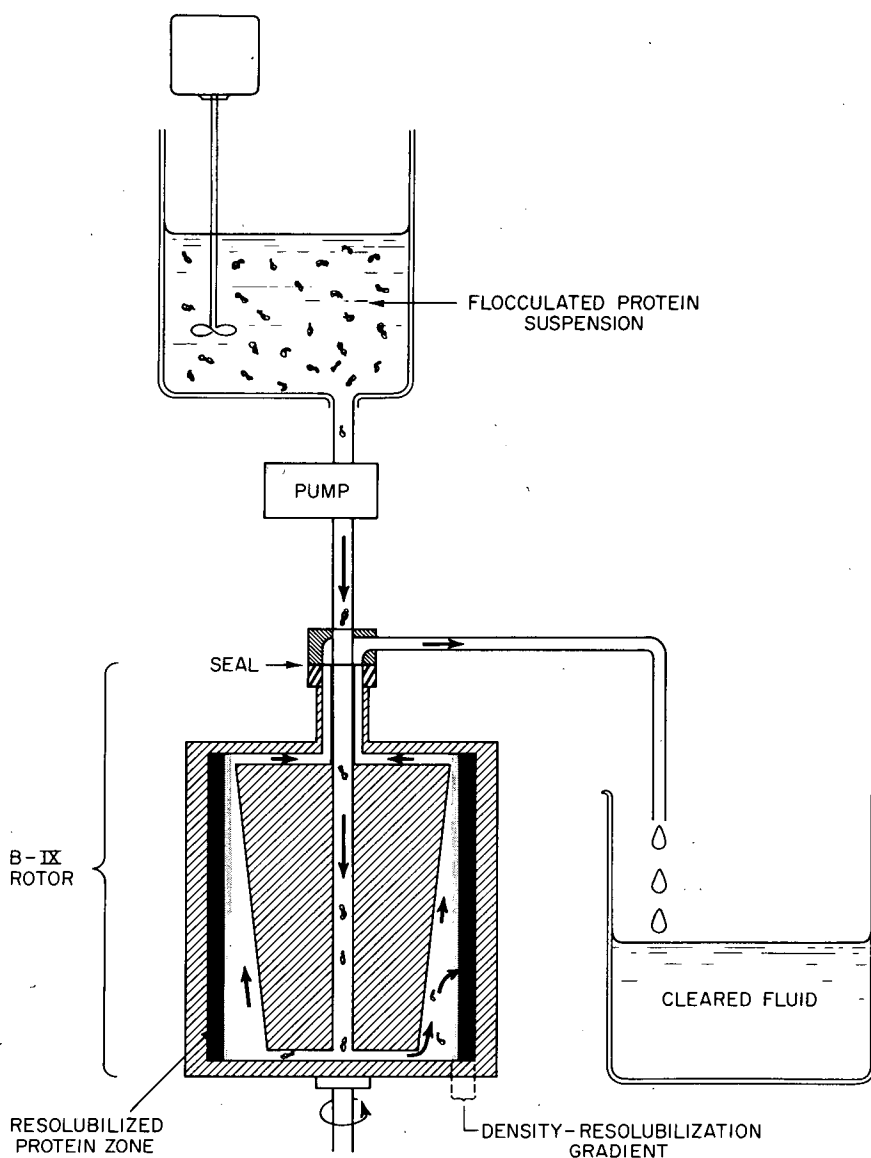


Fig. 1. Centrifugal Separation of Protein by Gradient Resolubilization in a Continuous-Flow Rotor.

gradient in the rotor until it either dissolves or bands isopycally. After centrifugation, the band is recovered. The method has been applied to the problem of concentrating adenovirus subunits and viruses from large fluid volumes; it is also applicable to concentrating and fractionating a variety of proteins, low-molecular-weight materials, and nucleic acids.

Precipitation in a Gradient, Followed by Isopycnic Banding

Under the proper conditions, a substance in the sample layer may be precipitated or crystallized at the centripetal end of a density gradient in which the substance is insoluble. The particles then may be centrifuged to their isopycnic levels

and recovered. The banding densities of crystals and precipitates reflect the densities and arrangement of the atoms in the molecules and the way in which the molecules may be packed together. Rather small changes in the configuration of a molecule may produce appreciable changes in the density of precipitates or crystals.

In practice, water-insoluble organic substances dissolved in a water-miscible organic solvent may be layered over an organic solvent-aqueous density gradient in which either crystalline or amorphous particles of the organic solids will band. With proper choice of solvents, all levels of the gradient and sample layer may be made denser than water, which is layered over the sample. As water diffuses into the sample layer, precipitation occurs, and particles move out through the gradient to their isopycnic levels. Similar systems using water-soluble materials layered over gradients prepared from dense, water-miscible organic solvents have also been explored. These concepts extend the usefulness of zonal-centrifuge rotor systems to the separation of molecules that are too small to sediment under ordinary conditions and to the fractionation of subcellular particles into their constituent molecular species.

High-Resolution Continuous-Flow Centrifuge Systems

For many purposes, very large amounts of one or more subcellular particles may be required. There is, therefore, need for systems for large-

scale isolation of nuclear, mitochondrial, lysosomal, microsomal, and ribosomal units. These may be isolated by cascading continuous-flow centrifuges of increasing speed or gravitational fields. It is desirable to have a very sharp cut-off point: particles having a sedimentation rate above a certain value should be retained in the rotor, while those below that value should stream through it. The principles used to approach this requirement are shown diagrammatically in Fig. 2. A fluid flowing centripetally in a sector-shaped compartment in a gravitational field is (1) subjected to a centrifugal field that decreases directly with radius and (2) flowing at a rate that increases inversely with the radius. A particle in such a fluid must settle faster than the stream is flowing centripetally in order to reach the rotor wall. However, any particle that has not begun to move toward the wall when the fluid is at a maximum radius (and minimum rate of flow centripetally) will not do so since the flow rate increases and the centrifugal field decreases during movement toward the axis. By flowing the particle-containing fluid in over a density gradient in sector-shaped compartments, a separation is made in a narrow zone at the surface of the gradient. Either the particles sediment at once into the gradient, or they are swept inboard and out of the rotor. The particles left in the rotor may be allowed to sediment to the rotor wall (Fig. 2) or against an immiscible, dense, fluid barrier (Fig. 3). They may also be banded isopycnically in a gradient. By cascading a series of such rotor systems, highly enriched fractions can be obtained.

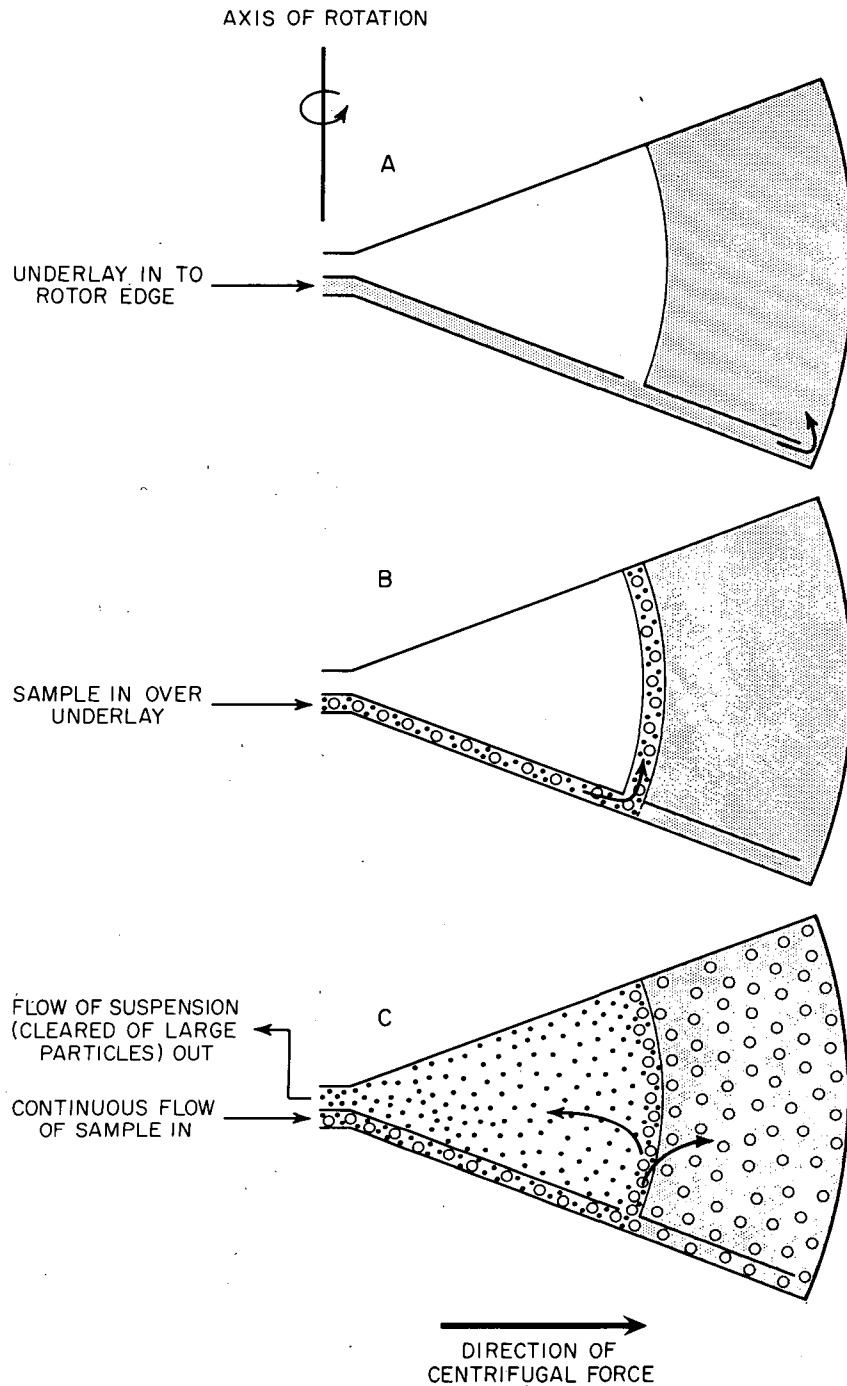


Fig. 2. Step-by-Step Procedure for the Separation of Particulate Materials in Sector-Shaped Compartments by Continuous-Flow Centrifugation. Large or heavy particles sediment to the rotor wall. In (A) a dense fluid is introduced into a sector-shaped compartment in a spinning rotor. The sample suspension is then pumped into the rotor (B), where it begins to flow over the surface of the dense underlay. As more sample streams through the rotor, particles having a sufficiently large sedimentation rate sediment out through the underlay (C) while particles with a smaller sedimentation coefficient are swept inboard and out of the rotor.

ORNL-DWG 66-7504

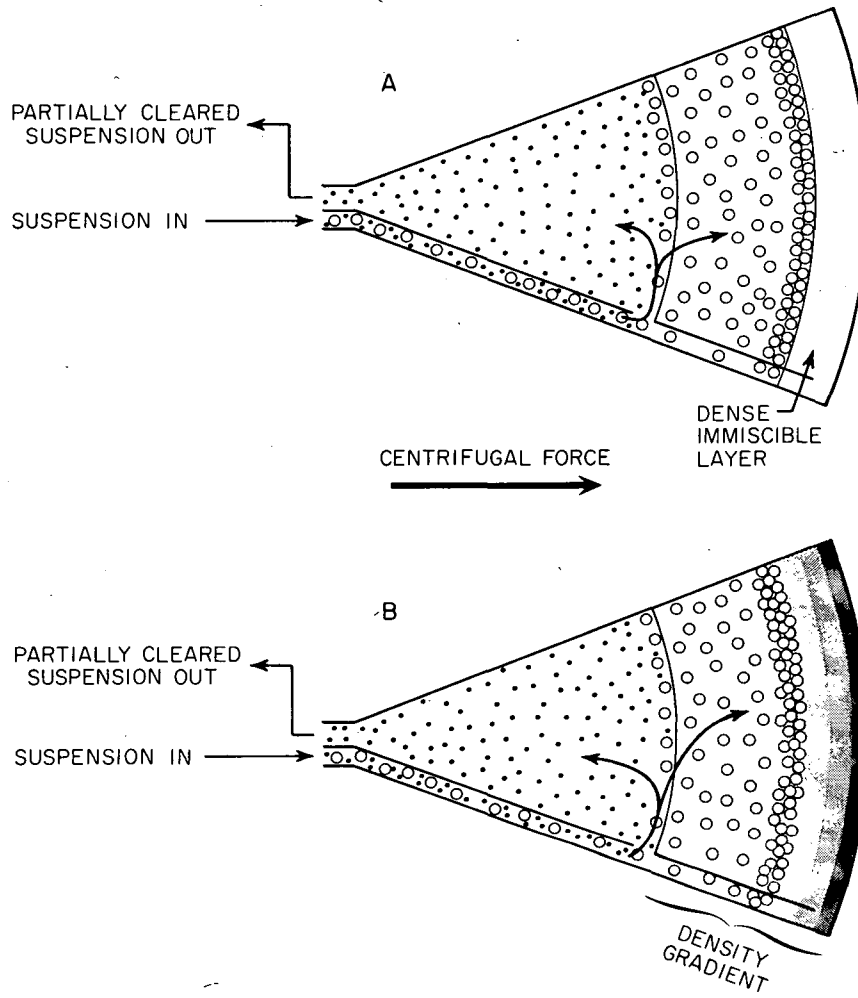


Fig. 3. Separation of Particulate Materials in Sector-Shaped Compartments by Continuous-Flow Centrifugation. Large or heavy particles sediment to a dense liquid (A) or are banded isopycally in a density gradient (B).

2. The B-Series Zonal Centrifuge Rotors

DESIGN AND EVALUATION OF B-XIV AND B-XV ROTORS

N. G. Anderson G. B. Cline
D. A. Waters C. E. Nunley
C. T. Rankin, Jr.

Zonal centrifuges have been developed for the mass separation of subcellular particles and viruses on the basis of either sedimentation rate or buoyant density.¹⁻⁸ They have been used to isolate major subcellular components, viruses,^{4,5,9,10} ribosomal RNA,¹¹ and serum macroglobulins.¹² An advantage of the B-IV zonal rotor previously described^{6,13} is that it may be

easily converted into a high-speed continuous-flow rotor with¹⁴ or without¹⁵ isopycnic banding during operation. A disadvantage of this rotor is that a special centrifuge with extended armor, a cooled upper bearing, and a high-speed seal are required. Where the continuous-flow capability is not needed, a much simpler removable-seal rotor, which can be spun in unmodified preparative centrifuges, appears to offer several advantages. Because the centrifuge has no upper bearing, however, the rotor configuration must be changed so that it is stable when supported from below by a flexible shaft. Two prototype steel rotors (B-X and B-XI) were developed during this work⁸ in order to demonstrate the feasibility of the concept. The rotors described here, B-XIV and B-XV, are advanced versions of the earlier prototypes and are suitable for routine separations.

¹N. G. Anderson, "The Zonal Ultracentrifuge. A New Instrument for Fractionating Mixtures of Particles," *J. Phys. Chem.* **66**, 1984-89 (1962).

²N. G. Anderson and C. L. Burger, "Separation of Cell Components in the Zonal Ultracentrifuge," *Science* **136**, 646-48 (1962).

³N. G. Anderson, "Development of Zonal Centrifuges," *Federation Proc.* **22**, 674 (1963).

⁴N. G. Anderson, "Virus Isolation in the Zonal Centrifuge," *Nature* **199**, 1166-68 (1963).

⁵N. G. Anderson, C. L. Burger, and W. W. Harris, "Virus Separation in the Zonal Ultracentrifuge," *J. Cell Biol.* **19**, 12A (1963).

⁶N. G. Anderson *et al.*, "The B-IV Zonal Ultracentrifuge," *Life Sci.* **3**, 667-71 (1964).

⁷N. G. Anderson, "An Introduction to Particle Separations in Zonal Centrifuges," in *The Development of Zonal Centrifuges and Ancillary Systems for Tissue Fractionation and Analysis*, ed. by N. G. Anderson, Mono. 21, J. Natl. Cancer Inst. Mono. Ser., 1966.

⁸N. G. Anderson *et al.*, "Zonal Rotors with Removable Seals. Rotors B-X and B-XI," in *The Development of Zonal Centrifuges and Ancillary Systems for Tissue Fractionation and Analysis*, ed. by N. G. Anderson, Mono. 21, J. Natl. Cancer Inst. Mono. Ser., 1966.

⁹C. B. Reimer *et al.*, "An Evaluation of the B-V (Continuous Flow) and B-IV (Density Gradient) Rotors Using Live Polio Virus," in *The Development of Zonal Centrifuges and Ancillary Systems for Tissue Fractionation and Analysis*, ed. by N. G. Anderson, Mono. 21, J. Natl. Cancer Inst. Mono. Ser., 1966.

¹⁰C. B. Reimer *et al.*, "Influenza Virus Purification with the Zonal Ultracentrifuge," *Science* (in press).

¹¹J. R. B. Hastings *et al.*, "Fractionation of Ribonucleic Acids in the Zonal Ultracentrifuge," *Nature* **208**, 646-49 (1965).

¹²W. D. Fisher and R. E. Canning, "Isolation and Characterization of Rat Macroglobulin," in *The Development of Zonal Centrifuges and Ancillary Systems for Tissue Fractionation and Analysis*, ed. by N. G. Anderson, Mono. 21, J. Natl. Cancer Inst. Mono. Ser., 1966.

¹³N. G. Anderson *et al.*, "The Design and Operation of the B-IV Zonal Centrifuge System," in *The Development of Zonal Centrifuges and Ancillary Systems for Tissue Fractionation and Analysis*, ed. by N. G. Anderson, Mono. 21, J. Natl. Cancer Inst. Mono. Ser., 1966.

¹⁴N. G. Anderson *et al.*, "Continuous-Flow Centrifugation Combined with Isopycnic Banding," in *The Development of Zonal Centrifuges and Ancillary Systems for Tissue Fractionation and Analysis*, ed. by N. G. Anderson, Mono. 21, J. Natl. Cancer Inst. Mono. Ser., 1966.

¹⁵H. P. Barringer, N. G. Anderson, and C. E. Nunley, "Design of the B-V Continuous-Flow Centrifuge System," in *The Development of Zonal Centrifuges and Ancillary Systems for Tissue Fractionation and Analysis*, ed. by N. G. Anderson, Mono. 21, J. Natl. Cancer Inst. Mono. Ser. 1966.

A brief description of these rotors has appeared elsewhere.¹⁶

Rotor Design

In overall dimensions rotors B-XIV and B-XV are similar to B-X and B-XI previously described.⁸ However, the rotors have been greatly simplified, and measures have been taken to ensure better temperature control during loading and unloading.

Operating Principles. — Both rotors consist of two semihemispheres held together by buttress threads and sealed with an O-ring. The operation of the rotor is graphically shown in Fig. 1. The internal volume of the rotor is divided into four sector-shaped compartments by four septa which are an integral part of the core (Fig. 2). A coaxial seal^{1,6,13} permits fluid to be pumped through the core to the rotor edge or to the inmost surface of the core. The seal is attached to the rotor during loading and unloading at low speed (~3000 rpm) and is removed and replaced with a small cap for high-speed operation.

Overall Configuration. — The B-XV rotor is shown partially assembled in Fig. 2 and completely assembled in Fig. 3. Two versions have been fabricated — one with the center piece extending through the lower hemisphere (not shown) and the other with the center piece protruding only through the upper hemisphere. The ratio of the moments of inertia of a rotor was chosen to ensure stability when the rotor is supported and driven from below with no upper bearing.¹⁷

Construction of the Seal. — The removable static seal is attached to the rotor through a stainless steel sealed bearing that centers the static seal and maintains its alignment against the flat surface of the rotating seal. Two flexible arms are attached to a ring in the Spinco model L centrifuge chamber to prevent rotation of the static seal. These are also used as handles for inserting and removing the seal.

When the rotor is in place in the centrifuge, a Lucite cover is positioned directly over the rotor to reduce air flow and to assist the maintenance of low temperature during loading and unloading. The seal assembly is mounted above the Lucite plate (Fig. 4). An additional two-piece Lucite closure is used in place of a metal lid during loading and unloading to further diminish the flow of warm air through the centrifuge.

For high-speed operation, the static seal is manually removed and replaced with a rotating seal and a cap that permits it to be grasped safely when the seal is placed on or removed from the rotor (Fig. 5).

The Rotor Core. — The rotor core is similar to that of the B-X and the B-XI,⁸ with a few modifications. The septa, which are an integral part of the core, divide the internal rotor space into four compartments and serve to prevent mixing and swirling due to Coriolis forces during loading and unloading and to accelerate and decelerate the entire rotor contents uniformly. The edge lines, which are drilled through the septa, are shown in Fig. 2.

The center seal line connects to the rotor center, and the edge seal line to the rotor edge. To equalize the gradients in each sector, clearance is provided between the septa and the rotor wall. The flat center-core faces funnel the density and particle zones toward a point on their upper center surfaces, where connection is made to the center fluid line, as shown in Fig. 6.

Rotor Data

The pertinent data on the B-XIV and B-XV rotors are shown in Table 1. In addition to speed advantages gained by titanium construction, rotors constructed of this material may be steam-sterilized and do not corrode in most salt solutions or at pH's used in biological studies.

The suggested operating speeds which are maximum safe speeds for the B-XIV and B-XV rotors, as functions of the specific gravity of the fluid used, are shown in Fig. 7. Note that when a dense, homogeneous fluid is centrifuged for a long period of time, a gradient is gradually formed which will markedly increase the wall pressure in the rotor. For safe operation, the density of a gradient is considered as that of its densest portion.

¹⁶N. G. Anderson *et al.*, "Two New Simple Zonal Centrifuge Rotors: B-XIV and B-XV," *Federation Proc.* 25, 421 (1966).

¹⁷H. P. Barringer, "The Design of Zonal Centrifuges," in *The Development of Zonal Centrifuges and Ancillary Systems for Tissue Fractionation and Analysis*, ed. by N. G. Anderson, Mono. 21, J. Natl. Cancer Inst. Mono. Ser., 1966.

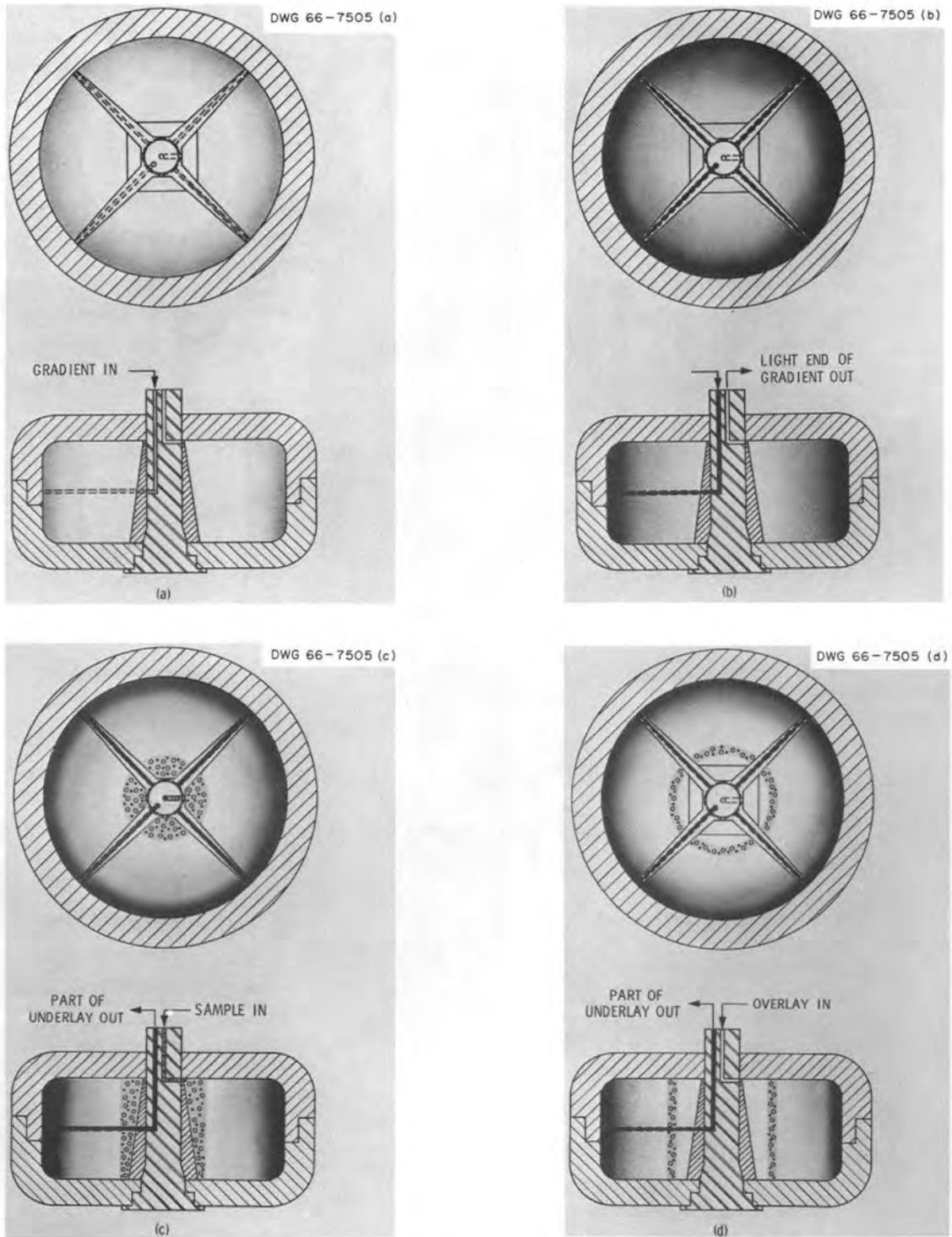


Fig. 1. Schematic Diagrams of the Operation of B-XIV or B-XV Zonal Centrifuge Rotors. A rotor is shown at various stages of loading and unloading in top and side view: (a) start of gradient introduction into rotor which is spinning at low speed, (b) completion of loading of gradient, (c) movement of sample layer into the rotor through the center line, (d) introduction of overlay into rotor in order to move the starting zone away from the core faces, (e) separation of particles at high speed, (f) displacement of separated zones out of rotor at low speed, and (g) completion of unloading and collection of sample tubes.

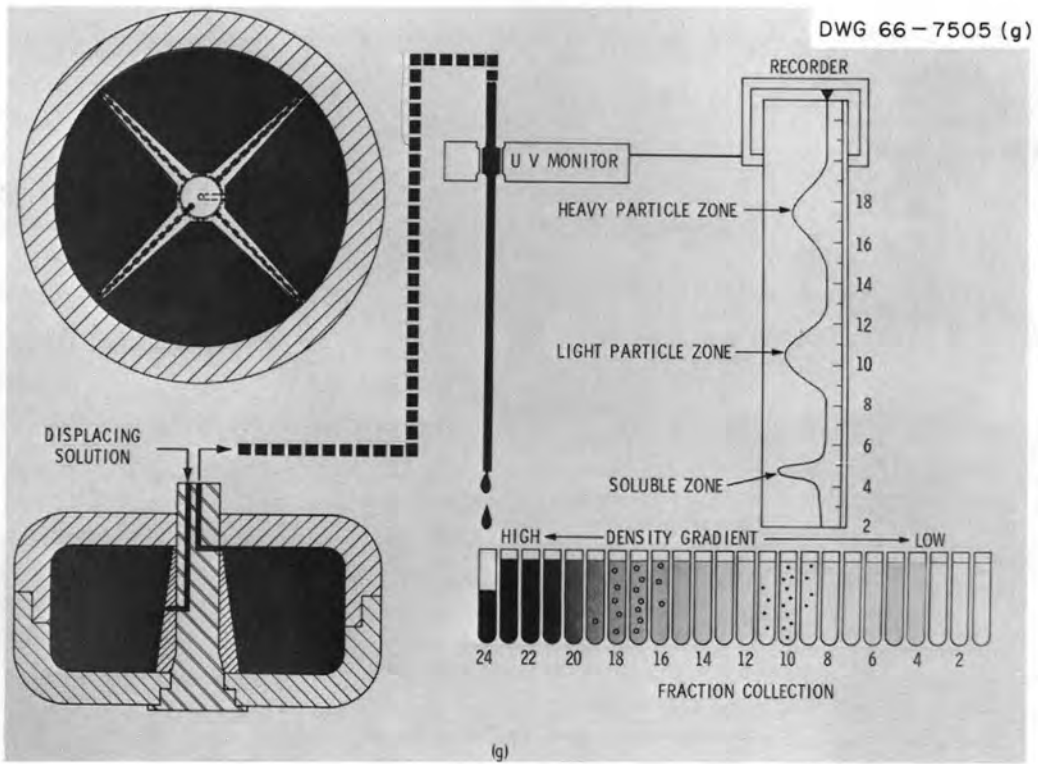
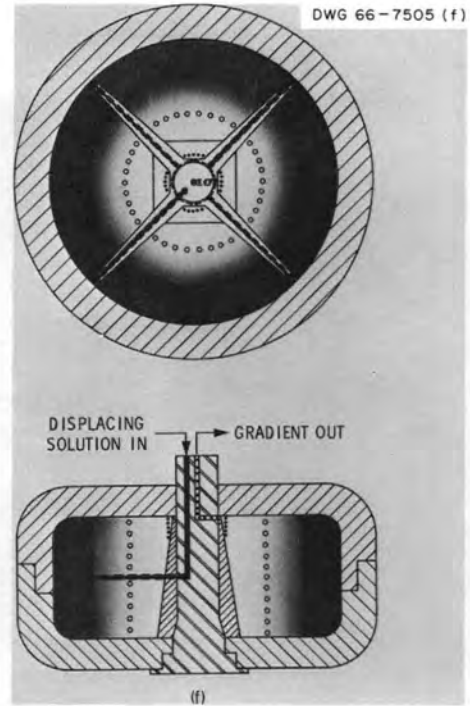
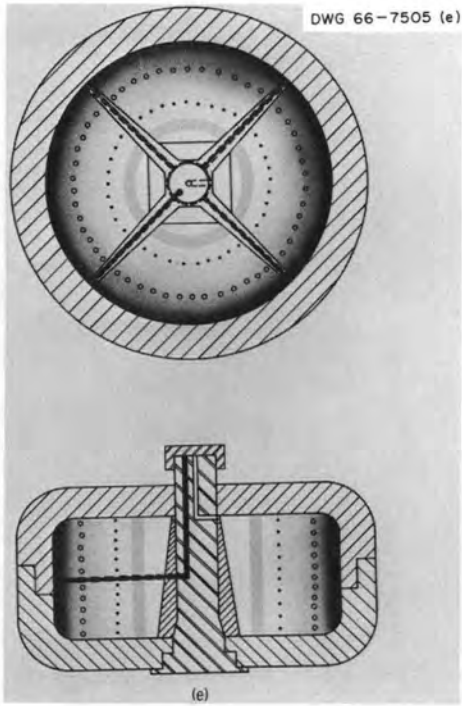


Fig. 1. Continued.



Fig. 2. Partially Assembled B-XV Rotor. Upper section of rotor (right) screws into lower section (left).

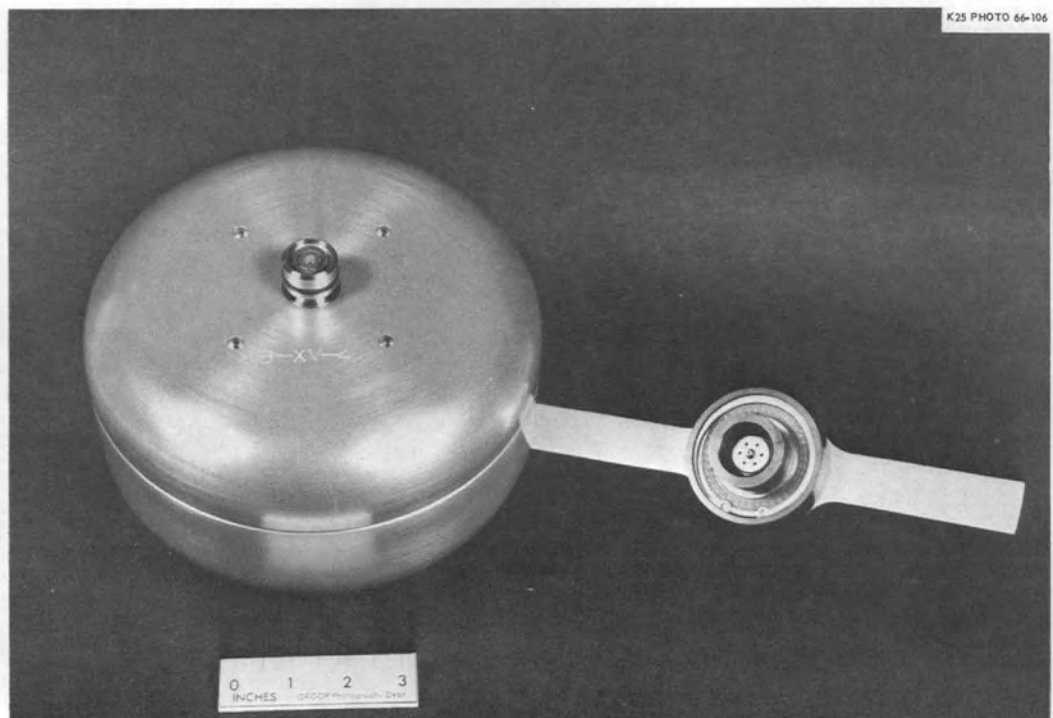


Fig. 3. Completely Assembled B-XV Rotor. Removable upper seal is shown at right.

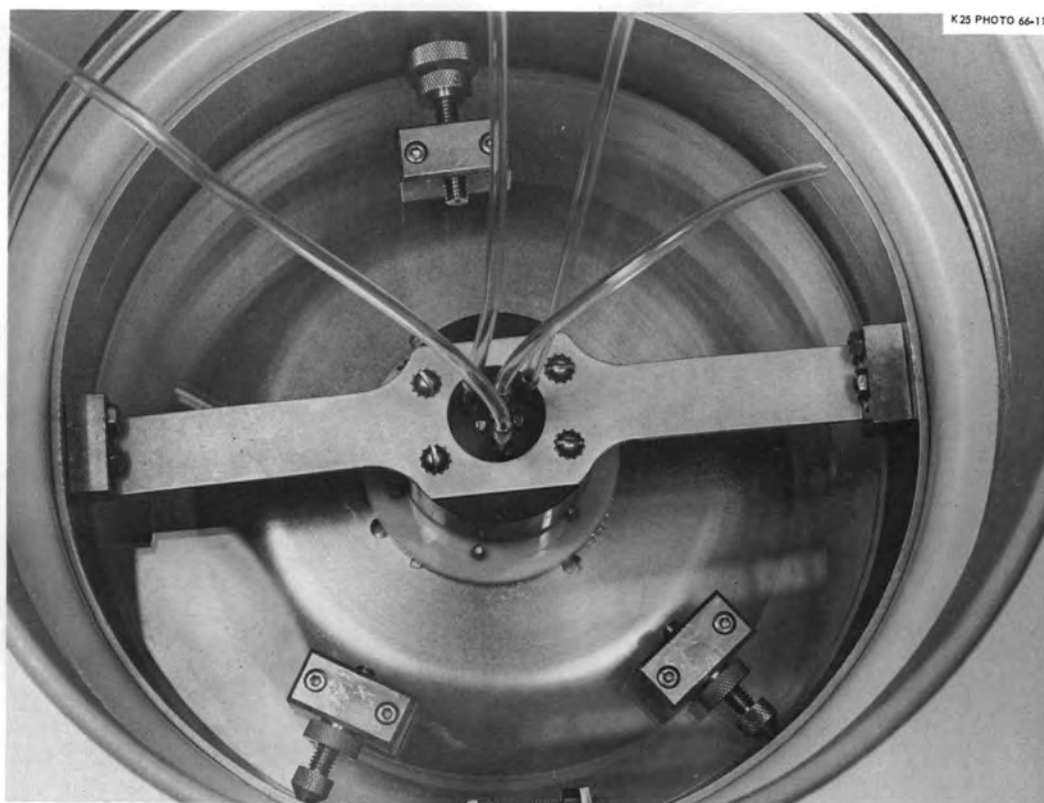


Fig. 4. Rotor and Seal in Place in Spinco Model L Preparative Ultracentrifuge.

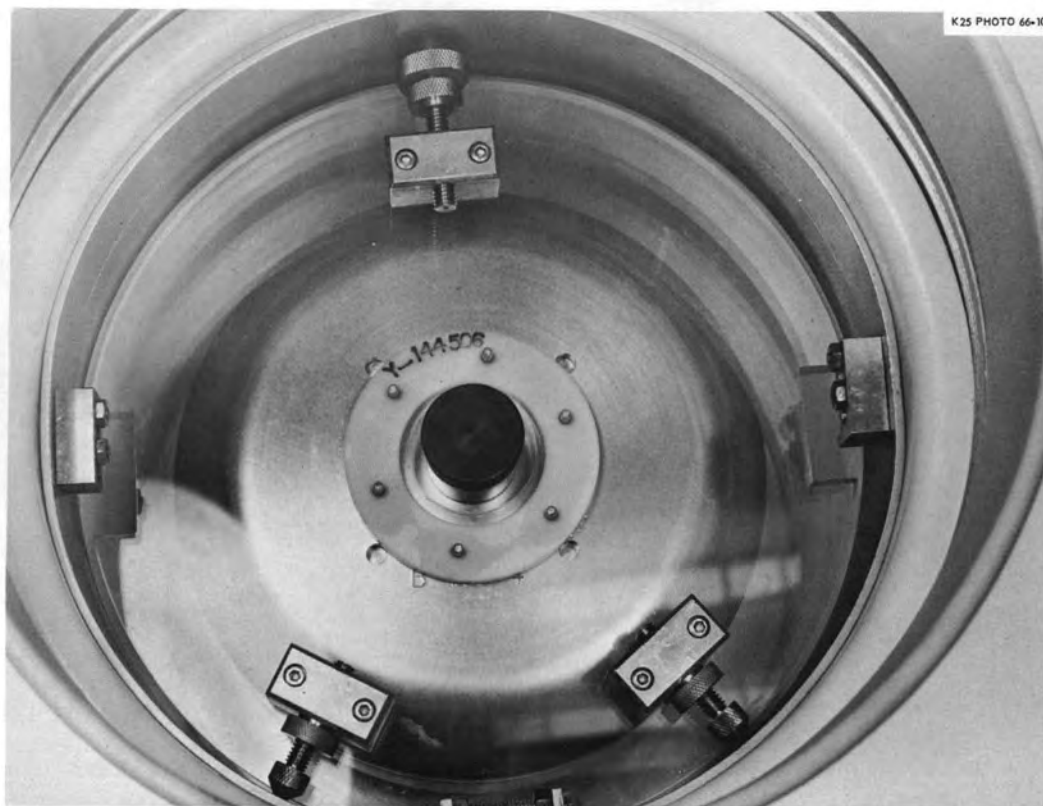
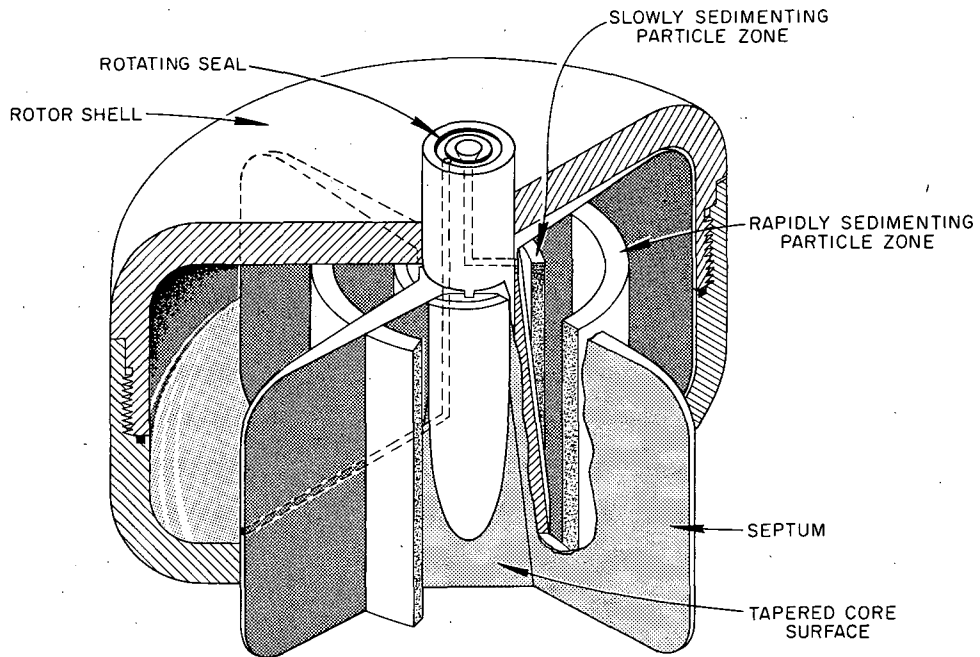
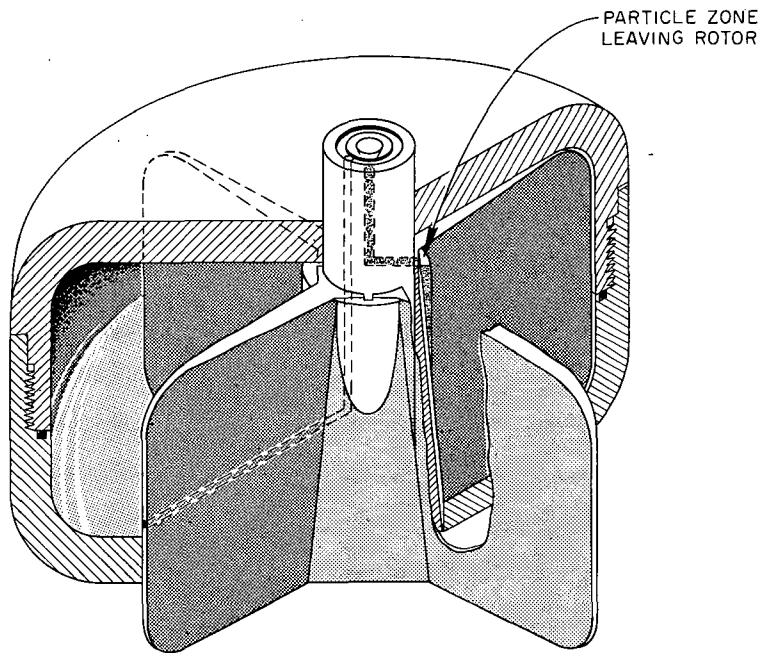


Fig. 5. Assembled B-XV Rotor. The protective cap (in place) covers the rotating seal during high-speed operation.



(a)



(b)

Fig. 6. Flow of Particle Zones Across Core Face During Unloading. In (a) one zone is close to the core face while a second has just made contact with it. In (b) a zone is being funneled across the core face into the exit line.

Table 1. Operating Data for B-XIV and B-XV Zonal Rotors

Parameter	B-XIV (Aluminum)	B-XV	
		Aluminum	Titanium
Weight (empty), kg	3.571	7.439	12.7 ^a
Volume, cc	649	1,666	
Speed, rpm	30,000	21,000	26,000
Maximum g , at rated rpm	60,000 at 29,400	45,000 at 21,500	60,000 at 24,000
Maximum radius, cm	6.62	8.79	8.79
Maximum stress (tensile), psi	50,000	50,000	82,000
Maximum radial growth, in.	0.013	0.0175	
Estimated maximum pressure, psi	5,000	5,400	8,000
Estimated maximum end load, lb	75,000	125,000	175,000

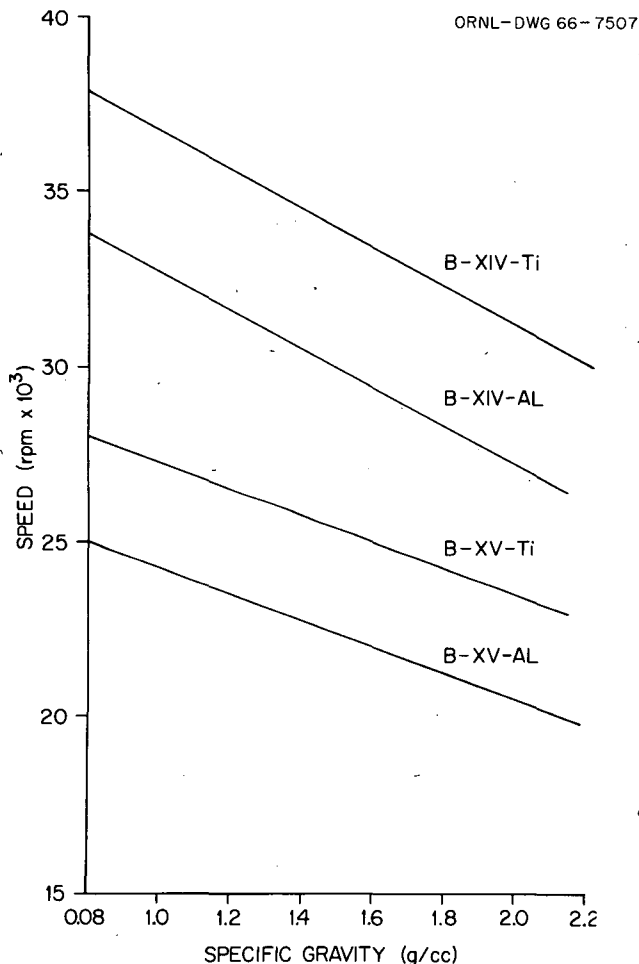
^aEstimated.

Fig. 7. Operating Speed of Aluminum and Titanium B-XIV and B-XV Zonal Rotors as a Function of the Density of the Fluids in the Rotor.

Analytical data can be obtained from the B-XIV and B-XV rotors if the starting position of a particle, its position at the end of the run, and the integral of $\omega^2 dt$ are known.¹⁸ The position of the starting zone and of recovered zones in the rotor can be calculated, providing that (1) the volume and the position of these zones among the recovered fractions are accurately known and (2) equations are available which relate recovered volume to radius in the rotor.

The plots of rotor volume vs radius are given in Figs. 8 and 9 for rotors B-XIV and B-XV respectively. These may be used to locate the position of a fraction in the rotor from the effluent analysis and to determine the width in the rotor of each fraction or peak obtained. The methods of calculation are discussed by Rutenberg under the heading "Calculation of Radius as a Function of Volume for the B-XIV and B-XV Rotors" in this chapter.

Rotor Performance

The first test of any new rotor system is to determine how closely the gradient recovered at the end of the run resembles the gradient introduced into the rotor. By use of a piston gradient pump,

¹⁸Barbara Bishop, "Digital Computation of Sedimentation Coefficients in Zonal Centrifuges," in *The Development of Zonal Centrifuges and Ancillary Systems for Tissue Fractionation and Analysis*, ed. by N. G. Anderson, Mono. 21, J. Natl. Cancer Inst. Mono. Ser., 1966.

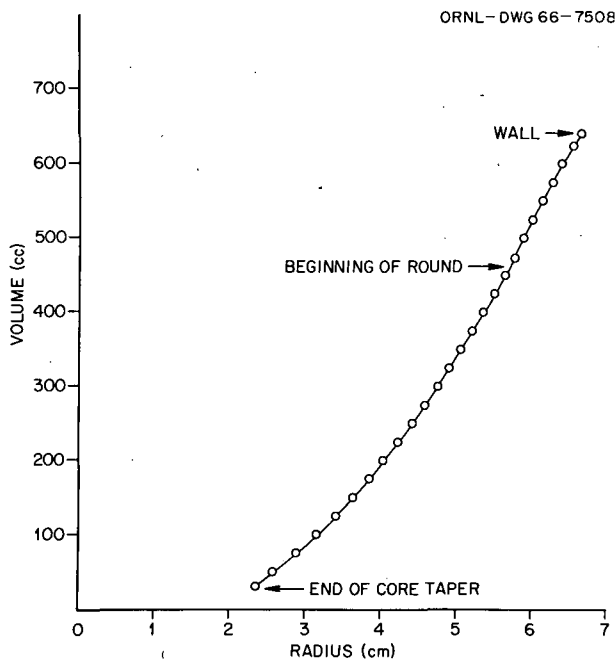


Fig. 8. Rotor Volume as a Function of Radius for the B-XIV Rotor. See Table 2 for dimensions used for calculations.

500-ml gradients, linear with volume, ranging from 17 to 55 wt % sucrose were: (1) collected in 40-ml fractions directly from the pump; (2) pumped into the B-XIV rotor at 3500 rpm and promptly displaced with additional 55 wt % sucrose; and (3) introduced into the rotor at 3500 rpm, accelerated to 30,000 rpm, run for 30 min, and then decelerated to 3500 rpm for displacement. The results for the B-XIV rotor are shown in Fig. 10. Similar studies with a 1200-ml gradient in rotor B-XV are shown in Fig. 11. In the latter instance, the third experiment was run at 20,000 rpm for 30 min. Little disturbance of the gradient occurs during passage through the rotor.

The boundary spreading that occurs when a sample is placed in the B-XV rotor and then recovered, with and without acceleration to high speed, was also examined. Samples containing 20 ml of 3 wt % bovine serum albumin stained with bromphenol blue in 5 wt % sucrose were layered over 1200-ml gradients extending from 17 to 55 wt % sucrose, followed by an overlay of 200 ml of distilled water. The sample was introduced and recovered at 3500 rpm; the results are shown in Fig. 12a. The width at half peak height equaled the sample volume (20 ml) and was equal to a

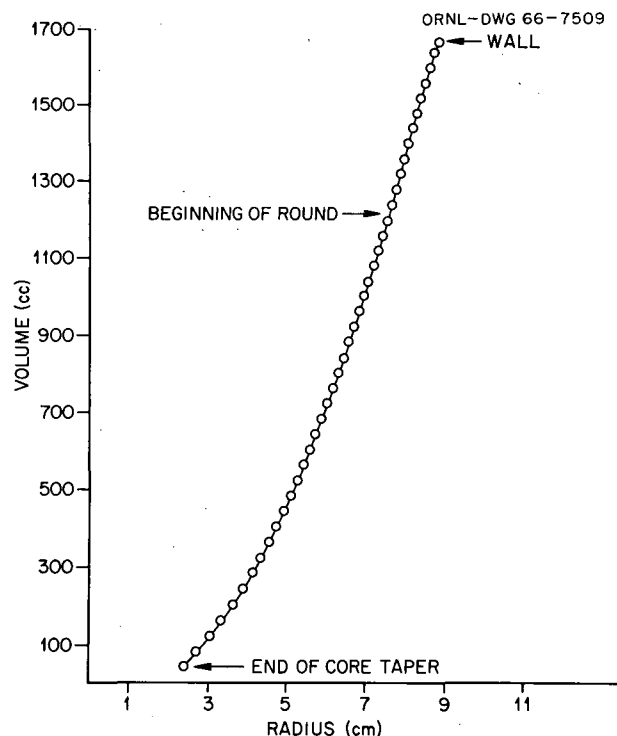


Fig. 9. Rotor Volume as a Function of Radius for the B-XV Rotor. See Table 2 for dimensions used for calculations.

band width of 0.12 cm in the rotor. Some widening was seen (Fig. 12b) when the rotor was accelerated to 20,000 rpm for 30 min, followed by deceleration to 3500 rpm for unloading. The width at half peak height in the latter instance was 30 ml or 0.19 cm in the rotor. Similar studies with the B-XIV rotor also showed that very little boundary widening occurred. A chart recording of one such experiment is shown in Fig. 13.

These experiments show that zones can be introduced into and recovered from the upper (less-dense) portion of the gradient with little loss in resolution. Sharp zones also can be formed and recovered from the area close to the rotor wall. To examine this point, ragweed pollen grains extracted with alcohol (1 ml of packed cells in 20 ml of 5 wt % sucrose) were placed on a 17 to 55 wt % sucrose gradient in the B-XIV rotor, followed by 50 ml of water as an overlay. Since the cells banded very quickly, it was not necessary to accelerate the rotor past 3500 rpm. The results are shown in Fig. 14 and indicate that sharp zones can be recovered far down the gradient. Similar studies at both low and high speeds

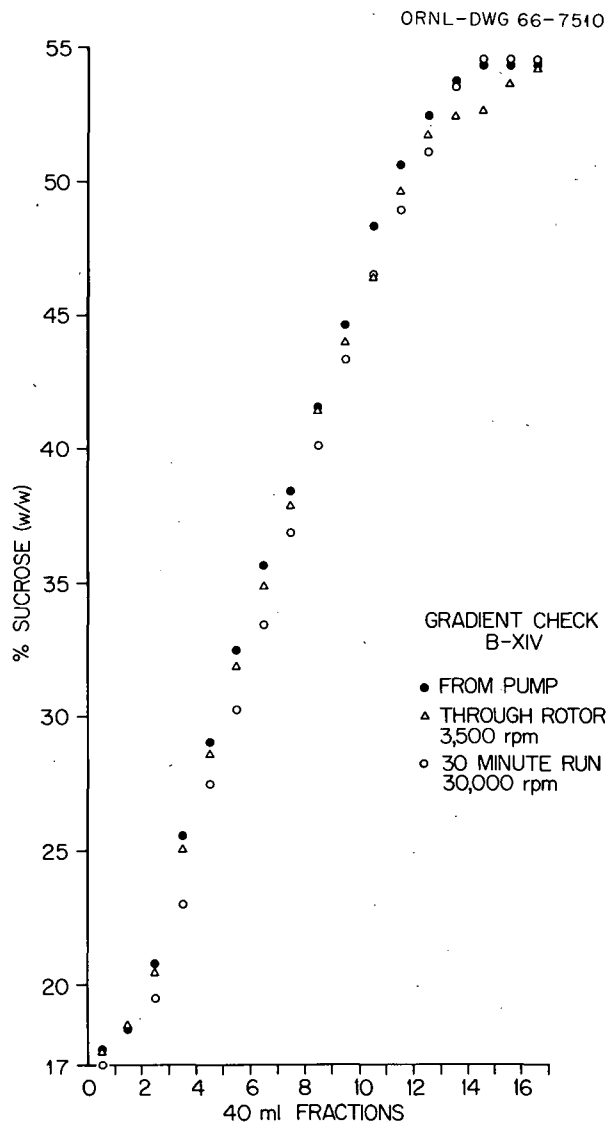


Fig. 10. Evaluation of B-XIV Rotor for Gradient Handling.

have been done in the B-XV rotors with good results. In some instances, however, multiple sharp peaks were observed which suggest that there were small differences in the rates at which different sectors of this rotor were unloaded. To avoid this difficulty, the distance between the outer edge of each septum and the rotor wall was increased at the point where the fluid line from the seal discharges at each septum edge. These results show that the rotor is operating satisfactorily from a purely physical viewpoint.

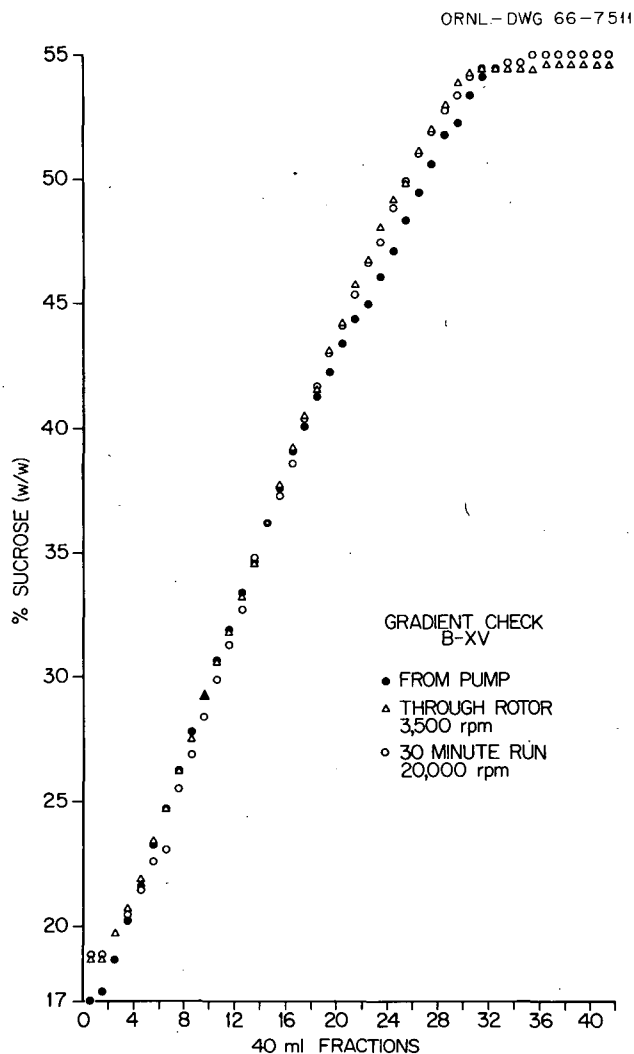


Fig. 11. Evaluation of B-XV Rotor for Gradient Handling.

Evaluation with Biological Test Particles

Ribosomes and ribosomal subunits, in addition to other subcellular particles,¹⁹ have been used as test materials in the B-XIV and B-XV rotors. With a sucrose gradient that was linear with rotor radius and with a sample containing approximately 31.9 mg of *Escherichia coli* ribosomes (partially

¹⁹J. R. Corbett, "Separation of Lysosomes by the B-XV Zonal Centrifuge Rotor," Abstracts, 10th Ann. Meet., Biophys. Soc., p. 90 (1966).

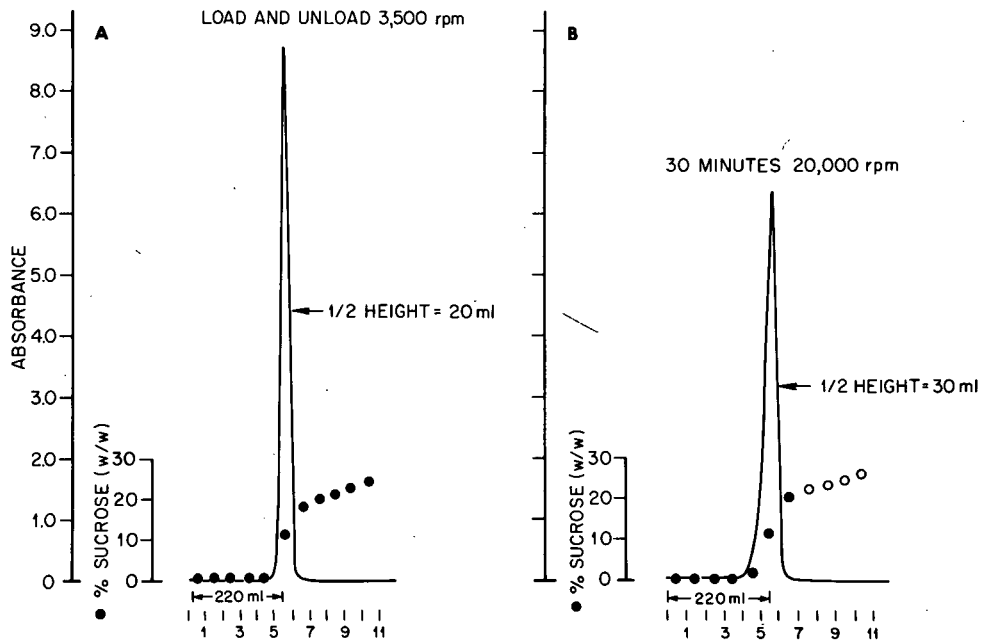


Fig. 12. Degree of Widening of Bovine-Serum-Albumin Sample's Boundary in B-XV Rotor. Sample composition and other details are given in text.

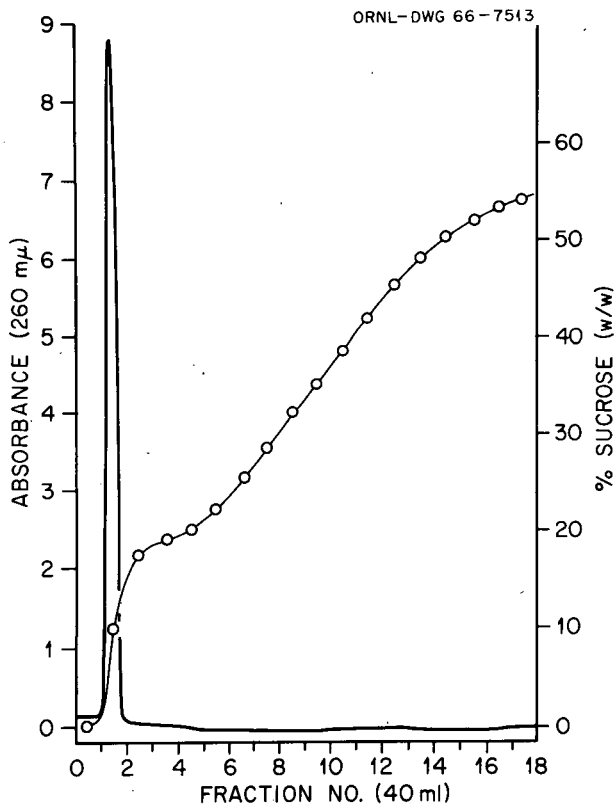


Fig. 13. Recovered Bovine-Serum-Albumin-Sample Zone from B-XIV Rotor. See text for details.

dissociated), the results shown in Fig. 15 were obtained. For this experiment, G_c was $280,460 \times 10^6$, which is equivalent to 17.75 hr at 20,000 rpm. It should be noted that the term G_c represents a direct reading and is calculated in units of 10^6 . Actually, $G_c = \int \omega^2 dt$.

Discussion

Two newly developed zonal centrifuge rotors allow large-volume, rate-zonal, and isopycnic-zonal centrifugation in conventional preparative ultracentrifuges. These rotors are loaded and unloaded at low speed through a seal that is removed for high-speed operation. The rotor may be used for a variety of fractionation problems, including the separation of lysosomal activity from mitochondria.¹⁹

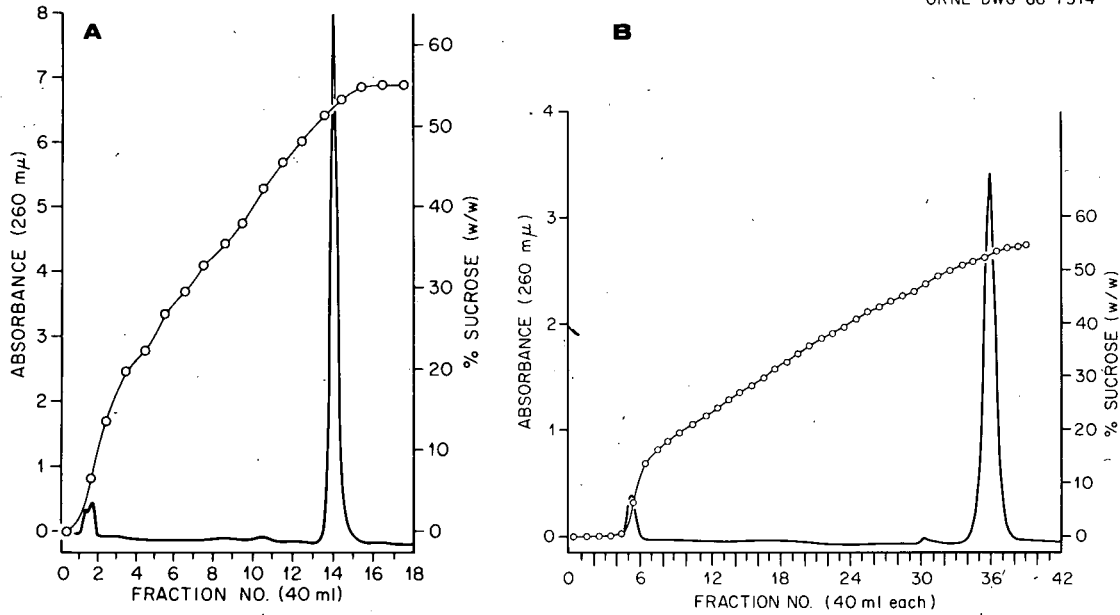


Fig. 14. Recovery of Banded Ragweed Pollen in (a) B-XIV and (b) B-XV Rotors.

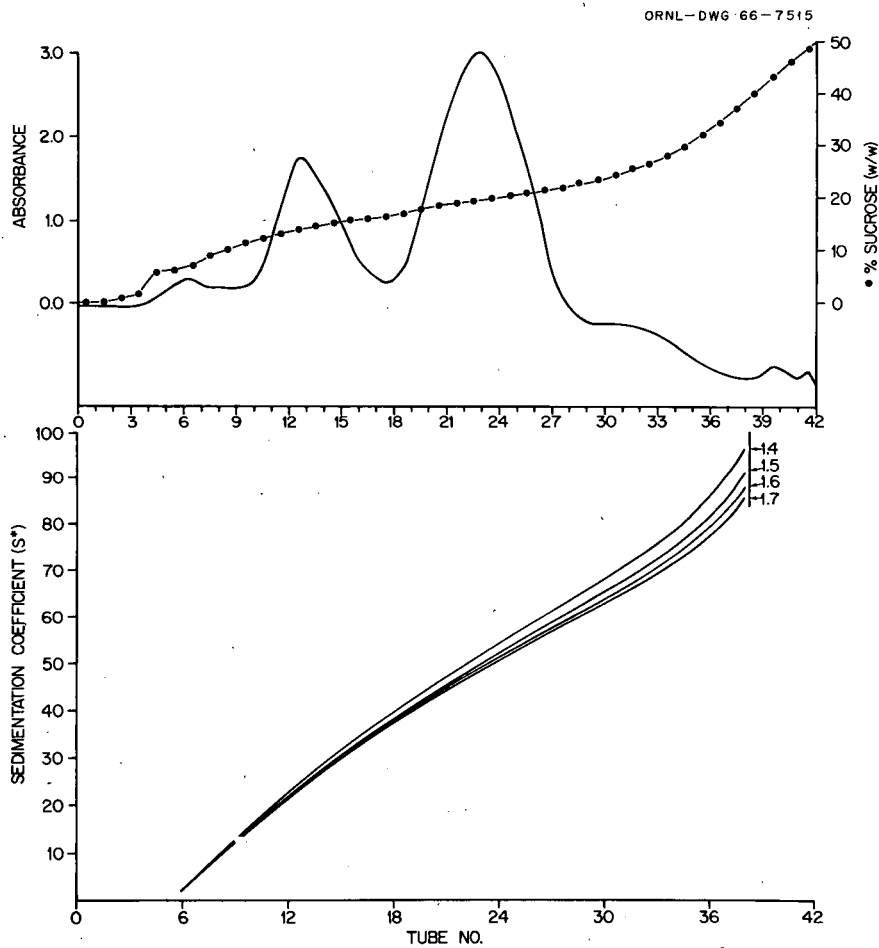


Fig. 15. Separation of Ribosomes and Ribosomal Subunits in the B-XV Rotor. Absorbance was recorded at 260 mμ.

**CALCULATION OF RADIUS AS A FUNCTION
OF VOLUME FOR THE B-XIV
AND B-XV ROTORS**

Elizabeth L. Rutenberg

The object of the following work was the computer calculation of radial distance from the center of a rotor for any fraction of its total volume.

In some cases, areas are calculated for simplicity, and volume is obtained by multiplying the area in question by L , the internal height of the rotor, for liquid or metal.

The metal area of the core and septa which is included in a circular area containing the area of the liquid in question must be calculated to give the corresponding radius r with respect to liquid volume. The x and y coordinates of a septum, with respect to r or the equation for the sloping side of a septum, are formulated in the following way (see Fig. 16):

The equation for a line is:

$$y = mx + c,$$

where

y = y coordinate,

x = x coordinate,

m = slope of line,

c = some constant.

Thus, by transposition

$$c = y_1 - mx_1,$$

and also

$$m = \frac{y_2 - y_1}{x_2 - x_1} = \frac{t - b'}{r_m - b} = -\frac{b' - t}{r_m - b},$$

where $y_1 = b'$, $y_2 = t$; $x_1 = b$, $x_2 = r_m$. From these equations, a computer program can be derived for any number of septa. Since the B-XIV and B-XV rotors have four septa, $b = b'$. For $y_1 = b$ and $x_1 = b$:

$$c = y_1 - mx_1 = b + \left(\frac{b-t}{r_m-b}\right)b = b + \frac{b^2 - bt}{r_m-b} = \frac{br_m - b^2 + b^2 - bt}{r_m-b},$$

$$c = b\left(\frac{r_m-t}{r_m-b}\right).$$

For any value of x and y ,

$$y = mx + c = -\left(\frac{b-t}{r_m-b}\right)x + b\left(\frac{r_m-t}{r_m-b}\right).$$

In general:

$$x^2 + y^2 = r^2.$$

Substituting for y :

$$x^2 + \left[-\left(\frac{b-t}{r_m-b}\right)x + b\left(\frac{r_m-t}{r_m-b}\right)\right]^2 = r^2,$$

$$x^2 + \left(\frac{b-t}{r_m-b}\right)^2 x^2 - 2\frac{(b-t)(r_m-t)}{(r_m-b)^2}xb + b^2\left(\frac{r_m-t}{r_m-b}\right)^2 - r^2 = 0,$$

$$x^2(r_m-b)^2 + (b-t)^2x^2 - 2[(b-t)(r_m-t)]xb + b^2(r_m-t)^2 - r^2(r_m-b)^2 = 0,$$

$$[(r_m-b)^2 + (b-t)^2]x^2 - 2b[(b-t)(r_m-t)]x + b^2(r_m-t)^2 - r^2(r_m-b)^2 = 0.$$

This quadratic equation may be solved for x using

$$x = \frac{-B + \sqrt{B^2 - 4AC}}{2A}, \quad (1)$$

where

$$A = (r_m - b)^2 + (b - t)^2,$$

$$B = -2b[(b - t)(r_m - t)],$$

$$C = b^2(r_m - t)^2 - r^2(r_m - b)^2.$$

We may now solve for x in terms of any radius. If x and r are known, y may be calculated.

The area for $\frac{1}{2}$ septa at a radius r (see Fig. 16) is then calculated:

$$A_1 = \frac{\pi r^2 \tan^{-1}(y/x)}{2\pi} + \text{area of triangle OWY},$$

ORNL-DWG 66-7516

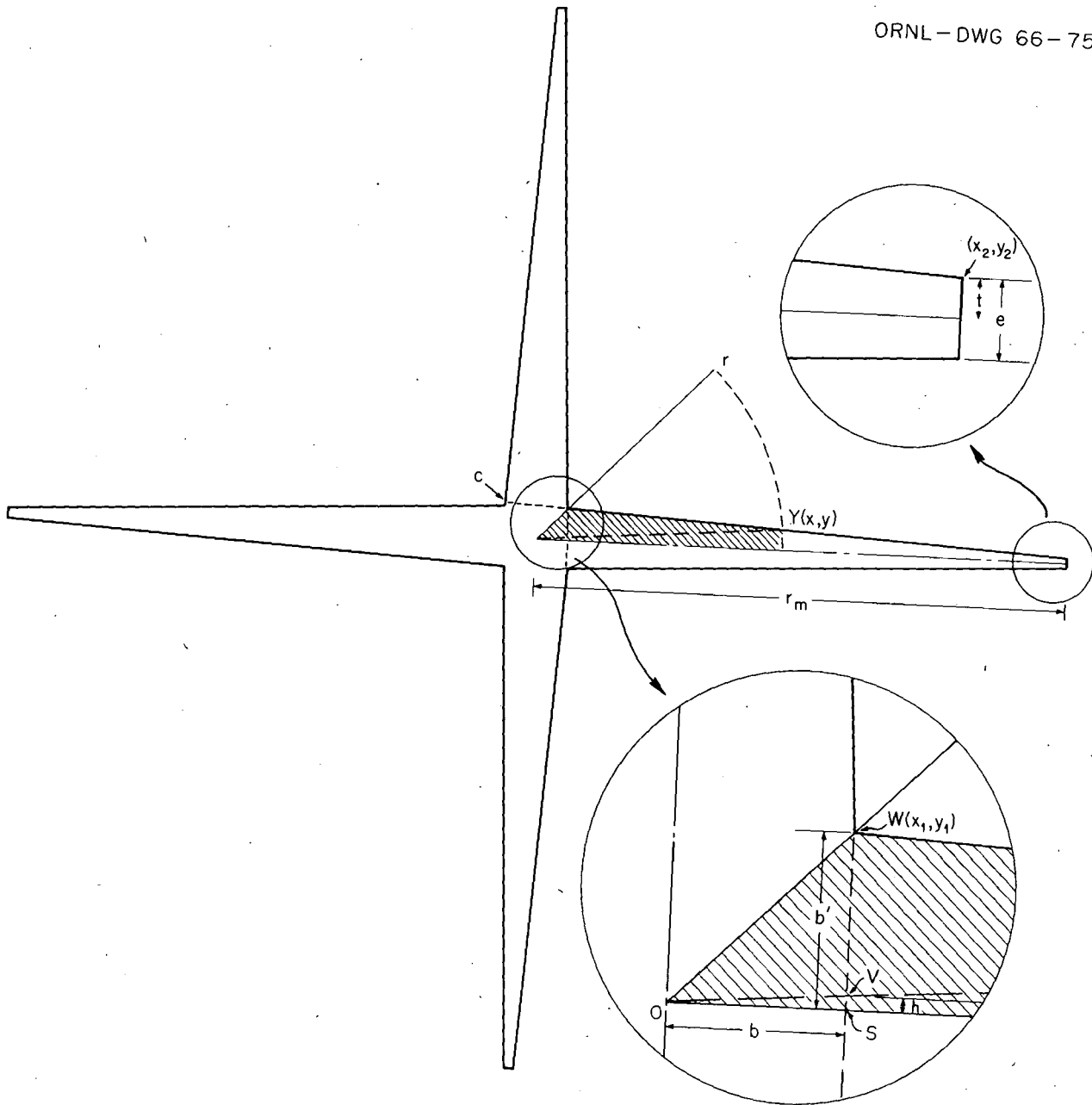


Fig. 16. Derivation of Area of Septum.

$$A_1 = \frac{r^2 \tan^{-1}(y/x)}{2} + \text{area of triangles} \\ (WVY + OWS - OVS), \\ y/x = h/b, \\ h = by/x.$$

The following areas of triangles may be obtained:

$$WVY = (1/2)(b-h)(x-b) \\ = (1/2)[b - (by/x)](x-b), \\ OWS = (1/2)b^2, \\ OVS = (1/2)bh = (1/2)b^2y/x; \\ OWY = WVY + OWS - OVS \\ = (1/2)[b - (by/x)](x-b) + (1/2)b^2 \\ - (1/2)b^2y/x \\ = (1/2)[xb - b^2 - by + (b^2y/x) + b^2 - (b^2y/x)] \\ = (1/2)(xb - by).$$

Thus:

$$A_1 = [r^2 \tan^{-1}(y/x) + bx - by]/2. \quad (2)$$

Since the known volumes (Fig. 17) can be related to known areas by dividing the volumes by the height L of the rotor, we can estimate a radius R for calculation of the actual r .

$$A_2 = A_L + A_S + A_C,$$

where A_C is the metal area of the sloping core and A_L is the liquid area in question.

Actually, the volume of the liquid is partially in the core region since the core tapers; but since the metal volume of the core has been calculated and is constant,

$$\frac{\text{metal volume} + \text{liquid volume}}{L}$$

is the same as $A_C + A_L$. Any volume calculated for radius must exceed the tapered or sloping core.

The circular area A_2 used to estimate r is:

$$A_2 = A_L + A_S + A_C,$$

where A_S is minimum area of a septum (actual septum area will be calculated from a test radius R);

$R^2 = A_2/\pi$ is the first test radius, is used to solve Eq. (1), and enables us to obtain a corresponding test x and y .

Now we can calculate a new area, A_N , where

$$A_N = A_L + A_C + 8A_1, \quad (3)$$

where A_1 is Eq. (2). Since these equations are solved and tested by the computer, this method might not be the best one for manual computations.

With the first calculations:

$$A_N = A_{i+1} \quad \text{or} \quad A_N = A_2, \\ A_i = A_L + A_C + A_S \quad \text{or} \quad A_1 = A_L + A_C + A_S, \\ R_{i+1}^2 = A_i/\pi \quad \text{or} \quad R_2^2 = A_1/\pi, \\ i = 1;$$

so:

$$A_2 = A_L + A_C + 8 \frac{\pi R^2 \tan^{-1}(y/x)}{2\pi} + \frac{bx - ay}{2}.$$

With the second calculation:

$$A_N = A_3,$$

$$R_{i+1}^2 = A_2/\pi.$$

Each time, new x and y values are calculated, which correspond to the estimated R , until A_N is the same as the previous A_N or $A_i = A_{i-1}$ to the sixth digit. At this point $r^2 = A_i/\pi$. This is true because A_{i-1} was used to obtain the R_i from which A_i was calculated. Since $R_i = R_{i+1}$, it is the desired r .

The preceding calculations yield volume vs radius for the cylindrically shaped part of the rotor. Near the rotor wall, the cylinder is rounded off (Fig. 18). The following calculations yield volume vs radius for this remaining part of the rotor.

The volume is divided into two parts - a volume of the difference of two cylinders having radii R_i and r , and a volume generated by forming a half circle of the rounds and revolving the half circle about the rotor center with a radius $R_1 +$ distance to the center of gravity of the half circle.

To calculate the radius corresponding to part of the rounded area, it is necessary to use the center of gravity for a circle or partial circle to find the actual length of the arm of rotation which goes from the center of the rotor to the center (of gravity) of the area.

ORNL-DWG 66-7517

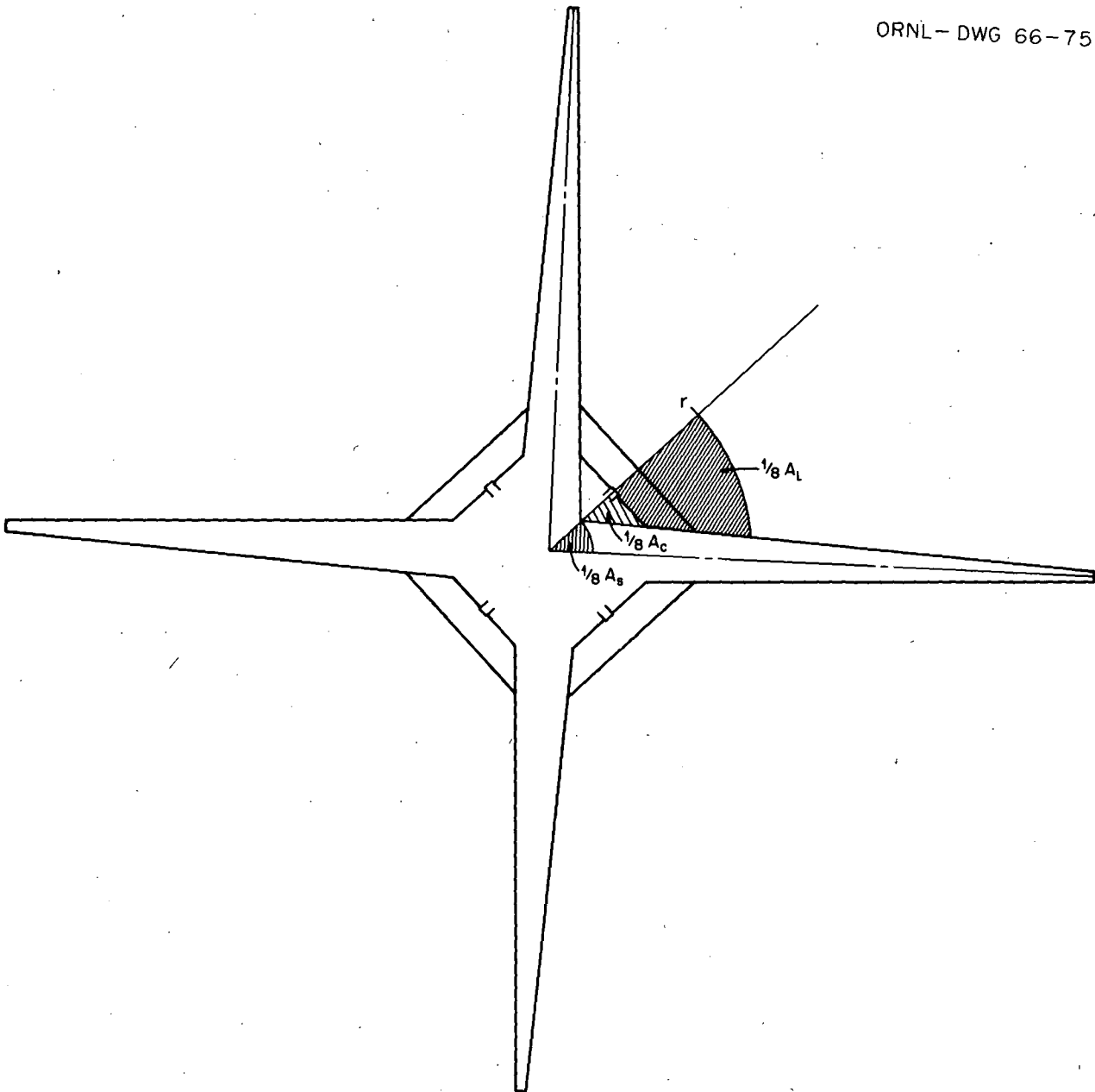


Fig. 17. Computation of Radius Corresponding to a Given Liquid Volume up to Rounded Portion.

ORNL-DWG 66-7518

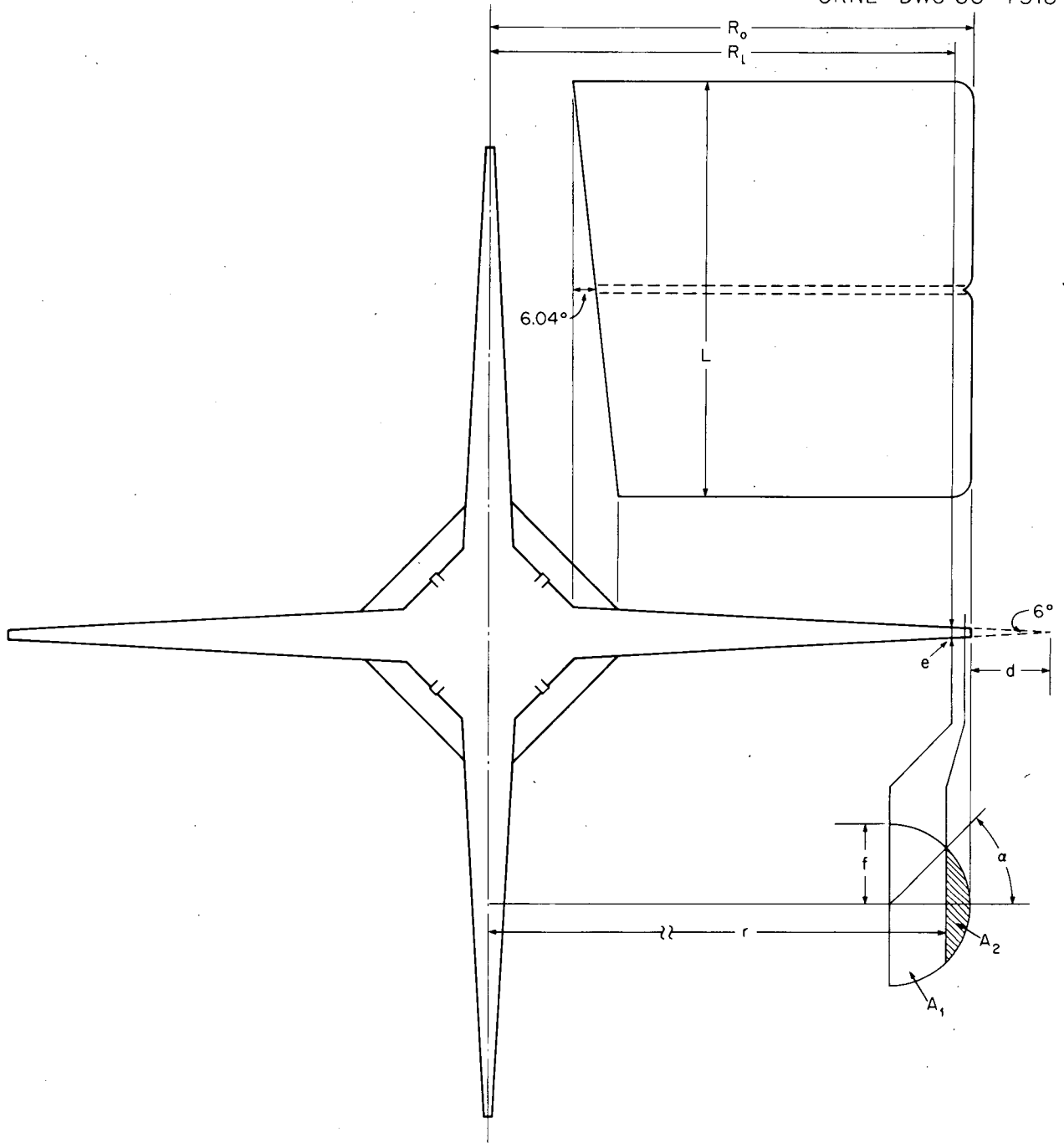


Fig. 18. Computation of Radius Corresponding to a Given Liquid Volume in the Rounded Portion.

The center of gravity b_T for the half circle is

$$b_T = 4f/3\pi, \quad (4)$$

where f is the radius of the circle.

The center of gravity b_2 for a sector is

$$b_2 = (2f^3 \sin^3 \alpha)/3A_2.$$

The volume of liquid for which we wish to calculate radius r is V_1 .

$$V_1 = (V_T - V_2) + V_3 - V_{\text{septa}}, \quad (5)$$

where:

V_T = the volume generated by revolving the entire half circle,

V_2 = the volume of the revolved leftover sector,

V_3 = the cylindrical volume between the two quarter rounds,

$$A_T = \frac{1}{2} \pi f^2,$$

$$V_T = A_T \cdot 2\pi(R_L + b_T) = \pi^2 f^2 \left(R_L + \frac{4f}{3\pi} \right),$$

$$A_2 = f^2 \alpha - \frac{f^2 \sin 2\alpha}{2},$$

$$\alpha = \cos^{-1} \frac{r - R_L}{f},$$

$$V_2 = A_2 \cdot 2\pi(R_L + b_2).$$

To get the average width, w_0 , of the septa for an area determined by r ,

$$w_0 = (e + z)/2,$$

where

$$z = \frac{e}{d + f} (d + R_0 - f \cos \alpha - R_L)$$

and z is the variable width of the septa depending on r . The volume for the septa at radius r :

$$V_{\text{septa}} = 4w_0 [(\pi f^2/2) - A_2] + L(r - R_L),$$

$$V_3 = \pi(r^2 - R_L^2)L.$$

Test radii

$$R_L + \frac{f}{2},$$

$$R_L + \frac{f}{3},$$

and

$$R_L + \frac{f}{4}$$

Table 2. Dimensions of B-XIV and B-XV Rotors

Dimension	Constants	B-XIV	B-XV
1/2 septa tip width	t or $(1/2)e$	0.137 cm	0.145 cm
Radius to beginning of rounds	r_m or R_L	5.712 cm	6.62 cm
1/2 septa width at intersection of septa	b' or b	0.416 cm	0.518 cm
Internal height of rotor	L	5.428 cm	6.638 cm
Radius of round	f	0.952 cm	1.27 cm
Maximum radius	R_0	6.665 cm	8.89 cm
Added length if septa sides intersected	d	1.697 cm	1.501 cm
Volume of metal from rotor center to septa intersection	V_S	2.786 cm ³	4.277 cm ³
Volume of tapered metal core	V_C	30.5 cm ³	32.1 cm ³
Volume of liquid in taper of core	V_{min}	30.4 cm ³	44.2 cm ³
Maximum liquid in rotor	V_{max}	640.3 cm ³	1667.2 cm ³

are used to calculate volumes (Eq. 5). These volumes are compared with the known V_1 's, and if one of these volumes is not the same as V_1 to the eighth digit, the original three estimated radii are divided and volumes calculated. This procedure is continued until a volume is calculated which matches V_1 . The radius used to calculate the match is r . The computer method used for this fit is similar to a curve-fitting method.

Based on information shown in Table 2, curves for rotor volume as a function of rotor radius were obtained. These are shown in Figs. 8 and 9.

IMPROVEMENTS TO B-SERIES ROTOR SYSTEMS

C. E. Nunley

A number of improvements have been made to B-series rotor systems. A one-piece cap and shaft was designed for the B-II rotor, the B-V core was redesigned, the B-IX rotor was designed, and seals have been reworked for the B rotors.

B-II Rotor

Weak points in the design of the B-II rotor²⁰ were detected upon prolonged, frequent use of the system, especially at high speeds. Several mechanical and operational modifications were necessary to improve the reliability of the system under these conditions.

With increased operating speed, higher stresses and higher frequencies tended to loosen the steel shaft pressed into the aluminum upper rotor cap. A loose shaft caused instability in the rotor, excessive seal vibration, and seal leakage. An integrated aluminum cap and shaft were designed with the same spring rate as the combination steel-aluminum cap; thus, no change in damper bearings or other hardware was necessary. The upper end of the shaft has a tapered, press-fitted, steel journal bearing that matches the existing damper bearing and seal system. The one-piece cap-shaft has the same mechanical characteristics as the original two-piece, steel-aluminum cap-

²⁰N. G. Anderson, "The Zonal Ultracentrifuge. A New Instrument for Fractionating Mixtures of Particles," *J. Phys. Chem.* 66, 1984-89 (1962).

shaft. Figure 19 shows the cap-shaft assembled to a rotor.

A straight-through manifold (also shown in Fig. 19) was designed for use with the B-V and B-IX cores, which are used in continuous-flow systems.^{21,22} However, experience has shown that resolution is not adversely affected in rate sedimentation studies with the B-IV system²³ when a straight-through manifold is used. This manifold is more easily fabricated than the cross-over manifold.

B-V Rotor

The prototype B-V core²¹ was a solid aluminum bar weighing approximately 11.75 pounds. The core has been redesigned as a hollow core and weighs 5.25 pounds. The reduction in weight takes some strain off the drive-system bearing, and the core is easier to handle. A complete drawing of the core is shown in Fig. 20.

B-IX Rotor

The B-IX core was designed from information obtained from the prototype B-VIII core.²² The B-IX core, like the B-V core, is hollow to reduce weight.

A drawing of the B-IX core is shown in Fig. 21. Note the $\frac{1}{2}^\circ$ axial taper on the core body and the facets around the circumference of the body. The $\frac{1}{2}^\circ$ taper provides (1) a holdup volume in the rotor that gives the sedimenting particles time to move into the gradient and (2) a funneling effect for the banding particles as the gradient is pushed from the rotor. Since the vanes are an integral part of the core, conventional lathe turning of the core body was impossible. However, because

²¹H. P. Barringer, N. G. Anderson, and C. E. Nunley, "Design of the B-V Continuous-Flow Centrifuge System," in *The Development of Zonal Centrifuges and Ancillary Systems for Tissue Fractionation and Analysis*, ed. by N. G. Anderson, Mono. 21, J. Natl. Cancer Inst. Mono. Ser., 1966.

²²N. G. Anderson *et al.*, "Continuous-Flow Centrifugation Combined with Isopycnic Banding: Rotors B-VIII and B-IX," in *The Development of Zonal Centrifuges and Ancillary Systems for Tissue Fractionation and Analysis*, ed. by N. G. Anderson, Mono. 21, J. Natl. Cancer Inst. Mono. Ser., 1966.

²³N. G. Anderson *et al.*, "The B-IV Zonal Ultracentrifuge," *Life Sci.* 3, 667-71 (1964).

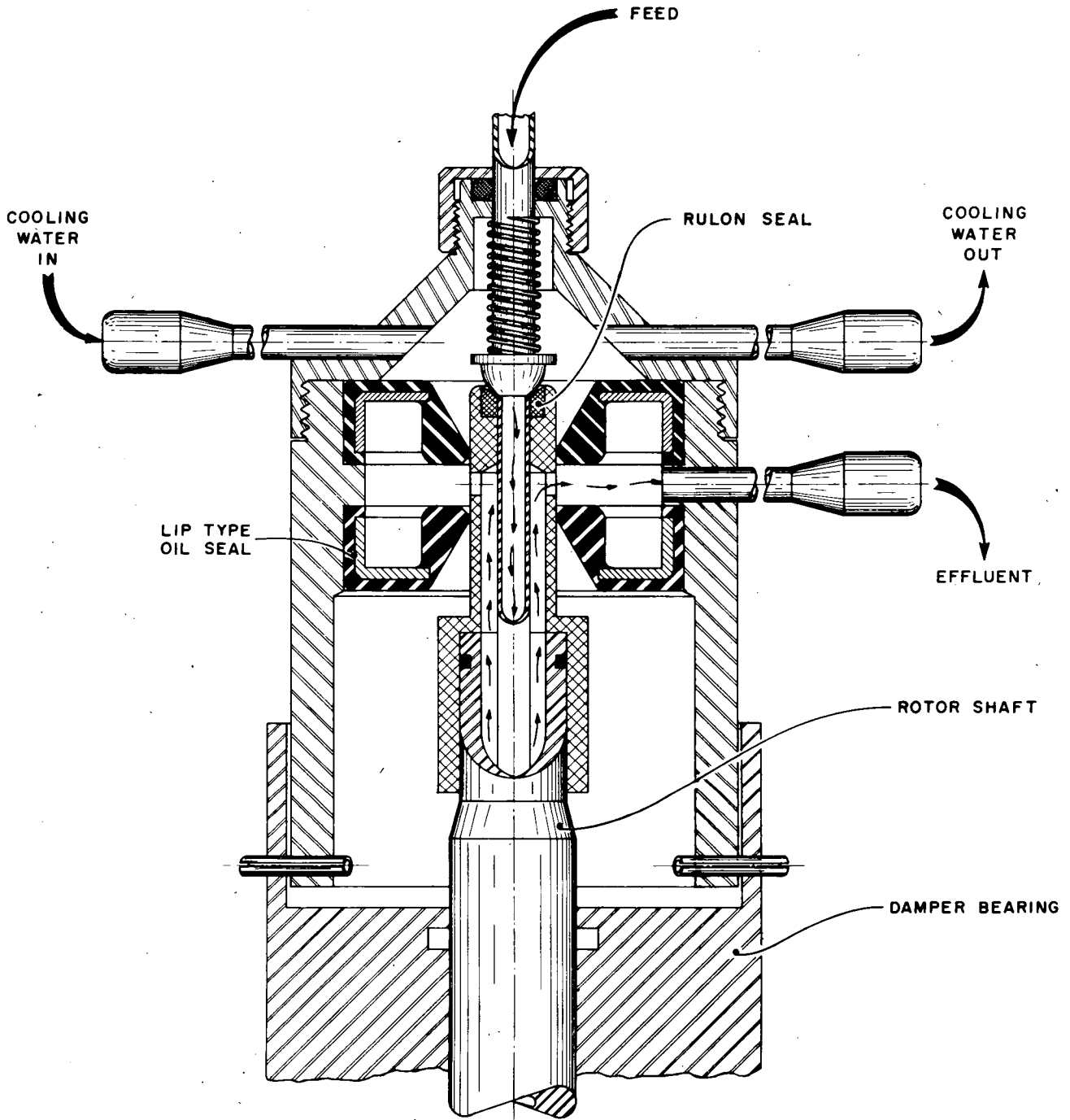


Fig. 19. One-Piece Cap-Shaft Assembled with Rotor End Core.

ORNL-DWG 66-7519

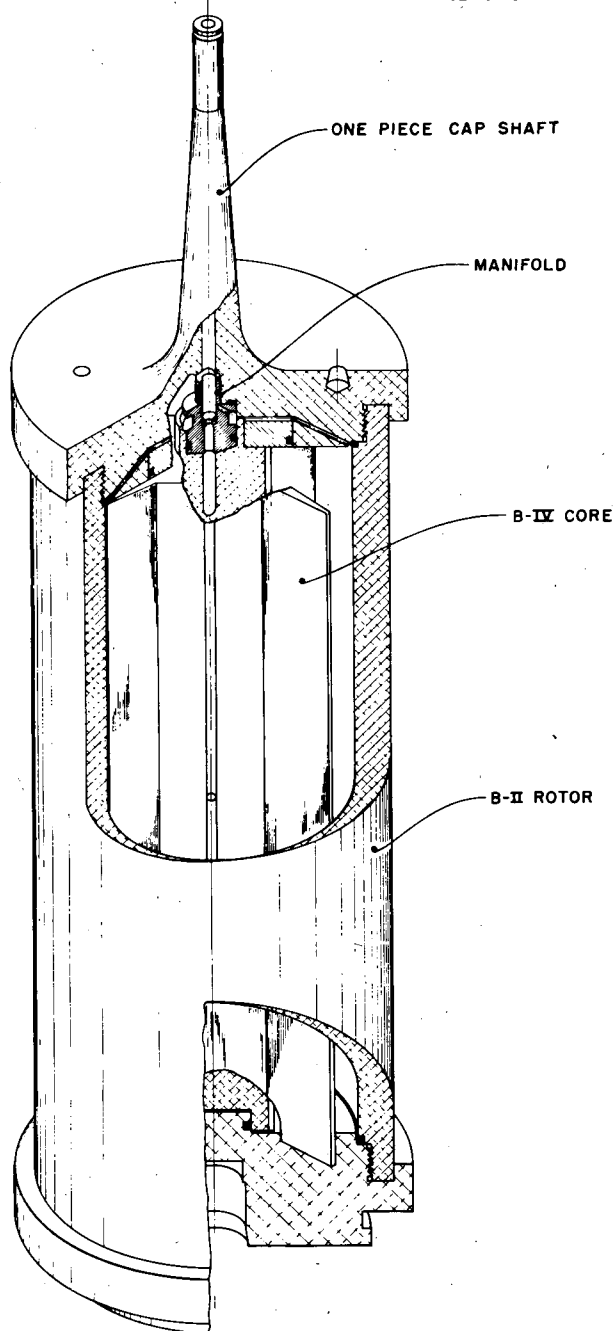


Fig. 20. The Redesigned B-V Rotor Core.

a circular or near-circular core body was desirable for equal distribution of the fluid flowing over the gradient, a compromise was reached by machining the core body with 76 facets and integral vanes. The vanes were desirable for operator convenience, and more important, the weight of the vanes in a high centrifugal field was supported by the core rather than by the highly stressed rotor wall.

Seals

B-Type Seal. — The long stem of the B-type²¹ seal assembly reached its natural frequency at approximately 28,000 rpm. The vibration of the resonating stem disturbed the rotating seal faces and sometimes caused leakage. To reduce the amplitude of the vibrating stem, a metal spider-like device has been attached to the steel stem with the arms engaging the inner surface of the hollow rotor shaft. Satisfactory operation of the hollow seal has been obtained with this modification.

New Seal Design. — The search for a high-speed seal that will be less vulnerable to accidental damage, less expensive to maintain, and more reliable is continuing. Oil seals that are resistant to operate on a shaft are inexpensive, resistant to accidental damage, and easy to replace; however, little data are available concerning their reliability in liquids other than oil at high surface speeds.

A seal has been designed (Fig. 22) to investigate the performance of lip-type oil seals in the zonal centrifuge. The seal was designed primarily for continuous-flow centrifugation. The fluid was pumped into the rotor through a spherical metal seal mated with Rulon. The spherical seal was very insensitive to fluid line pressure; therefore, spring loading and frictional heat could be kept to a minimum. The effluent was contained by two oil seals. Pressure on the oil seals was limited to 10 psi, an adequate pressure for loading and unloading a gradient. This seal has had very limited testing, but the results look promising. No leakage was observed up to 25,000 rpm, but excessive heating in the oil seals prevented testing at higher speeds. Modification and testing will continue.

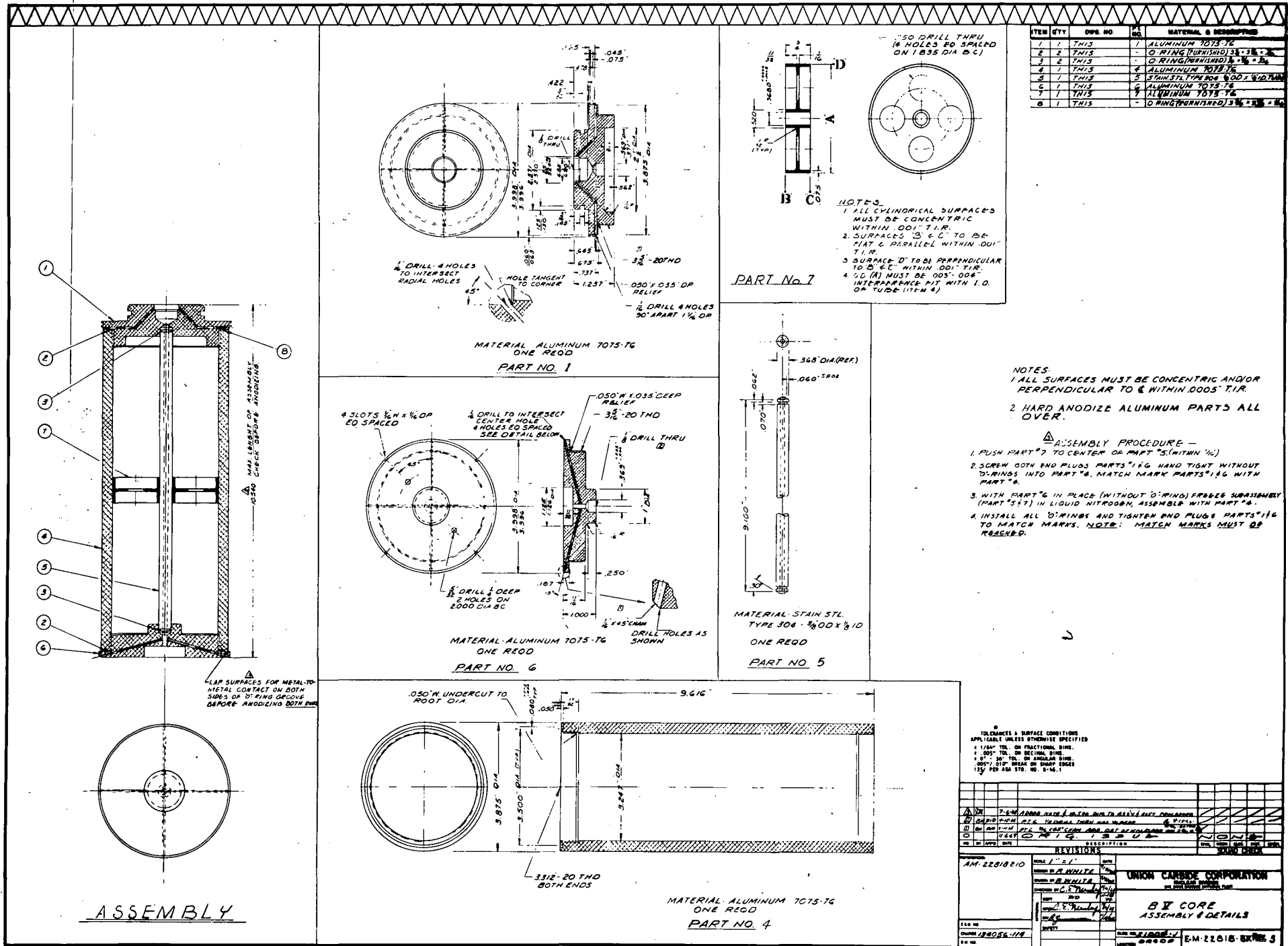


Fig. 21. Design of B-IX Core.

3. Continuous-Flow Centrifuges for Large-Scale Virus Isolation

The K-series zonal rotors are a part of the second generation of centrifuge systems for the isolation and concentration of small particles. Rotors of this type may be used for rapid processing of large volumes of virus suspensions and are of interest to various commercial firms for use in vaccine production. The K-I prototype was primarily a proof-of-principle rotor. The K-II rotor was the first of the series designed to do a specific task.

THE K-I ZONAL ROTOR

G. B. Cline D. A. Waters
R. F. Gibson N. G. Anderson

The K-I rotor is a prototype continuous-flow rotor of the B-IX design which operates in the conventional air-driven Sharples centrifuge. It was not designed for production capacities of materials, but it is useful for volumes of solution up to 10 liters where the total content of suspended solids is a few milligrams.

Materials and Methods

Simplicity of operation and maintenance is of greater importance in the design of a production-scale system than in the design of a research-oriented one. The only changes made in the Sharples centrifuge system were to the rotor and its bottom damper-bearing assembly (Fig. 1). Design speed for the rotor was 50,000 rpm, and it held 240 ml of liquid. Stress calculations indicated that speeds of the order of 60,000 rpm were safe; however, the characteristics of the drive system at speeds over

50,000 rpm are not known. Yield strength of the titanium alloy used was 137,000 psi, and at 50,000 rpm the safety factor of the bowl armor is approximately 3.2.

Friction damping in the bottom bearing allowed the rotor to spin freely about its own axis during changes of center of rotation caused by rotor contents. The damper took a minimum of energy out of the spinning rotor, and characteristic vibration amplitudes of a properly designed rotor were satisfactory. The bottom bearing was lubricated by applying a small amount of light grease to the shaft before each run. Typical runouts of the rotor as a function of speed, as well as the mode shapes of the two rotor critical speeds, are shown in Fig. 2. It was noted that precession from the more dominant first rigid-body critical of the rotor was re-excited at higher operating speeds when the friction damper at the bottom of the machine seized.

The rotor was loaded and unloaded along the same fluid path. Initially, a buffer solution or water was introduced through a feed jet to a 0.25-in. tube running through the center of the core. The fluid passed up the central hole to the top of the core and was centrifuged to the rotor wall. Half of the rotor volume was filled in this manner, then a dense solution was pumped in by the same route to fill the rotor. The sample solution also followed this path, eventually leaving the rotor through the shaft exit holes at the bottom of the rotor. A hydrostatic pressure of about 30 in. of water was sufficient to obtain flow rates to 4 liters/hr; however, optimum flow rates for desired cleanout must be determined for each type of particle. The density gradient was removed from the rotor by pumping more displacing solution to the rotor wall, thus backing the density gradient and its banded particles out through the shaft exit

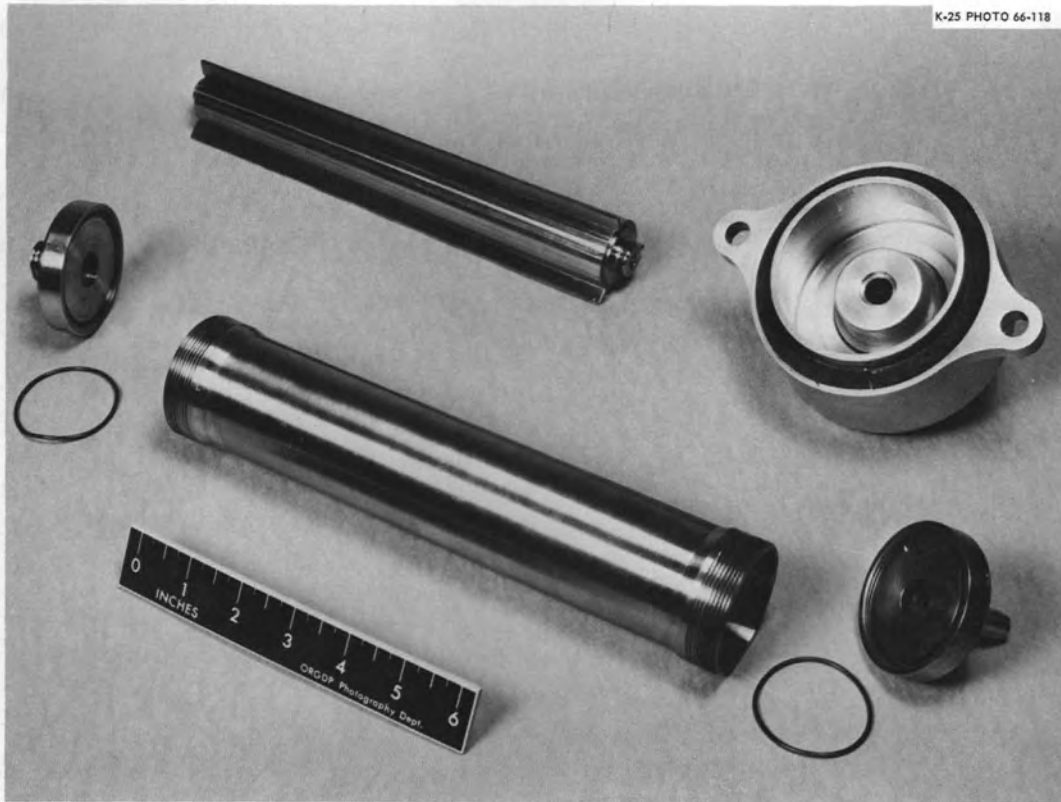


Fig. 1. K-1 Zonal Rotor and Seal for Sharples Model TI-P Centrifuge.

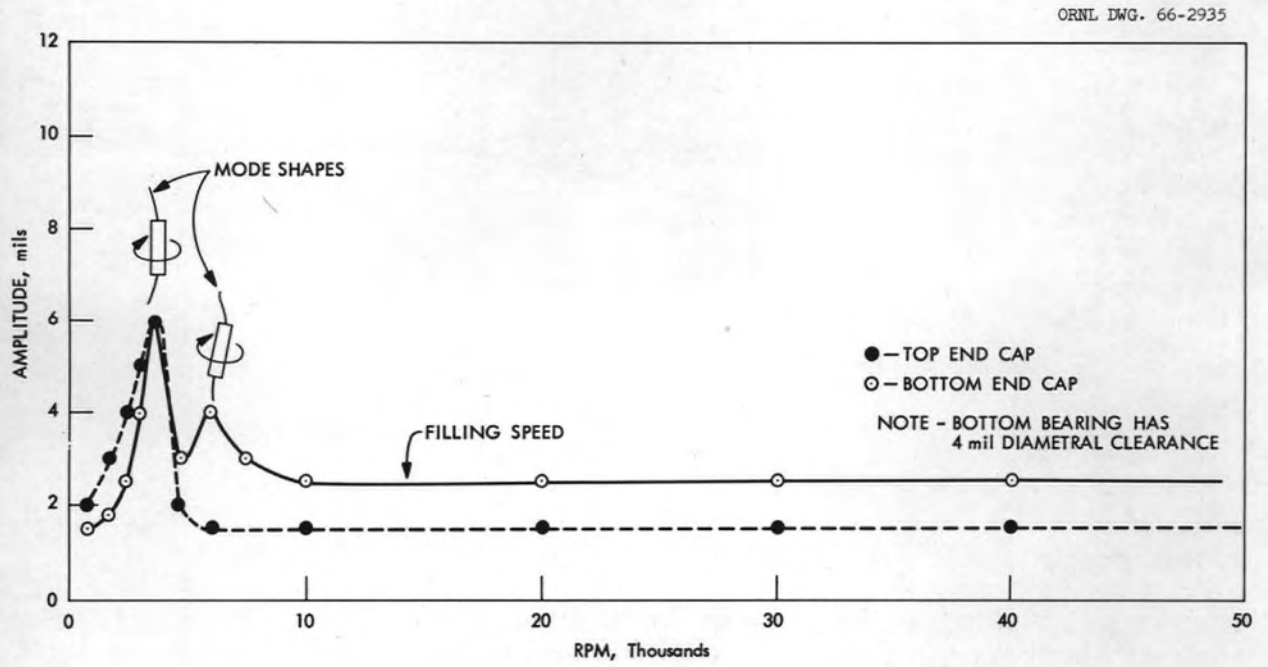


Fig. 2. Approximate Per-Revolution Runout of Titanium K-1 Rotor.

holes. As the gradient left these holes, it was funneled through the collection chamber and drain line into fraction tubes. Physical properties of the gradient may be monitored if the air is bled from the effluent stream. When decelerated to rest, the rotor drained by gravity.

Results

The results of cleanout and banding of ragweed pollen in a sucrose density gradient are shown in Fig. 3. A density gradient of sucrose was recovered from the rotor, and the pollen was concentrated in a zone within the gradient. The results of two cleanout experiments using Type 3 bacteriophage and lysate are shown in Fig. 4. The efficiency of cleanout at each flow rate was based upon the amount of virus remaining in the effluent stream after the flow rate had been established. It is apparent from these results that the K-I rotor can be used effectively for the isolation of T3 bacteriophage from fluid volumes in the liter range.

Ragweed pollen was banded into a zone within the sucrose density gradient. However, T3 phage was not banded into a distinct zone in a cesium chloride gradient even after an hour or more after completion of flow-through. Analysis of the gradient in such runs indicated that the displacing material was mixing with the gradient. Studies using sucrose gradients gave similar results.

The rotor core was modified to reduce the amount of mixing during unloading of the density gradient. A baffle arrangement ensured that the dense material migrated directly to the rotor wall. Mixing of the displacing solution with the gradient was thus limited to the swirling of the displacing solution as it flowed down the rotor wall, and the presence of the baffle limited this swirling action.

Although it could be shown that little or no mixing of displacing and gradient solutions occurred, no information is available yet to indicate that virus bands can be isolated without mixing. Banding studies with T3 phage in CSCI are under way. If these studies show that a zone of T3 can be

ORNL DWG. 66-2936

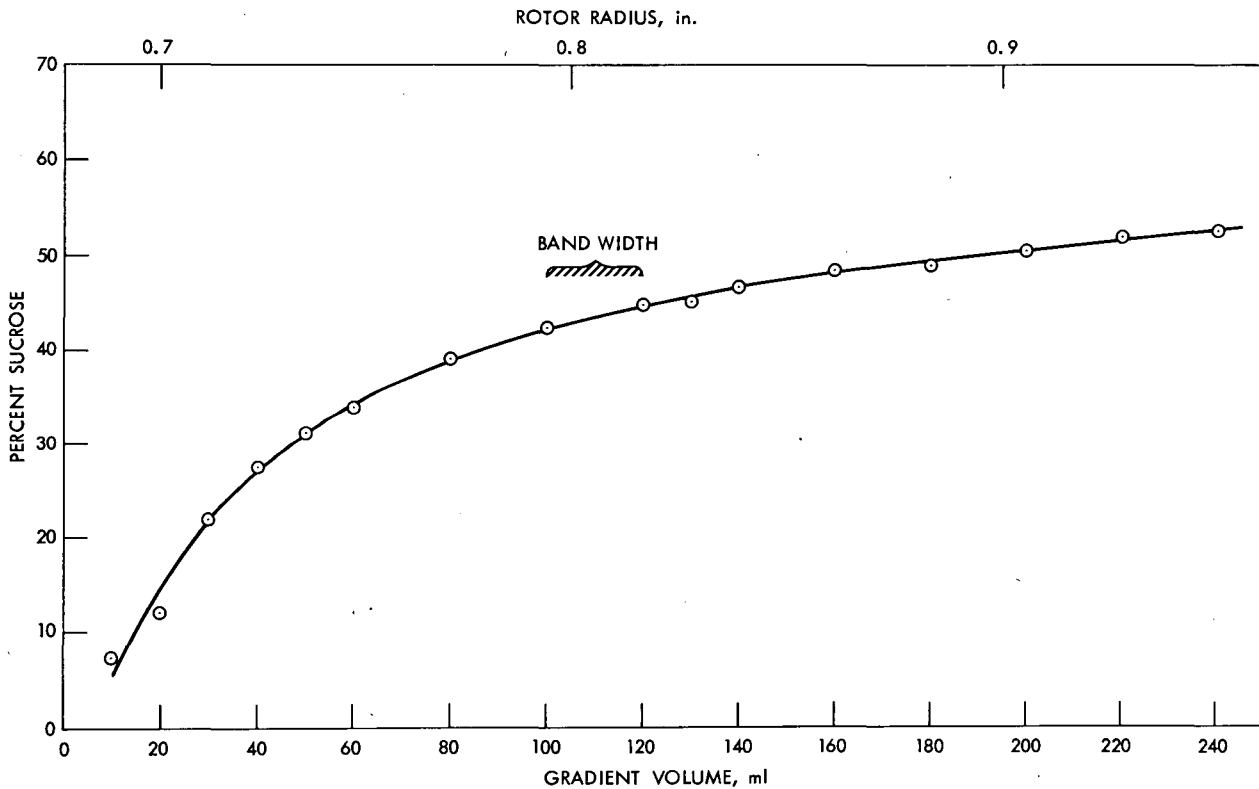


Fig. 3. Continuous-Flow, Isopycnic Banding of Ragweed Pollen in the K-I Rotor at 42,000 rpm.

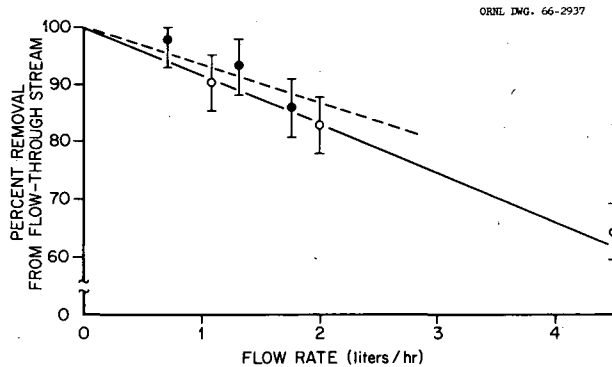


Fig. 4. Type 3 Bacteriophage Removal from Flow-Through Stream in the K-I Zonal Rotor as a Function of Flow Rate. The dashed and solid lines represent two experiments. The variability of results of the plaque assay of the T3 is estimated to be at least 15%. The solid line represents one experiment in which the starting time of T3 phage was 7×10^9 plaques per milliliter. The dotted line is a second experiment in which the titer was 1×10^9 per ml. Two liters of lysate were used in each experiment.

recovered after the flow-through operation, additional studies will be carried out at Eli Lilly and Company to determine whether flu virus can be isolated and recovered with this rotor.

These preliminary experiments with the K-I rotor indicated that production versions of this type of rotor might be used for vaccine production.

THE K-II ZONAL ROTOR

N. G. Anderson D. A. Waters

The success of the preliminary studies with the K-I rotor indicated that zonal rotors that combine the functions of continuous flow with isopycnic banding could be built to operate in a variety of centrifuges; however, the size of the K-I rotor limited its use in large-scale virus isolation. It was of considerable interest, therefore, to design a centrifuge rotor that would effectively do the work of several K-I rotors and, in addition, be simple in design and operation, low in cost, and work with either electric or turbine drives. The large-volume K-II rotor was designed to do a specific task: isolation of large viruses of low density

such as those of the myxovirus type. As the need arises, other production rotors may be designed to solve other specific separation problems.

Requirements and Limitations

The basic requirements of the K-II rotor system are listed in Table 1. Complete removal of virus particles from the flow-through zone was desirable, particularly for viruses growing to relatively low titers. The choice of a 10-liters/hr flow rate was arbitrary, although a machine of this capacity is already required. Other parameters were chosen to obtain optimum large-scale isolation of virus. A density of 1.193 was the observed banding density of flu virus in sucrose density gradients.

To evaluate the various possible types of continuous-flow rotors that could fulfill the goals of this machine, the comprehensive design curves shown in Fig. 5 have been prepared. These design curves are based on the chosen data in Table 1. The design curves may be scaled for any desired flow rate by means of the relation:

$$Q = L_e r_s^2 N^2, \quad (1)$$

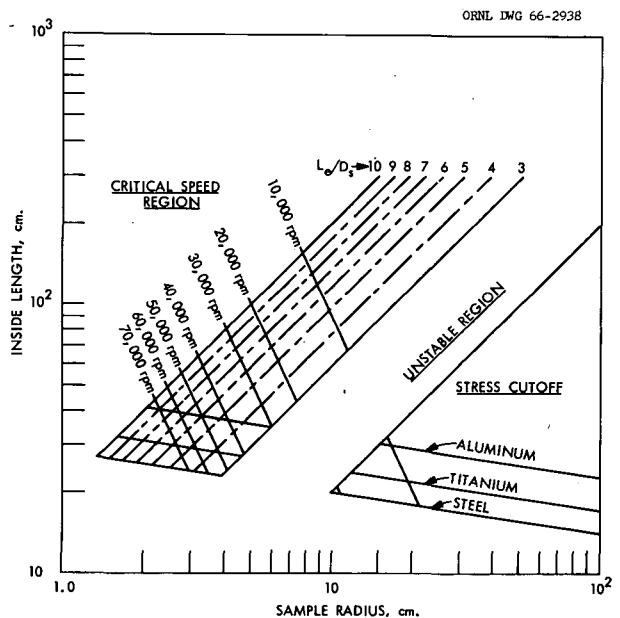


Fig. 5. Length, Speed, Sample-Zone Radius, and Weight of Rotor Required for 100% Cleanout of Virus at 10-Liters/hr Flow Rate. See Table 1.

Table 1. Performance Specifications for Design of K-II Rotor System

Parameter	Value
Cleanout from sample zone, %	100
Flow rate, liters/hr	10
Sample zone viscosity, poise	0.0152
Sample zone density, g/cm ³	1.05
Virus diameter, cm	8.2×10^{-6}
Banding density in sucrose, g/cm ³	1.193

where

L_e = effective rotor length,

r_s = outboard sample radius,

N = speed in rpm.

Five limitations were imposed on the K-II design: the rotor should

1. operate below its fundamental flexural critical speed,
2. be stable,
3. operate at some reasonable stress level,
4. be light enough so that one person could easily handle it and disassemble it for routine maintenance, and
5. be able to maintain a constant temperature.

The first three limitations are shown as areas in which a design is not allowed, and the fourth is indicated by the diagonal, dashed lines in Fig. 5. The unstable region is not an area where the rotor is truly unstable, but one where it is more difficult to design rotors for smooth operation because of problems with demands on the damper and suspension systems.

The rotor should be contained in a vacuum jacket to avoid overheating by wind friction. This friction (windage) became apparent when the horsepower lost (shown in Fig. 6) was related to the area of

interest in Fig. 5. Approximately $3\frac{1}{2}$ horsepower would be lost due to windage for any rotor in this region at atmospheric pressure — an intolerable condition for both the drive and the rotor contents.

Another practical limitation was speed. Although the maximum operating speed shown in Fig. 5 is well within the state of the art, there are not as many commercially available drives in this speed range as in lower speed ranges. By choosing higher rotor speeds, one makes a higher capital investment and at the same time loses some design flexibility. Therefore, the rotor system should be designed to operate at a speed consistent with the other design limitations and cost.

A secondary, but important, consideration with regard to the design flexibility was overspeed capability and its effect on the machine capacity. Note that the speed represented in Fig. 5 was not the maximum possible operating speed, but the speed required to permit 100% cleanout of flu virus at 10-liters/hr flow rate at the indicated rotor length and radius.

Design of the K-II Rotor

With the above limitations in mind, the design of the rotor was fixed with a sample radius of 5 to 6.5 cm, an operating speed of 25,000 to 30,000 rpm, an overspeed capability of about 40,000 rpm, and a maximum weight of 75 lb.

Four types of drives will operate under the speed and load conditions of the K-II rotor: air turbine, oil turbine, low-speed electric motor with speed increaser, and high-speed electric motor. All of these methods have been used successfully to drive high-speed centrifuges. It is probable that either a direct motor drive or an air turbine would be the most economical drive system. A choice depends primarily on the number of machines anticipated at a facility and the availability of compressed air. If a good supply of compressed air is already available, an air turbine would be clearly the most attractive choice.

ORNL DWG. 66-2939

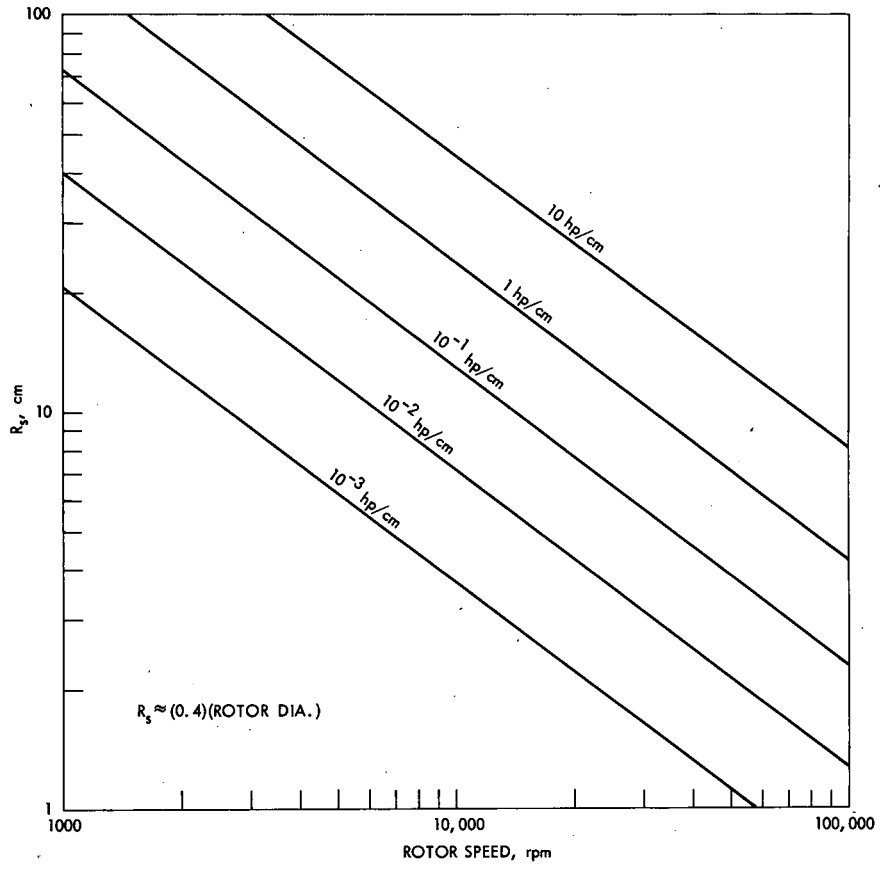


Fig. 6. Horsepower (per cm of Length) Required to Spin a Rotor in Air.

4. Advanced Rotor Concepts

HIGH-SPEED DRIVE SYSTEMS

H. P. Barringer

Production of high centrifugal fields requires high-strength rotor materials and high angular frequencies. Present centrifuges are limited by existing materials and low design frequencies. Thus, to obtain higher forces, we need higher frequencies when using present materials.

To find the useful maximum frequency or speed of a new drive system, the following items were considered:

rotor size and volume,
available hardware and development cost,
operational techniques,
reliability,
maintenance,
cost of a machine for small production runs,
largest step to be taken in the state of the art of high-speed systems,
power levels required, and
acceleration and braking rates of the rotor.

Major Requirements and Objectives

The preliminary design requirements were surveyed in three categories: (1) direct turbine drive by air and by oil, (2) direct motor drive, and (3) low-speed motor with speed increaser. Recent developments in power-transmission equipment show that the third category will have attractive advantages over other drive systems for use in biological laboratories.¹

¹F. J. Lavoie, "Unique Planetary Reducers Whirl at Super Speeds," *Machine Design* 37, 198-200 (1965).

The major objectives of the high-speed system were:

1. Maximum reliability should be attained with fluid-film bearings for 1000-hr operation at 150,000 rpm, or 1000-hr runs with overspeed capabilities of 200,000 rpm for less reliability.
2. All operating controls should be simple and reliable so they can be used by a trained, nonmechanically oriented laboratory technician.
3. The vertical high-speed spindle should extend upward for placing rotors, made by various vendors, on the quill.
4. Rotor speed should be capable of being set between 3,000 and 150,000 rpm. Speed control of the rotor should be ± 200 rpm over the speed range of 10,000 to 200,000 rpm. Speed control should be ± 400 rpm, from 3,750 to 10,000 rpm.
5. The drive system should be a standard, constant-torque (4000-rpm base speed) dc motor to which is attached a 50:1 speed increaser. The speed controller should be a solid-state device.
6. The drive system should be flexibly connected to a high-speed spindle that carries the rotor thrust and radial loads. The spindle should be equipped with a variable damping device which should be adjustable for different-sized rotors.
7. Acceleration and deceleration of the rotor could be accomplished in at least six different rates between 0 and 100% of rated motor capacity.
8. The rotor weight carried by the spindle could vary from $\frac{3}{4}$ to 50 lb. The spindle should be capable of handling 0.100 in. total indicator reading displacements of the rotor.
9. The vacuum system should rapidly evacuate the chamber to at least 1 μ in less than 5 min.

10. The refrigeration system should have proportional controls for sensing the rotor temperature and regulating the rotor temperature to $\pm 1^\circ\text{C}$.
11. Ancillary services such as air at high pressure, chilled water, sanitary water, oil, and electrical outlets should be provided at the working counter top of the centrifuge.
12. The system should be operable as an analytical or preparative centrifuge by the addition of miniature modules.

Design of the High-Speed System

Drive and Related Equipment. — A 4000-rpm-base-speed, constant-torque, $7\frac{1}{2}$ -hp, series-wound dc motor equipped with an integrally mounted ac tachometer was attached to a 50:1 speed increaser, permitting normal operation over the range of 3,000 to 150,000 rpm with overspeed capability to 200,000 rpm. The transmission operated at approximately 95% efficiency.

The high-speed spindle was connected to the transmission through a small, flexible quill. The spindle was equipped throughout with fluid-film bearings. Conventional journal bearings carried the radial loads, while a tilting pad thrust bearing carried the thrust loads. The bearings were lubricated by MIL-L-7808C oil, which has excellent lubricity, low viscosity, and extremely low vapor pressure.

A damping device, which was adjustable from outside the vacuum system, permitted optimum damping to be set for each rotor size and weight. A free, damped, vibration logarithmic decrement of about 0.6 was attempted. The spindle was fabricated and tested. The bearing spindle has adaptors that could be fitted between standard rotors made by other vendors and the drive quill; this gave more versatility than existing commercial centrifuges.

Centrifuge Housing. — The vacuum, refrigeration, and control equipment were installed in the cabinets. A small annunciator system was used to monitor the various interlocks and safety devices for more rapid use of the system. Since many lengthy centrifugation periods will be appreciably reduced when the drive is operated at 150,000 rpm, rapid acceleration of the system to

operational condition will be necessary for high-speed operation. Thus, extra capacity was added to vacuum, refrigeration, and monitoring equipment in order to expedite centrifugation. Preliminary tests with the vacuum system showed that a vacuum better than $1\ \mu\text{ Hg}$ could be obtained in less than 3 min.

Rotor Sizes

When a particular drive system has been chosen, an estimate of the rotor size can be made to cover a wide area of construction. Some information is presented below to characterize zonal centrifuges and other tubular rotors. Similar information can be derived for angle-head rotors.

The following design information is based on the use of Maraging steel at a 260,000-psi stress level in the centrifugation of dense cesium chloride. Two kinds of rotors are assumed: a long rotor with an inside-length-to-inside-diameter ratio of 8:1 and a short rotor with a ratio of 0.4:1.

From strength considerations,² we assume that the inside radius and wall thickness for both the long and the short rotors are:

$$a = 1.25 \times 10^5 / N$$

and

$$t = 0.288 \times 10^5 / N,$$

where a is the inside rotor radius (in.), t is the optimum wall thickness (in.), and N is the rotor speed (rpm). Thus, the lengths of the long and the short rotors are, respectively:

$$L = 16a = 20 \times 10^5 / N$$

and

$$L = 0.8a = 1 \times 10^5 / N.$$

The weight of each end cap (assuming the cap thickness equivalent to the wall thickness) is

$$W_{\text{cap}} = \pi(a + t)^2 t \rho = 0.62 \times 10^{15} / N^3.$$

²H. P. Barringer, *Joint NIH-AEC Zonal Centrifuge Develop. Program Semiann. Progr. Rept. Jan. 1-June 30, 1963*, ORNL-3502, p. 20.

The weight of rotor tube material is

$$W_{\text{tube}} = \pi[(a+t)^2 - a^2]L\rho,$$

so that

$$W_{\text{tube}_{LR}} = 14.7 \times 10^{15}/N^3$$

and

$$W_{\text{tube}_{SR}} = 0.735 \times 10^{15}/N^3.$$

The subscripts LR and SR designate the long and short rotors respectively. The weight of the rotor fluid is

$$W_{\text{fluid}} = \pi a^2 L \rho = 0.229 \times 10^{10} L / N^2,$$

so that

$$W_{\text{fluid}_{LR}} = 5.98 \times 10^{15}/N^3$$

and

$$W_{\text{fluid}_{SR}} = 0.299 \times 10^{15}/N^3.$$

Thus, the total weight for a long rotor and a short rotor is:

$$W_{LR} = 21.9 \times 10^{15}/N^3$$

and

$$W_{SR} = 2.27 \times 10^{15}/N^3.$$

These curves are shown in Fig. 1, with the limits of 50 lb maximum weight and 150,000 rpm maximum speed enclosing the design area.

The inside rotor length and radius are shown in Fig. 2. Figure 3 shows the maximum internal rotor volume, while Fig. 4 shows that the maximum g 's produced were

$$g_{\text{max}} = a\omega^2/g = 0.284 \times 10^{-4} a N^2 = 3.55 N.$$

A centrifuge constitutes a high inertia load that must be driven to rated speed, so an estimate of the expected rotor inertias must be determined to find acceleration times. The polar moment of inertia (I) of each end cap is:

$$I_{\text{cap}} = (W_{\text{cap}}/2g)(a+t)^2 = 1.92 \times 10^{22}/N^5.$$

The moment of inertia of the rotor tube is:

$$I_{\text{tube}} = (W_{\text{tube}}/2g)[(a+t)^2 + a^2] \\ = (6.39 \times 10^7 - W_{\text{tube}})/N^2,$$

so that

$$I_{\text{tube}_{LR}} = 93.9 \times 10^{22}/N^5$$

and

$$I_{\text{tube}_{SR}} = 4.69 \times 10^{22}/N^5.$$

The moment of inertia of the fluid is

$$I_{\text{fluid}} = (W_{\text{fluid}}/2g)a^2 = (0.00203 \times 10^{10}/N^2)W_{\text{fluid}},$$

so that

$$I_{\text{fluid}_{LR}} = 12.1 \times 10^{22}/N^5$$

and

$$I_{\text{fluid}_{SR}} = 0.606 \times 10^{22}/N^5.$$

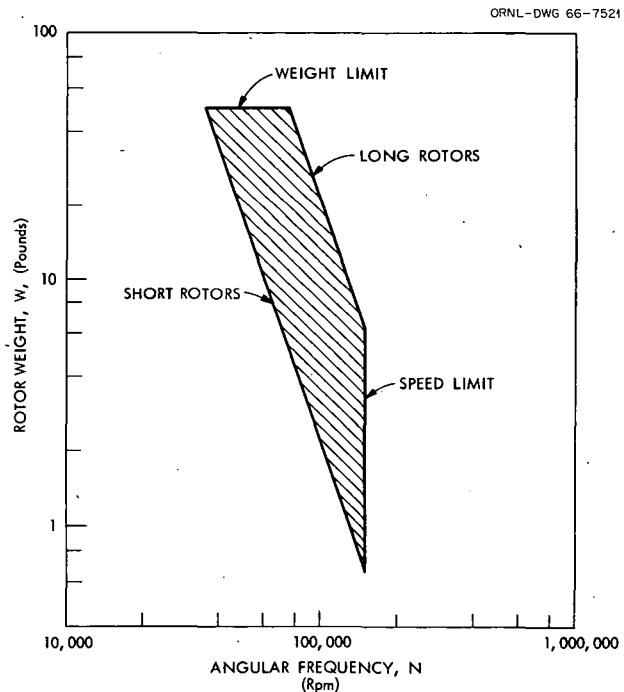


Fig. 1. Design Area of Weight and Speed for a High-Speed Centrifuge with Maraging Steel Rotors.

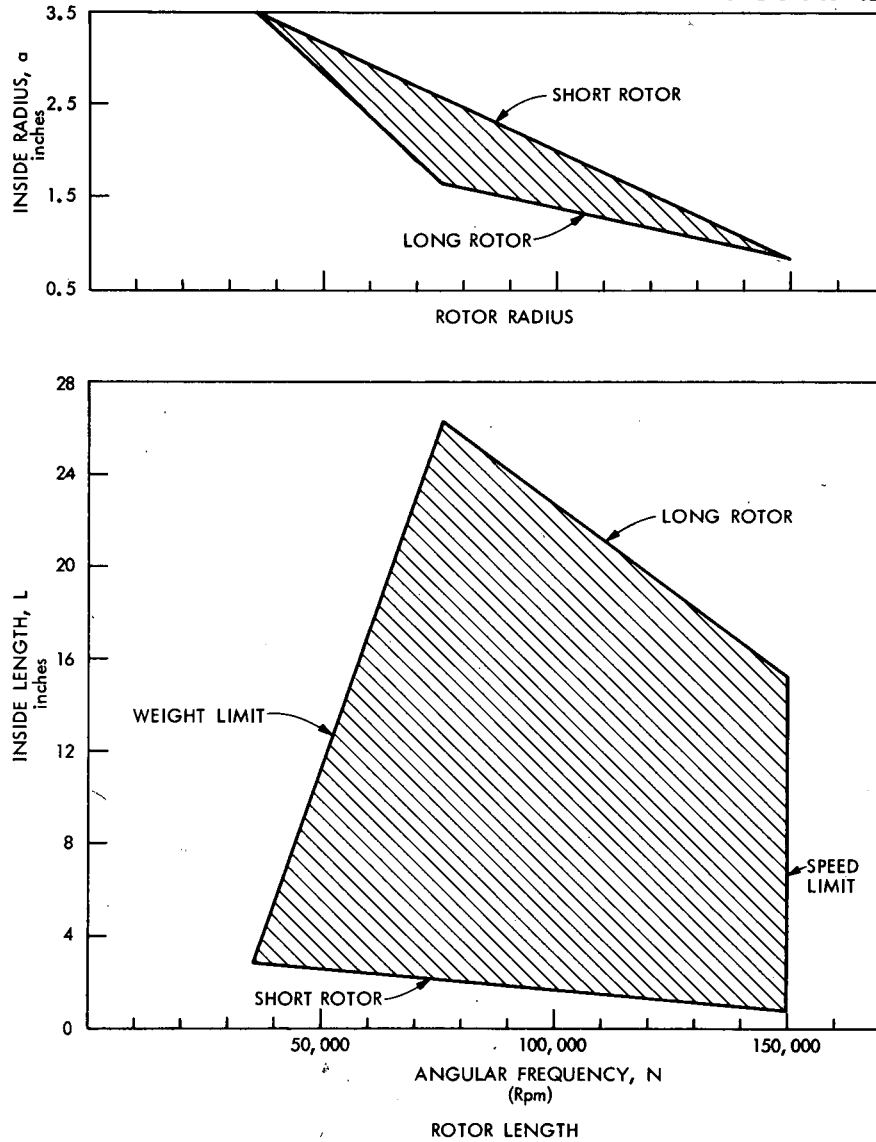


Fig. 2. Design Area of Inside Rotor Dimensions and Speed for High-Speed Centrifuge with Maraging Steel Rotors.

For a long rotor and a short rotor, the polar moments of inertia are:

$$I_{\text{polar}_{LR}} = 110.8 \times 10^{22}/N^5$$

and

$$I_{\text{polar}_{SR}} = 9.14 \times 10^{22}/N^5 .$$

Figure 5 shows the design area of interest.

At 100% efficiency, the constant-torque drive system could deliver a theoretical maximum torque (T) of 2.36 in.-lb to the rotor at all speeds.

Therefore, the angular acceleration rate will be

$$\alpha = t/I ,$$

and the time to accelerate from rest to speed will be

$$t = \omega/\alpha = \pi N/1800\alpha = \pi NI/1800T ,$$

which gives

$$t_{LR} = 8.11 \times 10^{20}/N^4$$

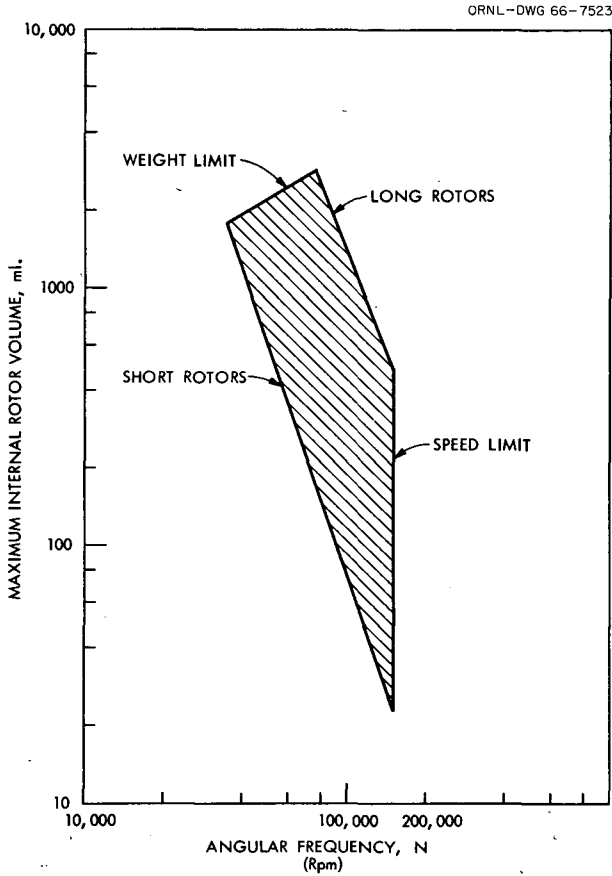


Fig. 3. Design Area of Internal Rotor Volume and Speed for High-Speed Centrifuge with Maraging Steel Rotors.

and

$$t_{SR} = 0.675 \times 10^{20} / N^4 .$$

Figure 6 shows the minimum acceleration times.

Power losses in the transmission and the high-speed spindle will cause the actual acceleration time to be greater than that shown in Fig. 6. Since the torque lost from the transmission will be approximately

$$T_{loss_t} = 7.0 \times 10^{-12} N^2 ,$$

and the torque lost from the bearing spindle will be approximately

$$T_{loss_s} = 6 \times 10^{-6} N ,$$

the torque available to the bearing spindle is

$$T_{net} = 2.36 - (6 \times 10^{-6} N) - (7 \times 10^{-12} N^2) .$$

The acceleration time can be found from equating the net torque to the product of the acceleration rate and the moment of inertia,

$$\frac{\pi}{1800} I \frac{dN}{dt} = T = 2.36 - (6 \times 10^{-6} N) - (7 \times 10^{-12} N^2) .$$

Then, integrating and solving for the acceleration time,

$$t = 346I \tanh^{-1} [(1.39 \times 10^{-6} N) + 0.595] ,$$

which gives

$$t_{LR} = (38 \times 10^{25} / N^5) \tanh^{-1} \times [(1.39 \times 10^{-6} N) + 0.595] ,$$

and

$$t_{SR} = (3.16 / N^5) \tanh^{-1} [(1.39 \times 10^{-6} N) + 0.595] .$$

The actual acceleration times are also shown in Fig. 6. Rotor weights greater than about 30 lb produce prohibitive acceleration times.

As shown in Fig. 7, other systems have torque-speed curves conducive to greater acceleration rates than the constant-torque motor. However, other factors such as power levels, speed control and adjustability, torque limitations of the system, cost, and availability must also be considered.

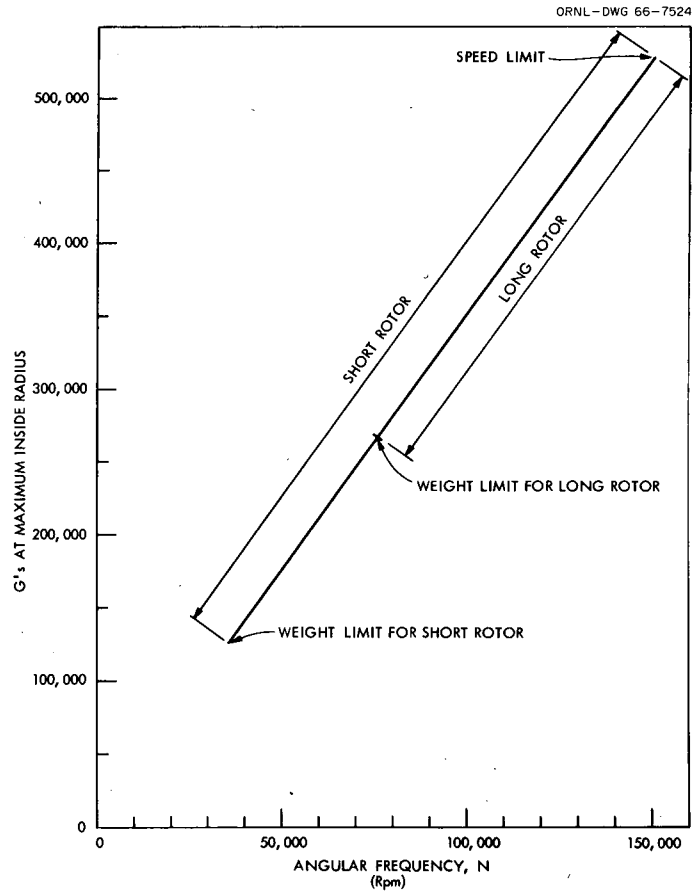


Fig. 4. Design Curve of Maximum Force and Speed for High-Speed Centrifuge with Maraging Steel Rotors.

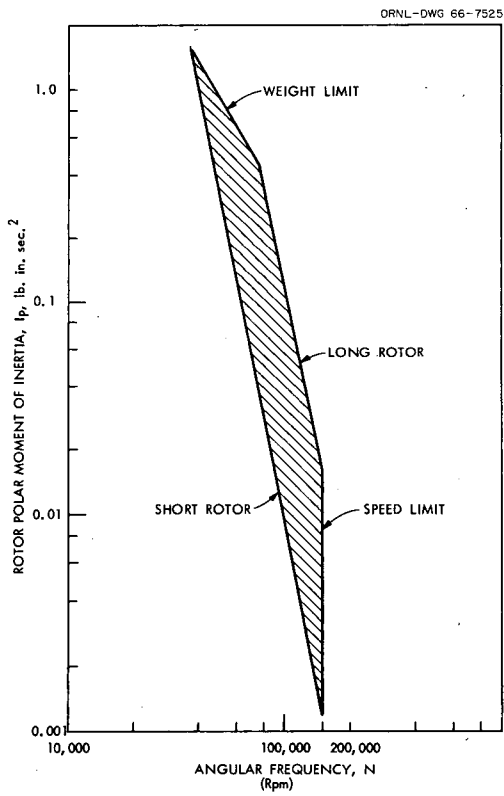


Fig. 5. Design Area of Polar Moment of Inertia and Speed for High-Speed Centrifuge with Maraging Steel Rotors.

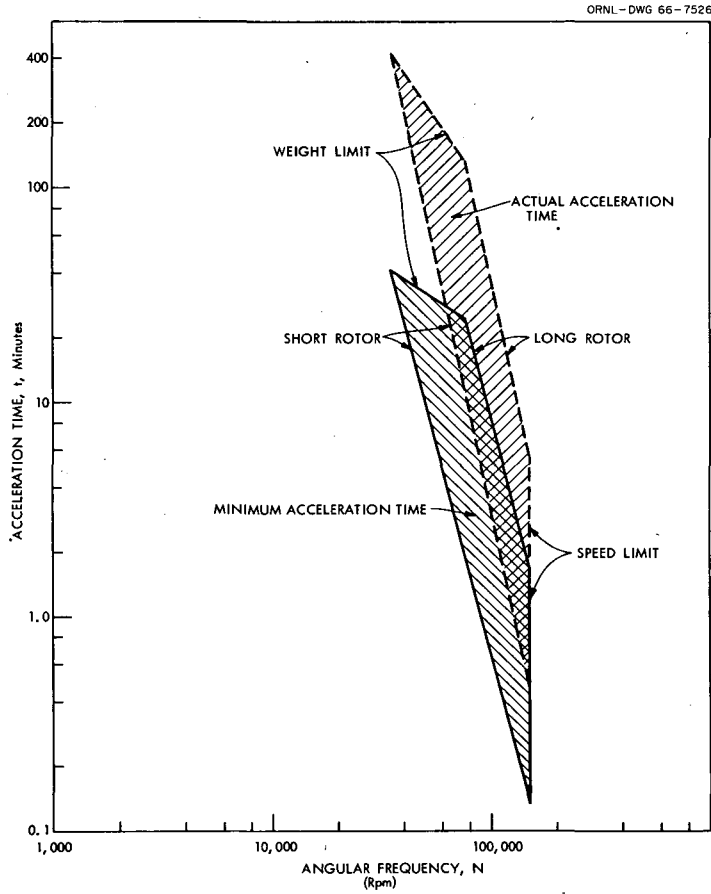


Fig. 6. Design Area of Actual and Minimal Acceleration Time and Speed for High-Speed Centrifuge with Maraging Steel Rotors.

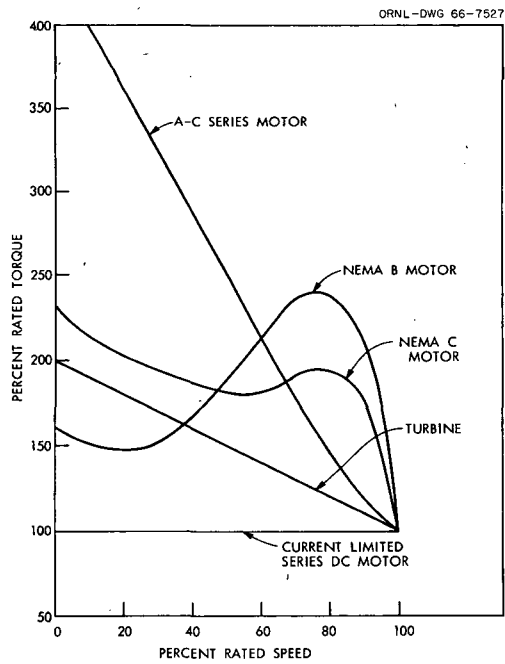


Fig. 7. Torque and Speed Curves for Various Drive Devices.

MAGNETICALLY SUSPENDED ROTOR SYSTEMS

E. C. Denny

Magnetically suspended rotors offer several distinct advantages over shaft-coupled systems. These advantages can be particularly worthwhile in certain types of centrifuge systems where large power transfer is neither necessary nor desirable. Systems falling in this category have extremely high g force rotors with ultimate speeds above those available from present bearings and equilibrium systems which require extremely constant conditions over extended time periods.

Advantages gained by magnetically suspending rotors are primarily those affecting resolution. While one would desire the highest resolution possible from any system, it is of prime importance in an equilibrium machine. Factors affecting resolution are (1) thermal gradients, which contribute to diffusion and convection; (2) vibration, which is caused by bearing friction, gear backlash, and unbalance; and (3) uniformity of speed over extended time periods.

Gravitational force on a rotor can be counterbalanced by the upward attraction of a magnet in a magnetically supported system. In many applications this upward attraction is merely used to support a portion of the thrust, thus reducing frictional forces. In applications such as those discussed here, the rotor is actually levitated. The force balance required for this condition can never exist in a static or truly equilibrium state. The system is basically unstable and requires servo action to maintain a balance between the two opposing forces of gravity and magnetic field. Techniques of achieving this balance have been discussed by various investigators.³⁻⁷ Applications of magnetic-support

techniques range from wind-tunnel test models through motor shafts to watt-hour meters.

Necessity for complicated circuits and complex control devices has limited use of such equipment in biological fields to a few special instances and applications. Apparently, no centrifuges with magnetically suspended rotors are available on the commercial market.

To render complex experimental systems suitable for general use, while at the same time improving resolution, several innovations have been made: use of modular components, conversion to solid-state electronics for high reliability, simplification of the high-vacuum system, and modification of the optical system.

In designing rotors for magnetically supported systems, two separate types, designated the D rotors and the equilibrium rotors, have been considered. The former are suitable for high-speed, high-force applications, and the latter give higher resolution than has been available with other analytical systems.

D Rotors

Data have been reported previously on the D system.⁸⁻¹⁰ While no modifications of importance have been made to the mechanics of the system, changes to the magnetic-support circuit warrant detailed discussion, since these features may be directly applicable in other biological systems or levitated devices.

Circuit Design. — Dynamics of rotors in a magnetic field and transfer functions for the control system are discussed in some detail by MacCosham.³ Basically, the action of the control circuit is straightforward. A detector (photoelectric, inductive, or capacitive) senses the position of the rotor in space. The signal output from the detector controls current through an electromagnet to restore the rotor to a given position

³V. J. MacCosham, *Ultracentrifugal Analysis*, pp. 249-62, ed. by J. E. Williams, Academic Press, N.Y., 1963.

⁴Y. Goto, Y. Miyazawa, and T. Sudo, "The Free-Running-Type Equilibrium Ultracentrifuge," *Bull. JSME (Japan Soc. Mech. Engrs.)* 4, 598 (1961).

⁵J. B. Breaseale, C. G. McIlwraith, and E. N. Dacus, "Factors Limiting a Magnetic Suspension System," *J. Appl. Phys.* 29, 414 (1958).

⁶J. W. Beams and L. B. Snoddy, "The Electrically Driven Ultracentrifuge," *Science* 85, 185 (1937).

⁷F. T. Holmes, "Axial Magnetic Suspensions," *Rev. Sci. Instr.* 8, 444 (1937).

⁸H. P. Barringer and D. A. Waters, *Joint NIH-AEC Zonal Centrifuge Develop. Program Semiann. Progr. Rept. July 1-Dec. 31, 1962*, ORNL-3415, pp. 57-58.

⁹W. W. Smith *et al.*, *Joint NIH-AEC Zonal Centrifuge Develop. Program Semiann. Progr. Rept. Jan. 1-June 30, 1963*, ORNL-3502, pp. 43-44.

¹⁰"Ultrahigh-Speed Rotors," *Joint NIH-AEC Zonal Centrifuge Develop. Program Semiann. Progr. Rept. July 1-Dec. 31, 1963*, ORNL-3656, pp. 34-35.

should any departure occur. With too-rapid response of the control system, with improper phasing, or with passage of too much current through the coils, the system may tend to oscillate or improperly levitate the rotor.

Initial parameters for the circuits may be calculated from known values of rotor mass, coil size, detector sensitivity, etc. In most cases actual values for optimum design may be derived more rapidly by experimental procedures. Final adjustments of circuit values usually must be made on the operating unit.

Circuits with adequate performance for use in levitation may be characterized by frequency response and phase shift. The frequency response may be described as having three ranges (see Fig. 8):

1. a small value of gain that is constant from dc to some low frequency called f_1 ,
2. a semilinear response from some frequency f_1 to a higher frequency f_2 with slope increasing at some rate between 3 db/octave to 12 db/octave, and
3. a higher but constant gain above the frequency f_2 rolling off at frequencies above a few thousand cycles per second.

Values of f_1 lie between 4 Hz and 16 Hz in most cases of interest, while in practice f_2 may vary between 100 Hz and 300 Hz. Gain at low

frequency is normally less than unity and at high frequency may range as high as 15 depending on rotor mass, etc. Phase shift varies to a maximum of about one radian at the midfrequency range between f_1 and f_2 .

It has been convenient in our work to make detector and output-stage response linear and to shape the entire circuit response in the intermediate stages. Two methods of shaping have been used in the circuits for D rotors and for equilibrium rotors. Neither system seems to hold an advantage, although the equilibrium-type circuit may offer more flexibility in making initial adjustments.

The high degree of reliability and the simplicity of modular units in solid-state design have made this approach to circuits attractive for this application. Solid-state control usually means current control as opposed to voltage control in the supporting coils. By controlling much larger values of current, coils may be greatly reduced in size and still produce the same magnetic forces. The complication of heat dissipation is dealt with by proper coil design, water cooling, and adequate heat sinks.

Support System. — In the design of the D rotor system, supporting coils have been placed at each end of the rotor to provide added stability through tighter coupling (i.e., increased magnetic spring rate). This feature is shown schematically

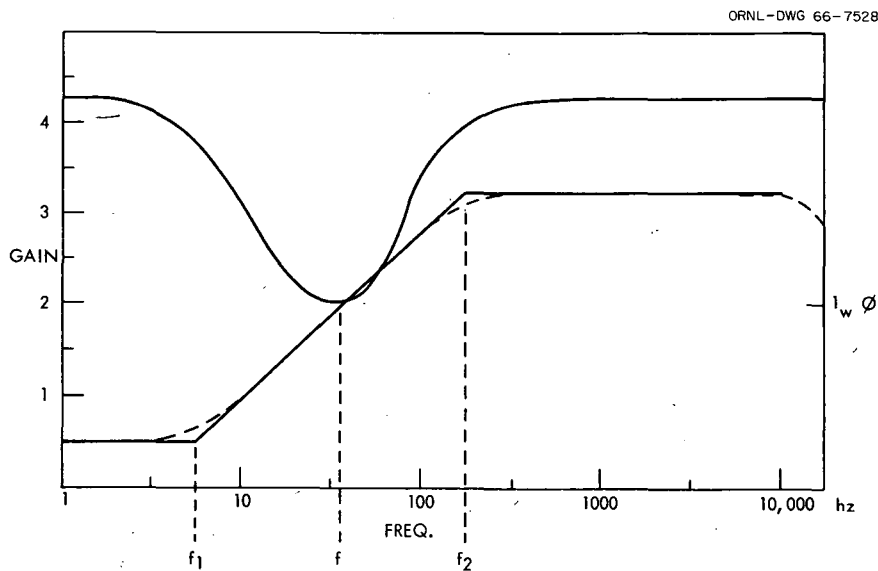


Fig. 8. Characteristic Frequency Response.

in Fig. 9. With this arrangement it has been possible to achieve lateral spring rates of 8 lb/in. with a gap spacing of 0.020 in. at each end of the rotor. Vertical stability of the rotor has been ± 0.000025 in. under these conditions. An added feature of the double-coil arrangement was that a complete flux path was provided through the rotor; the system thus was independent of external fields, which produce power losses and eddy-current heating.

Centrifuges with large length-to-diameter ratios will rotate in a stable condition around the long axis if properly constrained and damped. If support is given at the top end of the rotor only, then rotation at high speeds is difficult, if not impossible, to achieve. Thus, it would appear that not only are the advantages mentioned above useful for D rotors, but they are necessary to achieve high angular velocities.

Performance of the D rotors has been satisfactory at lower rotational speeds, and test operations have been made to speeds of 272,000

ORNL-DWG 66-7529

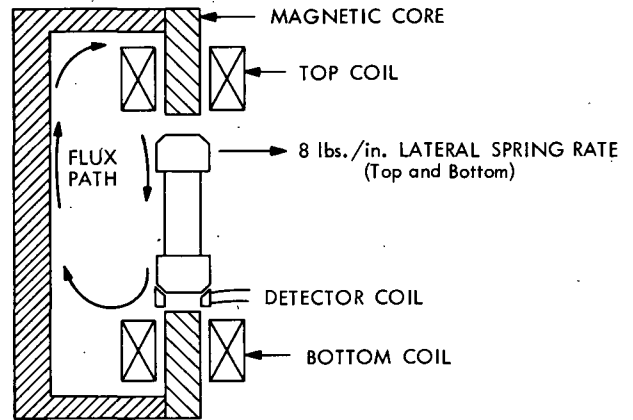


Fig. 9. D-Rotor Coil Arrangement.

ORNL-DWG 66-7530

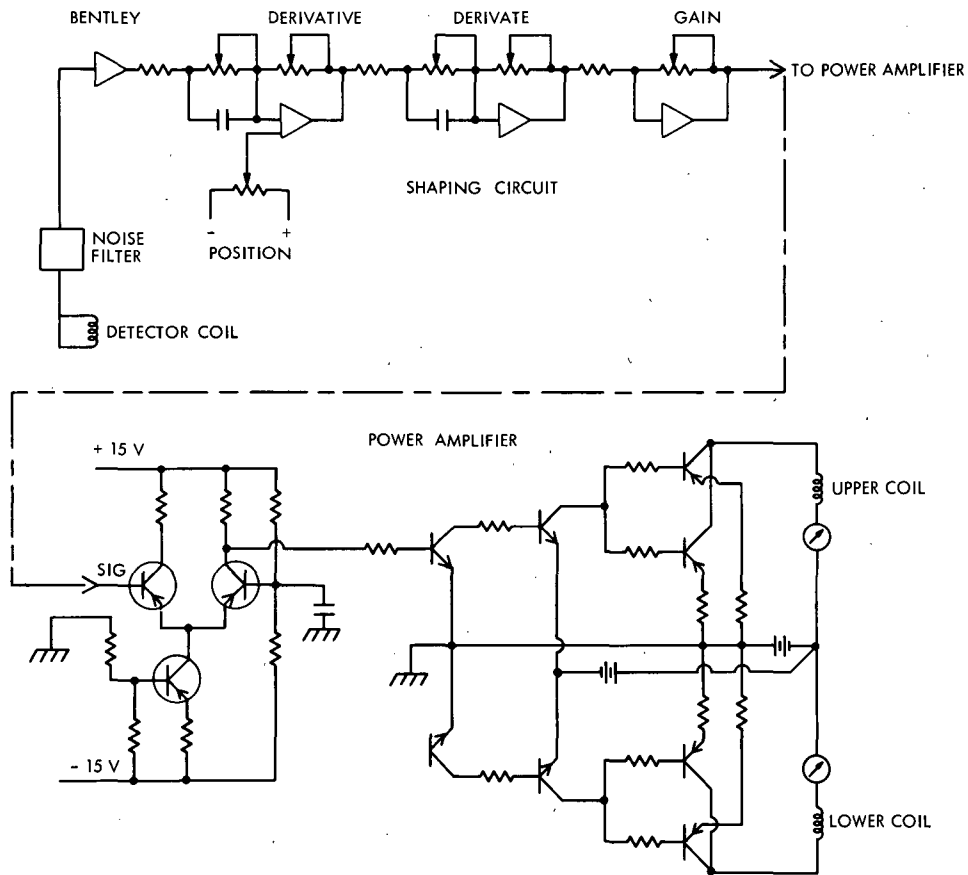


Fig. 10. Circuit Diagram for D-Rotor Magnetic Support.

rpm. Unfortunately, the design speed of 400,000 rpm has not been achieved. Analysis of rotor dynamics with an analog computer with measured values of parameters from a magnetically supported D rotor indicate that such speeds cannot be obtained with the present damper design. This behavior results from failure to damp certain of the precessional modes at higher speeds. The problem requires further study and modification of rotor shape and damper design.

The redesigned support circuit included the use of solid-state amplifiers and transistors for the output control. The entire support circuit was operable from storage batteries; thus, the unit was self-contained. This feature was added to minimize loss of costly samples in the event of power failures or fluctuations during extended runs. The system utilized readily available components to allow off-the-shelf servicing if necessary. A complete circuit diagram is shown in Fig. 10.

Operational amplifiers shown in Fig. 10 are Philbrick P-45LU's or P-65A's; any amplifier with similar output could be substituted. The proximity detector was a Bentley Nevada Corporation D-177 amplifier with a coil wound to fit the surface contour of the particular rotor being used and designed to oscillate at 3 Mc/sec. This modification increased sensitivity and minimized vertical hunting.

Equilibrium Rotors

The equilibrium system (Fig. 11) has particular design features that represent departures in concept. After final assembly of the components, the system will be ready for testing. Speed and power losses will be calculated, and temperature controls and the interferometer will be calibrated prior to introduction of biological samples.

Vacuum System. — Operation of an equilibrium centrifuge with a levitated rotor was accomplished by accelerating the rotor to speed and allowing it to coast suspended in the magnetic field. When speed losses were kept very low, this method approached true equilibrium. To reduce speed losses, one must remove the possibility of air drag on the rotor. This requires a vacuum of at least 10^{-5} torr or better.⁵

Demands of the space program have permitted a number of excellent high-speed, high-vacuum pumping stations to become available commercially. One of these — a 4-in., fully automated unit — was chosen to produce the high vacuum for this system. Design of the centrifuge chamber allowed complete hermetic sealing except where the rotor was inserted through an O-ring-sealed flange. Thus, the system could reach pressures of 1×10^{-7} torr or less with no bake-out. Operation of the system on a fully automatic cycle did not require the attention of the operator once the start switch was actuated.

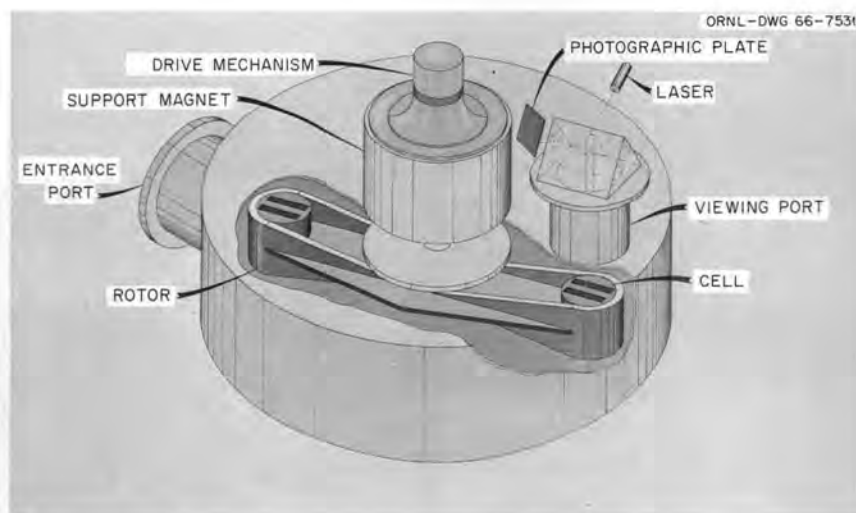


Fig. 11. Magnetically Supported Equilibrium Centrifuge.

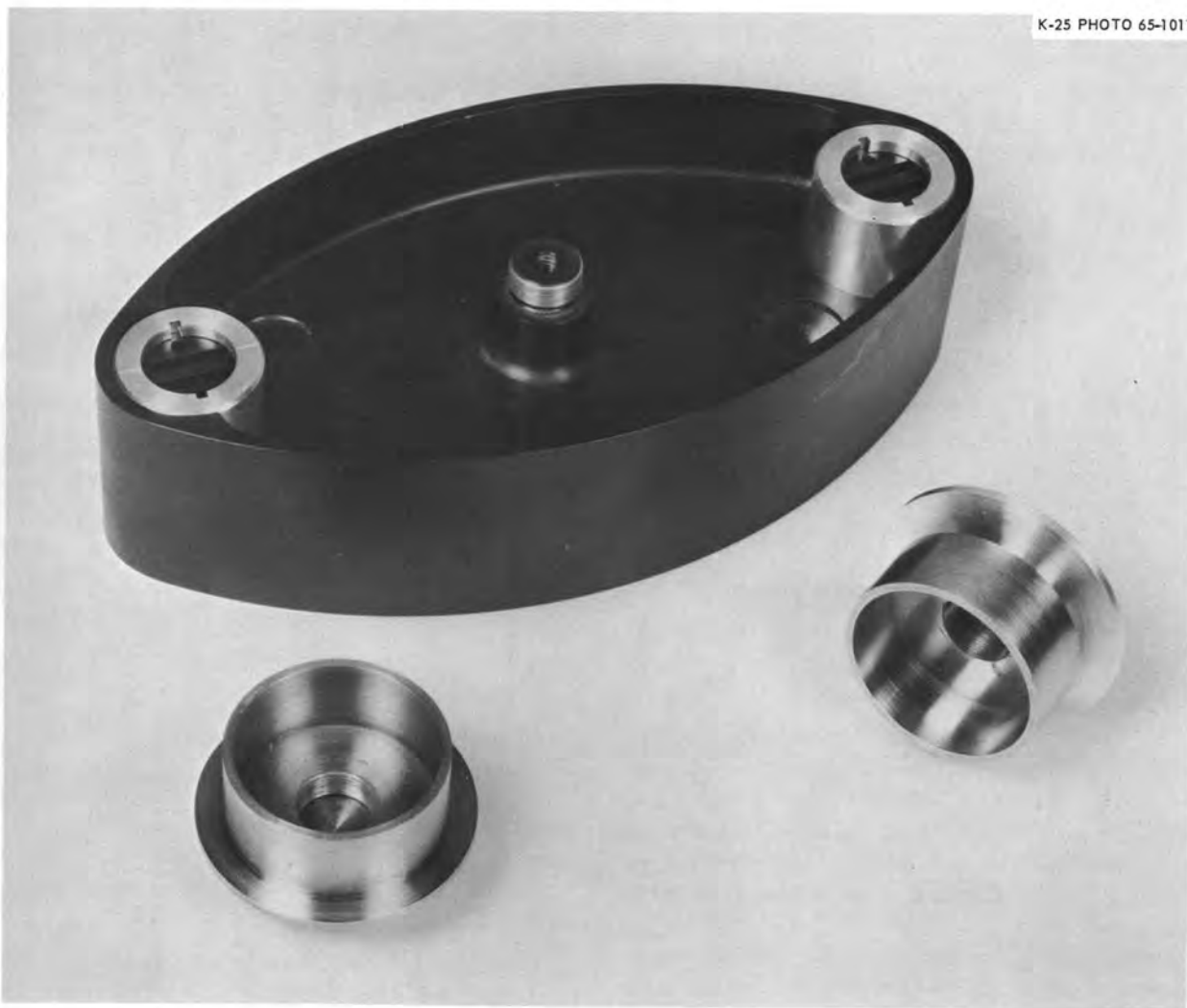


Fig. 12. Equilibrium Rotor.

Hollow Construction. — Early designs of centrifuge rotors demanded massive amounts of metal to obtain the desired strengths at operational speeds. Advances in metallurgy have now made alloys so strong that rotor design does not need these large masses of metal for the lower speeds desired in an equilibrium system. Consequently, the rotor for this system has been largely cut away, or hollowed out, as shown in Fig. 12. This lower-mass rotor allows reduced acceleration times and smaller power demands for the magnetic field. Less energy is stored in the rotor, a condition that would lessen the possibility of destruction should the support circuit fail. A

fail-safe feature was provided to prevent loss of costly samples. The rotor was allowed to spin to a stop on a needle-pivot and sapphire-jewel bearing. Rotor shape has been altered to an ellipse for ease of insertion through a vacuum flange. This feature makes operation of the high-vacuum system similar to that of an evaporator or bell jar and requires only an O-ring seal.

No equilibrium centrifuge system would be of value without a good method of obtaining necessary information from the rotor. Interference optical systems offer the greatest potential for resolution and sensitivity. In addition, results

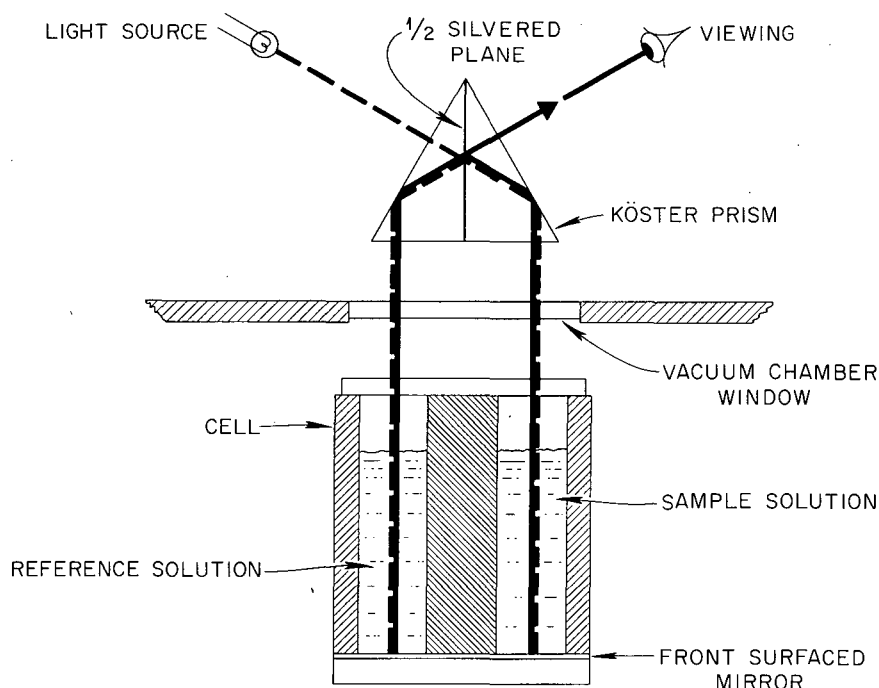


Fig. 13. Köster Interferometer Optics (Simplified).

are easy to interpret. Unfortunately, interference techniques have been avoided in many instances because of the complexity of initial adjustment and maintenance.

Interferometry. — Optical design of the interferometer used in the present work has been simplified and enhanced by use of Köster's prism.¹¹ The system eliminates the need for slits and lenses with their inherent reduction in light intensity. This feature enables one to obtain necessary information in much shorter exposure periods, thus improving resolution. The double length of the light path through the sample improved sensitivity and also aided resolution. In addition, only one movement of the prism was necessary for image formation, eliminating delicate optical alignment procedures. A schematic diagram of the optical system is shown in Fig. 13.

Levitation Control. — Exceptional simplicity was achieved in the design of the levitation-control circuits by making use of commercially available proximity devices, operational ampli-

fiers, and power supplies. A diagram of the levitation circuit is shown in Fig. 14, and a photo is shown in Fig. 15. The components used are as follows:

1. The proximity detector consisted of a Bentley Corp. D-177 amplifier and a coil wound to fit the pole-face dimensions for optimum sensitivity.
2. Operational amplifiers, Philbrick P-65A's, controlled the base current of a 2N1501 transistor, which programmed the prime power supply for the coil current.
3. The prime power to the coil was furnished by a solid-state supply capable of delivering ~5 amp into a coil of 220 turns of No. 14 AWG copper wire. This was capable of supporting the rotor weight with 1-lb samples at a distance of approximately 0.5 cm.

Reshaped Magnetic Field. — Power losses occur in the rotor from several sources: air drag, eddy currents inducted in the rotor, and hysteresis effects on the rotor. The latter are the most troublesome because they not only account for the gradual loss of speed, but also cause

¹¹J. B. Saunders, "The Kösters Interferometer," *J. Res. Natl. Bur. Std.* **58**, 27 (1957).

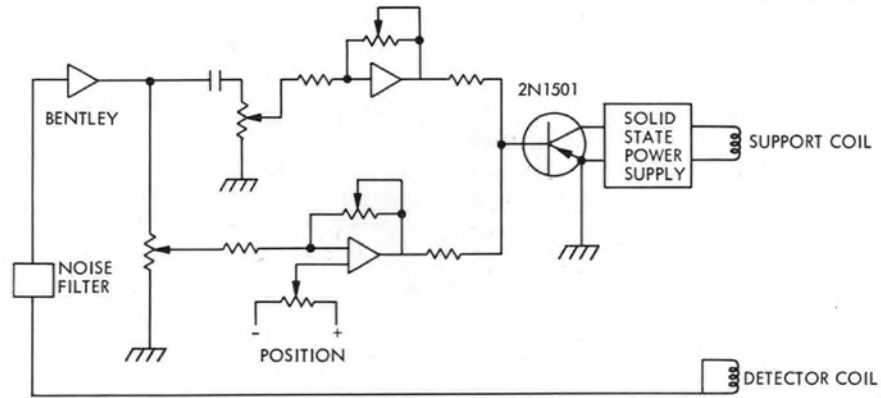


Fig. 14. Schematic of Equilibrium Magnetic-Support Circuit.

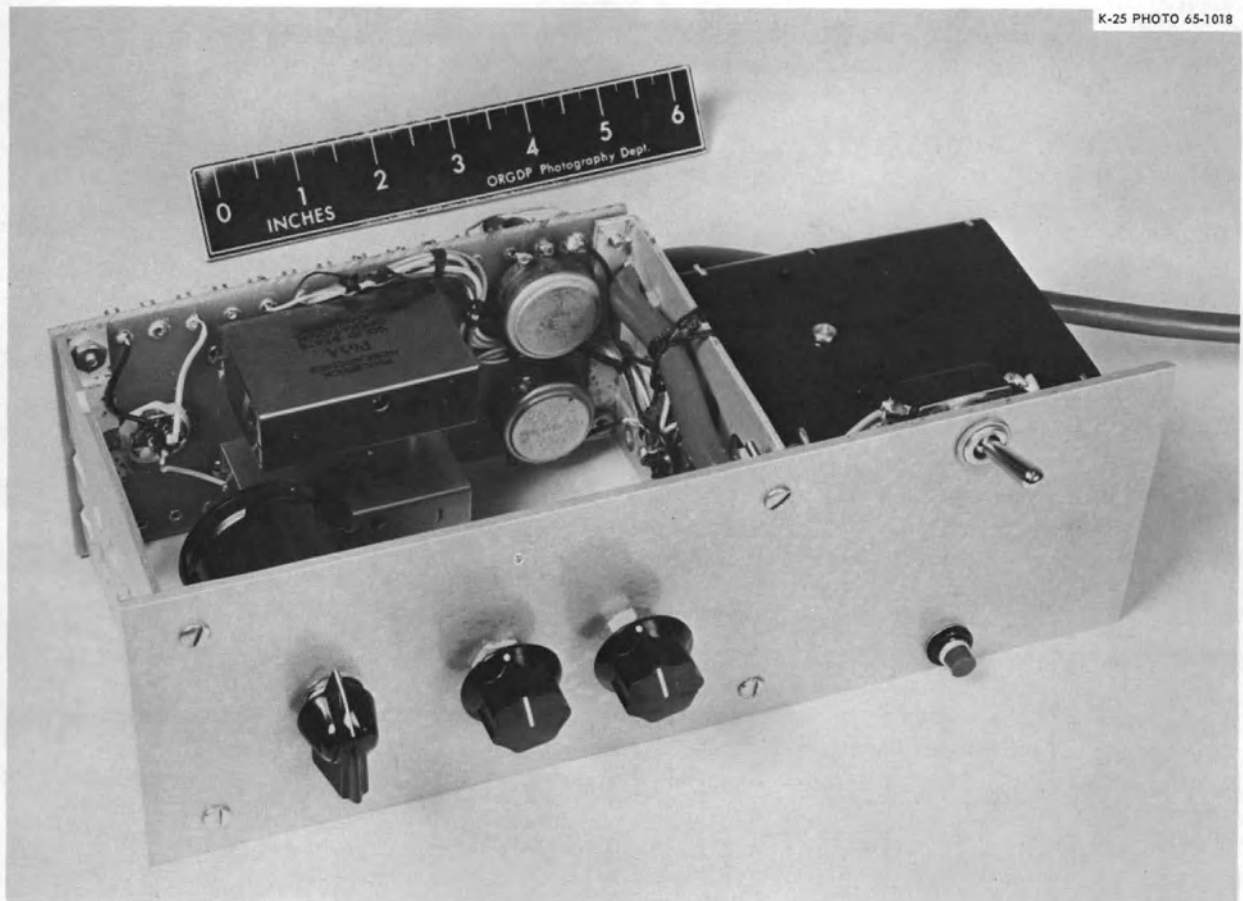


Fig. 15. Magnetic-Support Amplifier.

heating within the rotor itself. The heating decreases resolution and upsets equilibrium. Eddy currents and hysteresis losses are caused by inductive effects of the rotor spinning in an inhomogeneous magnetic field.⁵ In an equilibrium system, extraneous influences may disturb the shape of the field penetrating the rotor. Two steps were taken to alleviate this situation: the mass of conducting material through which the field passes was reduced by the rotor design, and a return flux path was provided around the outside of the rotor to ensure that all flux passed through the rotor without being disturbed by outside influences (Fig. 16).

Harmonic Drive. — The rotor was accelerated by a small universal motor operating through a hermetically sealed speed increaser called a harmonic drive, available from United Shoe Machinery, Beverly, Mass. A photograph of this drive assembly is shown in Fig. 17. No oil leaks in to contaminate windows and optical parts be-

cause the unit is hermetically sealed. After the rotor was accelerated to speed, it was detached from the drive shaft by lowering the rotor and allowed to coast in its levitated position, where no friction occurred to cause disturbances within the sample.

Other Design Features. — The equilibrium system has

1. temperature-control circuitry to maintain any preselected rotor temperature between 0°C to ambient conditions with proportional control,
2. electronic speed indication to give an accurate accounting of speed and speed changes with time,
3. all components mounted on one chassis for ease of operation and maintenance,
4. encapsulation of the entire chamber in foamed plastic for thermal isolation.

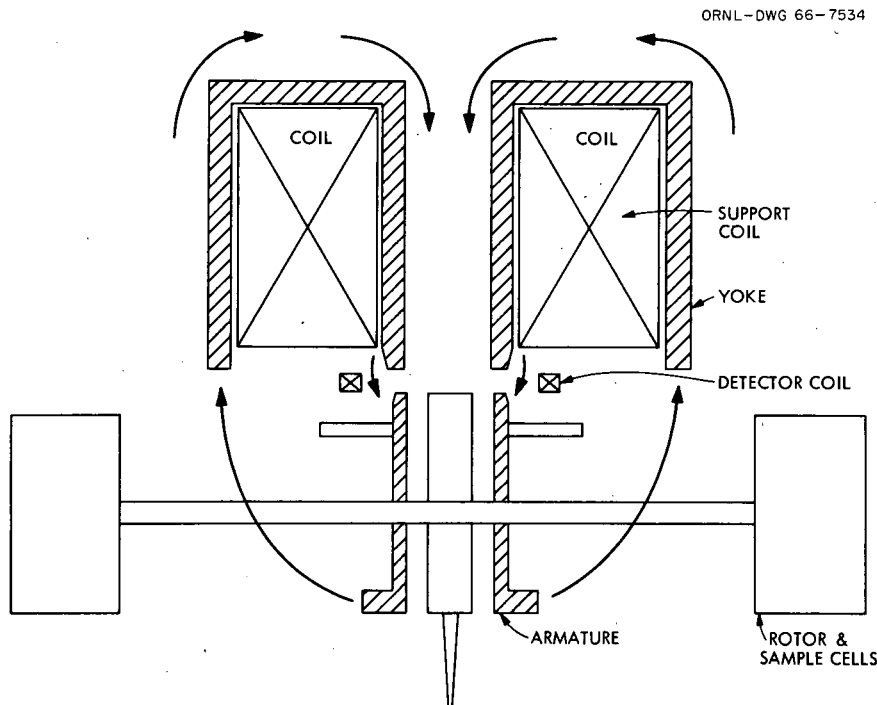


Fig. 16. Flux Path in Equilibrium Centrifuge.

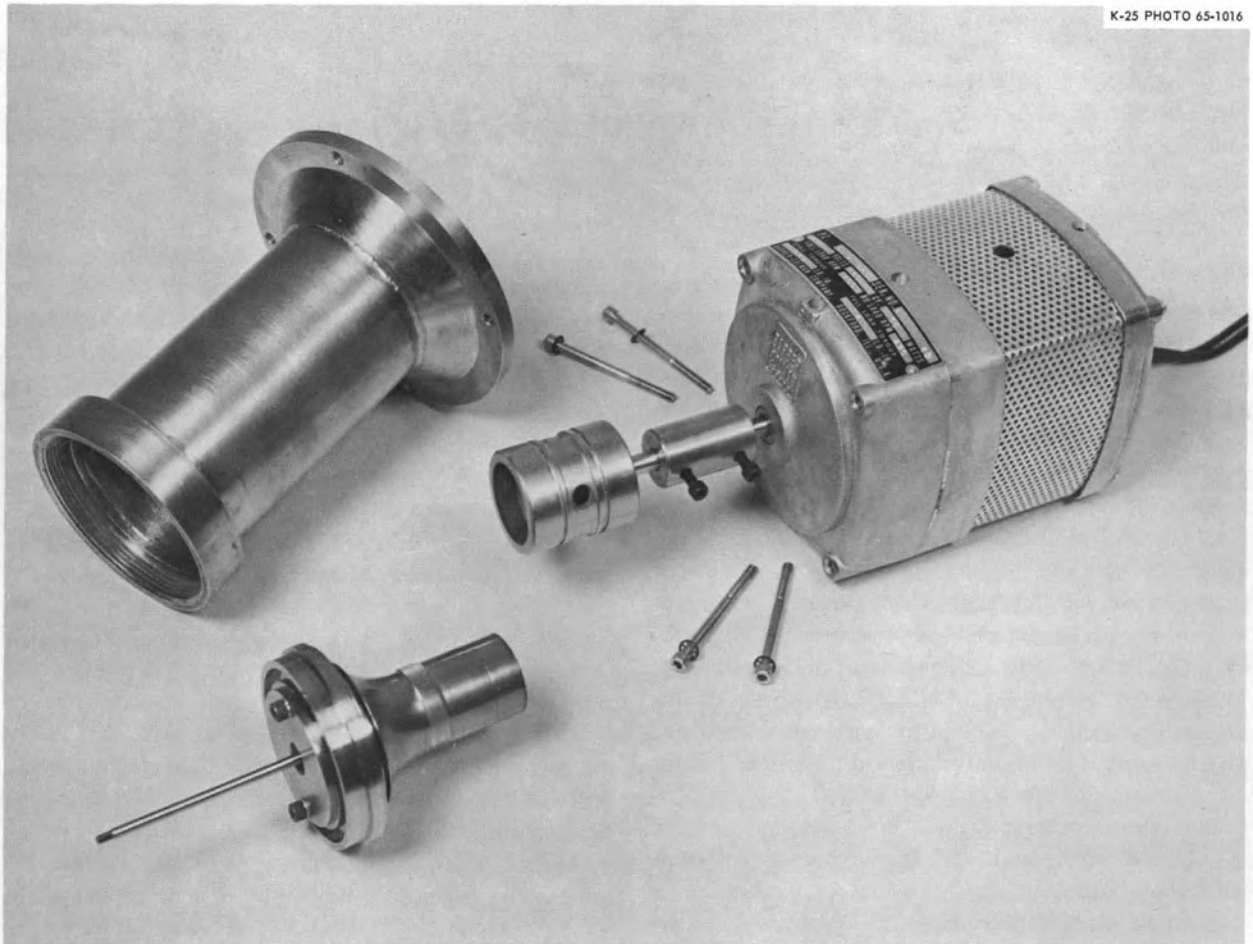


Fig. 17. Harmonic-Drive Assembly.

5. Experimental Separations

THE PURIFICATION OF LYSOSOMES

J. R. Corbett¹

Lysosomes are cellular organelles of mitochondrial size and contain hydrolytic enzymes that will attack nucleic acids, carbohydrates, and proteins at acid pH values.² The enzymes possess the property of latency, meaning they will show increased activity after such treatments as sonication, osmotic shock, or addition of a detergent. It is assumed that these treatments break a membrane surrounding the enzymes. This sac hypothesis is supported by electron micrographs of subcellular fractions enriched in lysosomes.³ The pictures show spherical structures which are surrounded by a single unit membrane and which contain a granular interior; similar bodies can be seen in sections of intact cells.⁴

The lysosome concept has been very successful in stimulating research, but the major difficulty with the current effort is that it is almost never concerned with highly purified lysosomes. The concept that the lysosome consisted of a bag of dangerous enzymes was intellectually attractive largely because it was open to experimental proof. The lysosome was seen as a destructive

organelle whose violence could be switched on and off by tampering with the membrane. Because of this, the lysosome has been implicated in biological processes as diverse as digestion, cancer, shock, and hormone action. A general approach is evident in much of this work. Animals are exposed to the desired factor, and a crude lysosomal fraction is made from a particular organ. The degree of latency of the lysosomal enzymes is measured, and if this differs from the control, it is concluded that lysosomes may be involved in processes affected by the particular factor under study. This approach was valuable in early work on lysosomes, but it may now be diverting too much attention from the study of the lysosome itself.

If lysosomes are important in cellular processes, and there seems little doubt among workers in the field that they are, it is imperative that more precise and fundamental questions be asked. What is the exact enzyme complement of the lysosomes? What is the molecular nature of the membrane? What is the mechanism of latency? Do lysosomes contain nucleic acids? These questions can only be answered if a purified fraction of lysosomes is available. Unfortunately, there is no general method available for the large-scale isolation of lysosomes; this preliminary report describes work undertaken to provide such a method.

Materials and Methods

Liver from adult, male Sprague-Dawley rats was used. The brei was made by grinding for 30 seconds with 8.5 wt % sucrose in a Waring blender. The brei was squeezed through cheesecloth and used directly for zonal centrifugation. The zonal runs illustrated in Figs. 1 and 2 used 11 to 12 g

¹On leave of absence from the Plant Biology Department, Rutgers, The State University, New Brunswick, New Jersey.

²C. de Duve, "The Lysosome Concept," p. 1 in *Lysosomes, Ciba Foundation Symposium*, ed. by A. V. S. de Reuck and M. P. Cameron, Little, Brown, Boston, 1963.

³P. Baudhuin, H. Beaufay, and C. de Duve, "Combined Biochemical and Morphological Study of Particulate Fractions from Rat Liver," *J. Cell Biol.* **26**, 219 (1965).

⁴A. B. Novikoff, "Lysosomes in the Physiology and Pathology of Cells: Contributions of Staining Methods," p. 36 in *Lysosomes, Ciba Foundation Symposium*, ed. by A. V. S. de Reuck and M. P. Cameron, Little, Brown, Boston, (1963).

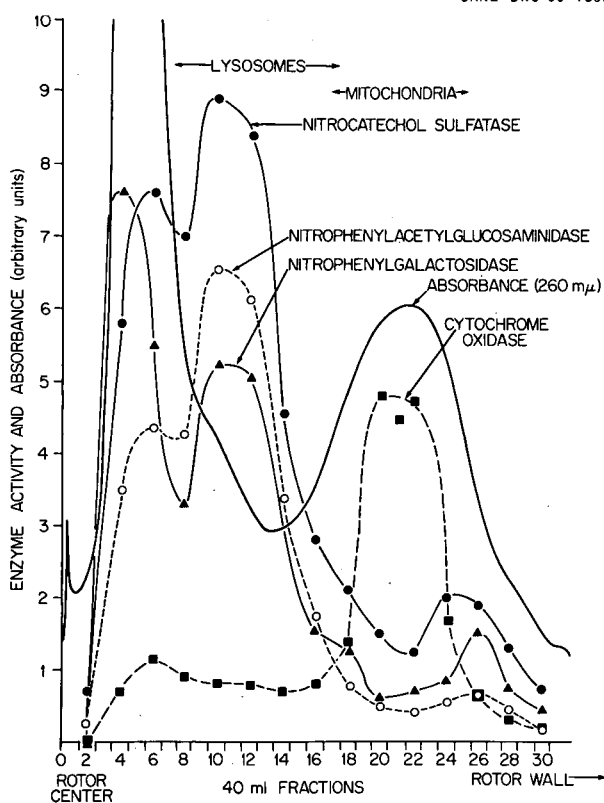


Fig. 1. Fractionation of Rat-Liver Brei with the B-XV Zonal Centrifuge; Lysosomes and Mitochondria.

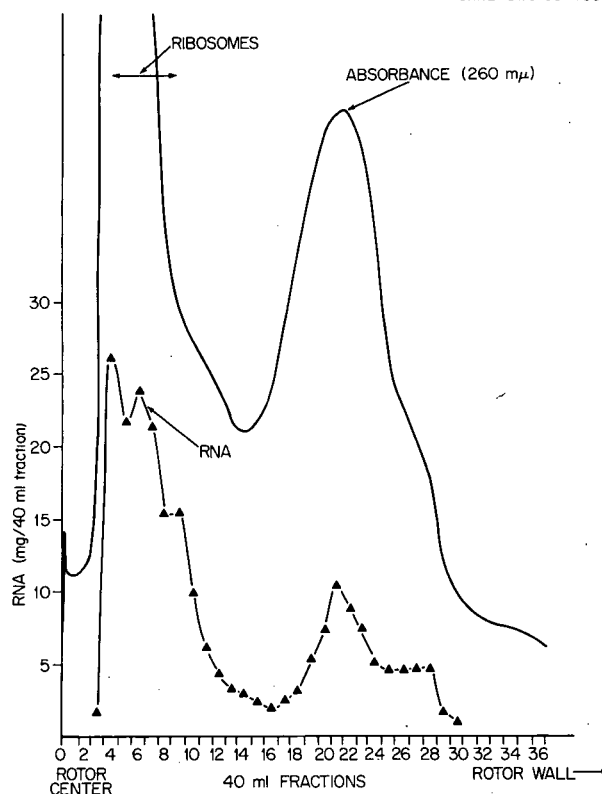


Fig. 2. Fractionation of Rat-Liver Brei with the B-XV Zonal Centrifuge; Ribosomes.

of fresh liver in the B-XV zonal rotor.⁵ The light mitochondrial fraction used in the zonal rotor was the F II of Sawant *et al.*⁶

The conditions used for the zonal runs are given in Table 1. At the end of the run, the solution was pumped out of the rotor and was continuously monitored at 260 $m\mu$ by a Gilford attachment on a Beckman DU spectrophotometer; 40-ml fractions were collected.

The following lysosomal enzymes were assayed automatically by a slight modification of the Technicon program described by Tappel:⁷ *p*-nitrophenyl-*N*-acetyl- β -D-glucosaminidase (EC 3.2.1.30), nitrocatechol sulfatase (EC 3.1.6.1),

p-nitrophenyl- β -D-galactopyranosidase (EC 3.2.1.23), phenolphthalein glucuronidase (EC 3.2.1.31), and *p*-nitrophenyl phosphatase (EC 3.1.3.2). These enzymes were assayed in the presence of 0.1% Triton X-100, except when the degree of latency was being determined. Cytochrome oxidase was measured according to Smith.⁸

To determine the amount of RNA in the fractions derived from the zonal centrifuge, a sample was centrifuged at 40,000 rpm in a 40 rotor (Spinco, model L), and the pellet was extracted selectively for RNA by the potassium hydroxide method

⁵N. G. Anderson *et al.*, "Two New Simple Zonal Centrifuge Rotors: B-XIV and B-XV," *Federation Proc.* **25**, 421 (1966).

⁶P. L. Sawant *et al.*, "Isolation of Rat Liver Lysosomes and Their General Properties," *Biochim. Biophys. Acta* **85**, 82 (1964).

⁷A. L. Tappel, "Automated Multiple Analysis of Hydrolytic Enzymes," p. 32 in *Technicon Intern. Symp. Automation in Anal. Chem.*, Technicon, Chauncey, N.Y., 1964.

⁸L. Smith, "Cytochromes a, a₁, a₂, and a₃," p. 732 in *Methods in Enzymology 2*, ed. by S. P. Colowick and N. O. Kaplan, Academic, New York, 1955.

Table 1. Conditions Used for Fractionation of Liver Homogenates in the B-XV Zonal Rotor

Condition	Sample	
	50 ml Whole Brei	50 ml Light Mitochondrial Fraction
Overlay	70 ml water, 50 ml 3 wt % sucrose	Same
Cam on gradient pump	Linear with volume	Linear with radius
Gradient	1200 ml of 17 to 55 wt % sucrose	1200 ml of 17 to 35 wt % sucrose
Underlay	300 ml 55 wt % sucrose	300 ml 40 wt % sucrose
Force	2.000×10^9 (~ 3 min at 20,000 rpm) ^a	Same

^aThis number represents a direct reading and actually is calculated in units of centrifugal force; see "Design and Evaluation of B-XIV and B-XV Rotors," Sect. 2.

of Schneider.⁹ The extract was assayed for RNA by the orcinol method, also described by Schneider.

Protein was measured by the Folin-Ciocalteu method as described by Layne,¹⁰ and corrections were made for the effect of sucrose, which was determined refractometrically.

Results

Separation of Lysosomes from Mitochondria in Whole-Tissue Breis. — Lysosomes differ markedly in size from ribosomes and nuclei, but they are similar to mitochondria in both density and size. It was assumed, therefore, that the major difficulty in the purification of lysosomes would be the removal of mitochondria. Fig. 1

⁹W. C. Schneider, "Determination of Nucleic Acids in Tissues by Pentose Analysis," p. 680 in *Methods in Enzymology* 3, ed. by S. P. Colowick and N. O. Kaplan, Academic, New York, 1957.

¹⁰E. Layne, "Spectrophotometric and Turbidimetric Methods for Measuring Proteins," p. 447 in *Methods in Enzymology* 3, ed. by S. P. Colowick and N. O. Kaplan, Academic, New York, 1957.

shows that the zonal centrifuge will separate these two particles easily. The sample zone extended to tube 4.25, so material beyond this region is essentially sedimentable. Figs. 1 and 2 show the distribution of 260- μ light absorbance, ribosomes, lysosomes, and mitochondria.

Phase and electron microscopy of various fractions confirmed the biochemical characterization of the organelles.

By using the same conditions as Fig. 1, except that the centrifuge was run for a longer time, we caused both the mitochondrial and lysosomal peaks to move farther out and to come to the same isopycnic position. Therefore, the separation shown is based on sedimentation rate.

260- μ -Light-Absorbing Capacity. — Since many of the fractions obtained from the centrifuge are turbid, it is concluded that light scattering as well as light absorption is implicated. There are two major peaks, one corresponding to the ribosomes and nonsedimentable material, and the other to the mitochondria. The light-absorption trace is reproducible (cf. Figs. 1 and 2) and can be used as a check on the rotor performance.

Ribosomes. — Figure 2 shows the distribution of RNA in the fractions; the main RNA peak presumably represents the ribosomes.

Lysosomes. — The following evidence suggests that lysosomes are in the fractions indicated. (1) Nitrophenylacetylglucosaminidase, nitrocatechol sulfatase, nitrophenylgalactosidase, phenolphthalein glucuronidase, and nitrophenyl phosphatase, all of which are lysosomal enzymes, were found in these fractions. Each enzyme had a soluble component as well as the sedimentable (lysosomal) component; the soluble component might be true soluble enzyme or lysosomal enzyme that had been released from lysosomes damaged during the blending process. (2) These enzymes showed latency (i.e., when Triton X-100 was omitted from the assay system, the activity decreased), particularly in the sedimentable component.

Mitochondria. — Cytochrome oxidase activity matches the sedimentable 260- μ light-absorption peak.

Purification of Lysosomes by Rate-Isopycnic Centrifugation. — The fractionation described above, which starts with whole brei, separates the bulk of the mitochondria from the bulk of

Table 2. Lysosome Purification

Fraction	Relative Specific Activity ^a
Unfractioned brei	1
Light mitochondria	8
Lysosomal fraction from B-XV rate run	36
Band from isopycnic separation in sucrose-D ₂ O	59

^aThe ratio of *p*-nitrophenyl- β -D-galactopyranosidase (EC 3.2.1.30) to protein.

the lysosomes, but still does not yield a particularly pure lysosome fraction as judged from enzyme data and electron micrographs. Furthermore, the yield is not particularly high. We therefore decided to use established methods to obtain a lysosome-rich, light-mitochondrial fraction and to use this as the starting material. With a combination of rate and isopycnic separations we obtained the purification shown in Table 2. At the moment, we obtain only about 1 mg of lysosomal protein in the final fraction even though we start with about 100 g of fresh liver.

Discussion

The work done so far has shown that the B-XV zonal rotor will easily separate the major cell organelles from a rat-liver brei. This separation could be useful in determining the intracellular localization of enzymes, drugs, and other materials. The separation is also a simple way of showing that lysosomes are a distinct class of organelles from mitochondria and ribosomes. De Duve² has pointed out that this is not an easy thing to do, but we were able to do it because the zonal centrifuge, particularly the B-XV rotor, is convenient for rate separations. This is not convenient with swinging tubes, where it is difficult to recover a sample which is half way down the supernatant solution without disturbing other zones.

We have also shown that lysosomes can be purified by a combination of rate and isopycnic separation. At present, this method is inferior to that developed for rat liver by Sawant *et al*;⁶

they obtain a 65- to 70-fold purification over the brei, and their yield is much higher. However, their method is difficult to repeat exactly and lacks flexibility. This is because it consists essentially of repeated differential centrifugation. The method that we have developed exploits two different physical properties of the lysosomes — their sedimentation rate and their density. It could be adapted, therefore, to lysosomes which differ in either of these properties from the lysosomes of rat liver.

THE *S*- ρ SEPARATION OF HUMAN-BREAST-TUMOR PARTICLES

E. L. Candler W. W. Harris
N. G. Anderson

In 1964, Anderson and Harris¹¹ isolated virus-like particles from a human breast tumor by rate-zonal and isopycnic centrifugation. These particles averaged 125 μ in diameter and had a central core about 100 μ in diameter. Long strands were also associated with these spherical particles. The present study was stimulated by the isolation of these interesting particles. A joint program was undertaken by the Laboratory and the National Cancer Institute to examine human breast tumors, normal breast tissue, and normal human milk for pleuropneumonia-like organisms and virus-like particles.

Breast tumors and normal breast tissues were supplied by the Viral Carcinogenesis Branch of NCI. Both breast tumors and normal breast tissues were removed surgically and frozen immediately to at least -60°C . Human breast milk was obtained from donors in the Oak Ridge area with newborn children. The milk specimens were always processed immediately.

Experimental Procedure

The separation procedure used in this work was as follows. A 10% tissue brei was prepared in 0.15 *M* sodium citrate, pH 7.0, by homogenizing for three 1-min periods with 30-sec intervals between the periods. The large cell and tissue

¹¹N. G. Anderson and W. W. Harris, *Joint NIH-AEC Zonal Centrifuge Develop. Program Semiann. Progr. Rept. Jan. 1–June 30, 1964, ORNL-3752, p. 8.*

fragments were removed from the brei by low-speed centrifugation at 2000 rpm for 30 min. The supernatant solution from this centrifugation was spun again at 24,000 rpm for 30 min in a Beckman No. 30 rotor in the model L centrifuge. The pellets were collected and homogenized in a Potter-Elvehjem glass homogenizer in 45 ml of 0.15 M sodium citrate. Of this, 40 ml was used as the specimen for zonal centrifugation, and the other 5 ml was used to prepare thin sections for electron microscopy. Two rotor systems were employed in this work, the B-IV and the newer B-XV. The zonal centrifuge was run until $\int \omega^2 dt$ reached 1.58×10^{10} and then was unloaded in 40-ml fractions. A portion of each zonal fraction was banded (isopycnicly) over cesium chloride (density = 1.86 g/cm^3) in polycarbonate tubes at 24,000 rpm for 2 hr in a Beckman No. 30 rotor. Selected bands were removed from the tubes and dialyzed to remove sucrose and salts. The nondialyzable material was mounted on grids, negatively stained with phosphotungstic acid, and examined by electron microscopy.

The procedures for breast tumors, normal breast tissues, and normal milk were identical except that milk did not require pretreatment for centrifugation. However, enough 0.15 M sodium citrate solution, pH 7.0, was added to the milk specimen to bring its volume to 40 ml, the standard volume for zonal centrifuge samples.

Results and Discussion

Electron microscopy of negatively stained fractions of milk, normal breast tissue, and breast tumor tissue has shown a low incidence of particles with possible viral morphology as well as particles resembling mycoplasma. Distribution of particle incidence between normal tissue and tumor tissue has been variable, and particle types have varied. Ultrathin sections stained with uranium and lead show different particle populations between normal and tumor tissue used for starting material for centrifugation. Our next step will be to select fractions containing the different particles of particular interest and to prepare ultrathin sections from them in order to distinguish among virus, mycoplasma, and granules that may be characteristic of cell types.

Collagen frequently shows up in the electron micrographs of normal breast tissue, but it ap-

pears only rarely in the micrographs of breast tumors. This is probably due to the change in cellular makeup of the breast tumor. Glycogen, conversely, is almost always seen in breast tumors, but is seldom seen in normal breast tissue. Both collagen and glycogen have a consistent banding density.

WATER ANALYSIS IN THE ZONAL CENTRIFUGE

G. B. Cline

W. W. Harris

The analysis of water for human consumption should indicate the quantitative and qualitative presence of bacteria, viruses, pesticides, insecticides, and colloids. Classical water analysis relies primarily on the presence or absence of certain sewage bacteria, notably *Escherichia coli*. However, for every type of sewage bacteria, there is a virus that preys on the bacteria and disrupts or destroys it. Thus, although the lack of viable bacteria has been taken to mean that the water was not contaminated from sewage, such a lack may also indicate the presence of a high titer of bacterial viruses, which, in turn, indicates an efficient septic-tank activity. Consequently, water may contain sewage seepage and not be typed as impure. Since several enteric viruses such as polio virus and hepatitis virus are carried in sewage water, this could be of considerable concern, although there is no evidence that these water-carried viruses have ever been responsible for specific infections.

On the basis of the above assumptions, preliminary studies were begun to determine whether natural waters contained viruses by using the zonal-centrifuge system which was designed specifically for small-particle and virus isolations. In preliminary studies, the B-V continuous-flow rotor and a known sewage virus, Type 3 coliphage, were used to determine the characteristics of the cleanout of this virus in the centrifuge system. Since this virus is one of the smallest sewage viruses, a thorough study of its trapping in a centrifuge would indicate the efficiency of using this system for water-analysis studies. Information gained from the initial T3 phage studies was then used to set flow rates and rotor speed for the potential isolation of virus-like particles from filtered sea water.

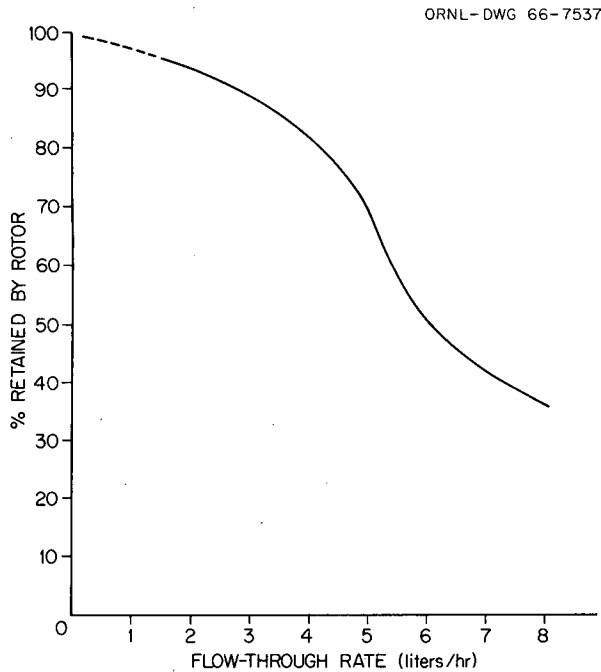


Fig. 3. Retention of T3 Phage in the B-V Continuous-Flow Rotor at 20,000 rpm as a Function of Flow-Through Rate.

Materials and Methods

Type 3 bacteriophage was grown on *Escherichia coli* strain B. The lysate titered at 2×10^{10} infectious virus particles per milliliter, as determined by plaque assay carried out as described by Adams.¹² The crude lysate was diluted 1:5 with 0.9% NaCl solution before being processed in the zonal centrifuge. The B-V zonal rotor system, which has been described elsewhere,¹³ was operated at 20,000 rpm for most of these studies. The sedimentation coefficient of the T3 phage in the lysate media was determined in the Model E analytical ultracentrifuge to be about 350. The T3 phage is reported to have an $S_{w, 20^\circ}$ of 473.¹⁴

¹²M. H. Adams, *Bacteriophages*, Interscience, New York, 1959.

¹³H. P. Barringer, N. G. Anderson, and C. E. Nunley, "Design of the B-V Continuous-Flow Centrifuge System," in *The Development of Zonal Centrifuges and Ancillary Systems for Tissue Fractionation and Analysis*, ed. by N. G. Anderson, Mono. 21, J. Natl. Cancer Inst. Mono. Ser., 1966.

¹⁴L. G. Swaby, "Some Biophysical Properties of the T3 Bacteriophage of *Escherichia coli*," Ph.D. Thesis, University of Pittsburgh (1962).

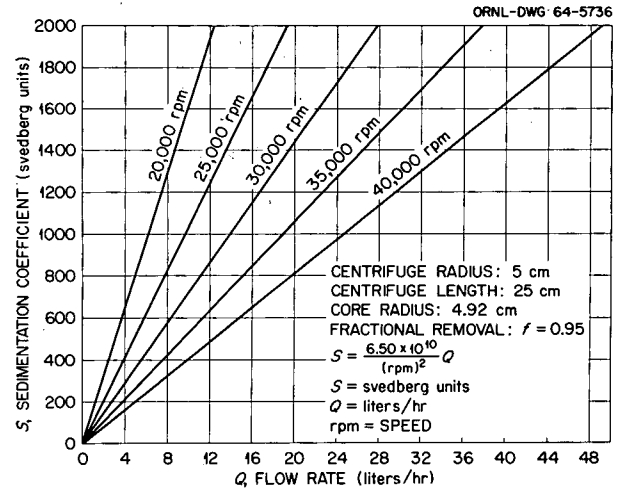


Fig. 4. Theoretical Cleanout Behavior of the B-V Rotor as a Function of Rotor Speed and the Sedimentation Coefficients of Retained Particles.

Figure 3 shows a cleanout curve obtained as determined by plaque assay of the T3 phage in the effluent stream from the rotor. The rotor speed was 20,000 rpm and the flow-through rate was varied from about 8 liters/hr to about 1.5 liters/hr. Operation of the B-V rotor at the top operating speed of 40,000 gives cleanouts of $\sim 99.99\%$ at 3 liters/hr, and greater cleanout can be obtained by slower flow-through rates. Figure 4 shows a family of theoretical curves calculated for 95% cleanout of any virus or particulate of any given sedimentation coefficient as a function of rotor speed and flow-through rate.¹⁵

Five gallons of filtered sea water from the Woods Hole Oceanographic Institute were passed through the B-V rotor at an average flow rate of 1.7 liters/hr at a rotor speed of 40,000 rpm. The material trapped in the rotor was recovered in a 155 ml volume. A portion of this concentrate was pelleted in the Oak Ridge No. 30 rotor tubes at 25,000 rpm for 48 hr. The pellet was resuspended in 1 to 2 ml of centrifuged sea water and examined in the electron microscope. The grids were prepared by a 10-sec contact of the sample with Formvar-coated copper grids and stained with 2% phosphotungstic acid. The samples were

¹⁵A. S. Berman, "Theory of Centrifugation. Miscellaneous Studies," in *The Development of Zonal Centrifuges and Ancillary Systems for Tissue Fractionation and Analysis*, ed. by N. G. Anderson, Mono. 21, J. Natl. Cancer Inst. Mono. Ser., 1966.

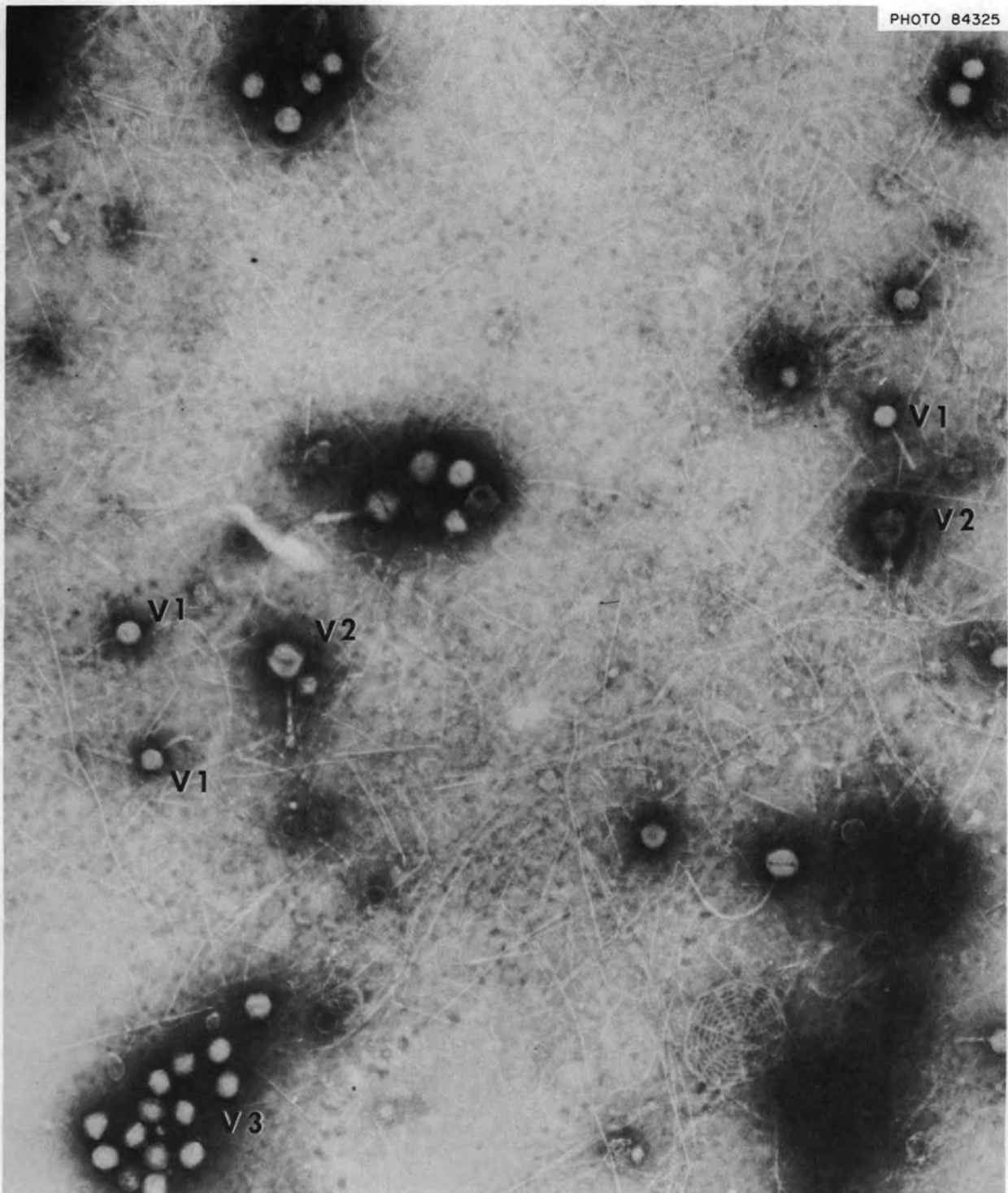


PHOTO 84325

Fig. 5. Electron Micrograph of Materials Removed from Sea Water in the B-V Continuous-Flow Rotor. Particles that appear morphologically to be virus-like are designated by the symbols V1, V2, and V3. 80,000 \times . Reduced 15%.

examined in an RCA EMU-3G microscope. A photograph obtained from one of these preparations is shown in Fig. 5.

Results and Discussion

The removal (cleanout) of the T3 bacteriophage from the crude phage lysate shows that the B-V zonal rotor is useful for the continuous-flow isolation of virus particles. At the rotor speed used for the T3 study, it was possible to vary the flow-through rate to obtain a sufficient number of samples to plot percent removal against flow rate and check the theoretical predictions. Good agreement between the theoretical and the experimental findings suggests that conditions can be programmed to isolate and concentrate particles of a certain size from large volumes of fluid.

Conditions chosen for the isolation of virus particles from natural water were such that particles having a sedimentation coefficient in sea water of 70 S or greater would be trapped with

better than 95% efficiency. This means that particles with sedimentation coefficients in the range of T2 phage (i.e., 1000 S) would be trapped with much greater than 95% efficiency. Although the particles reported here to be present in filtered sea water have not been thoroughly classified, there are many particles of various sizes in the range expected for bacterial viruses. The nature of the stranded material which comprises the background in the electron micrograph is not known. Material concentrated approximately 2000 \times from sea water is too highly concentrated for electron-microscopic analysis. In addition, it is evident that the largest number of particles detected are of the size and morphology of both odd-numbered and even-numbered coliphages. Identification of these particles as bacterial viruses would be presumptive evidence that the water they came from had a history of sewage. A more extensive survey of natural waters by this centrifugation technique possibly may permit certain mammalian enteric viruses to be isolated and characterized.

6. Development of Automated Chromatographic Systems

THE ASSAY OF SUGARS IN HUMAN URINE WITH THE PROTOTYPE CARBOHYDRATE ANALYZER

J. G. Green N. G. Anderson

The details of the design and application of an automated system for the analysis of soluble carbohydrates have been reported elsewhere.^{1,2} Whenever the system has been applied to an analytical problem, it has demonstrated a resolution superior to that of most other procedures. The assay of human urine appears to be another such case, since typical analyses reveal the presence of 21 to 26 discrete components of which ten have been previously described.³ This study was conducted to assess the feasibility of applying the automated system to urine samples and the suitability of such a study as a test problem for the more accurate, sensitive, and reliable system now being developed.⁴ Consequently, none of the studies have been carried to completion, and only preliminary survey results are reported here.

¹J. G. Green and N. G. Anderson, "Prototype Automatic Carbohydrate Analyzer," *Federation Proc.* **24**, 606 (1965).

²J. G. Green, "Automated Carbohydrate Analyzer: Experimental Prototype," in *The Development of Zonal Centrifuges and Ancillary Systems for Tissue Fractionation and Analysis*, ed. by N. G. Anderson, Mono. 21, J. Natl. Cancer Inst. Mono. Ser., 1966.

³J. F. Van Pilsum, pp. 186-90 in Sect. 53, *Biology Data Book*, ed. by Altman and Dittmer, FASEB, Washington, D. C., 1964.

⁴See "Automated Carbohydrate Analyzer: Status of a Laboratory Model" in this Section.

Experimental Procedures

First, we attempted to assess the diversity and variation of the soluble carbohydrates appearing in the urine of clinically normal subjects and to identify some of the components. The results of these studies are shown in Figs. 1 and 2. Attempts were made to conduct an elution in 8 hr, but the samples were too complex to permit the elution of the acidic and phosphorylated components in this time. However, these components have been separated with longer periods, though they are shown only in Fig. 2. In this system, where only simple linear gradients could be formed, most samples were found to fractionate best by elution with 200 ml of 15% stock buffer followed by a gradient consisting of 200 ml each of 30% and 60% stock buffer (54 g of sodium tetraborate and 17.5 g of boric acid in a liter), and acidic components were eluted with an additional 300 ml of stock buffer. The urine was buffered by the addition of stock buffer solution to 4% of total volume and 0.5 to 0.6 ml was placed directly on the column. The fact that a precipitate, which contained some carbohydrate, was formed when the urine was buffered indicated that additional study of sample preparation techniques should be performed. Effort to decolorize the urine with adsorbent carbon were successful, but some sugars also were removed by this treatment.

In another experiment, potential metabolic implications of the carbohydrates in urine were investigated. The urine samples obtained prebreakfast and after a high-carbohydrate meal were compared. To prevent obesity, one subject must restrict dietary intake, especially of carbohydrates, whereas the other individual gains no weight on

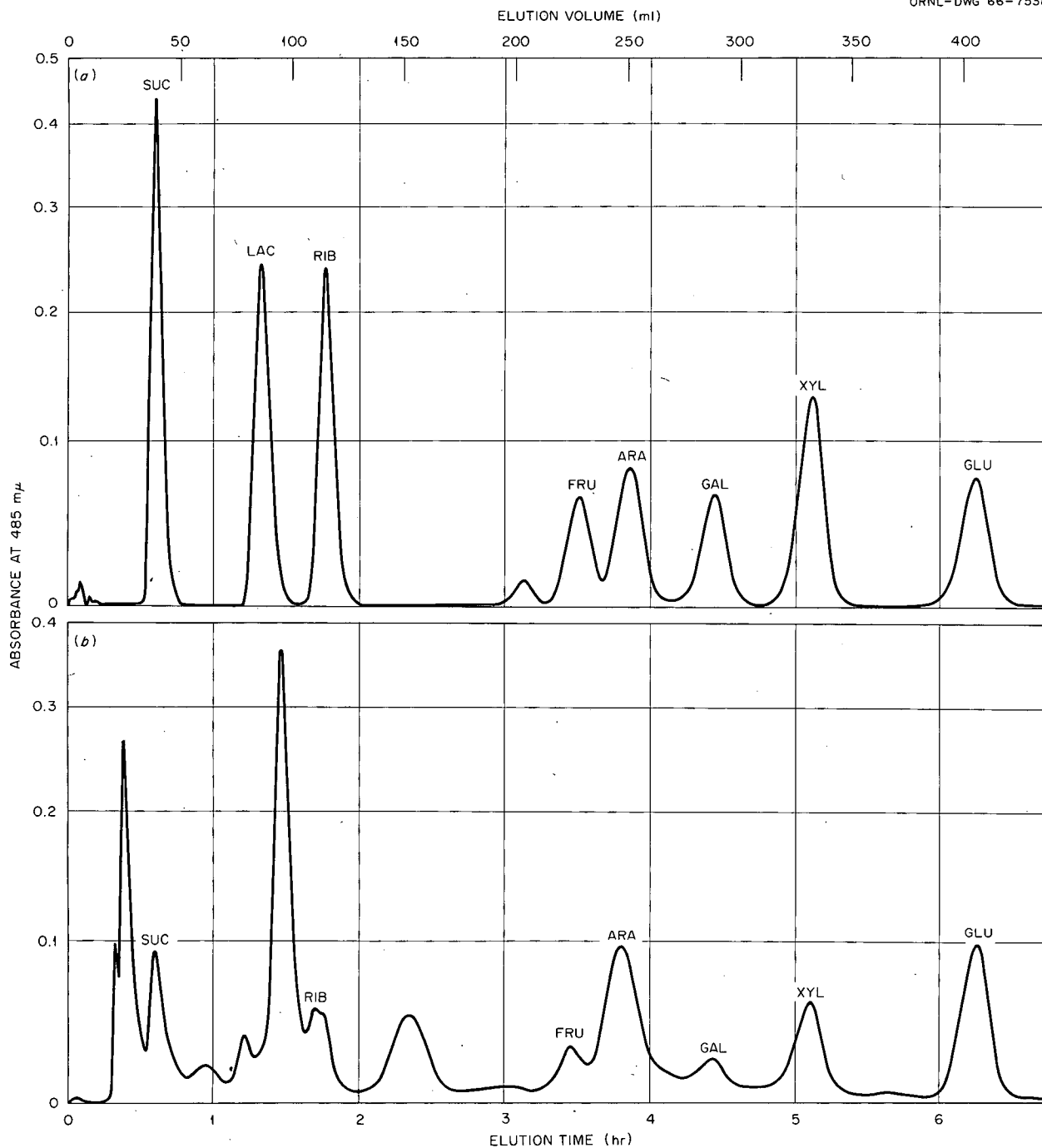


Fig. 1. Chromatograms Obtained from the Analysis of (a) a Mixture Containing $0.5 \mu\text{M}$ of Each of Eight Sugars Reported to Occur in Urine and (b) $600 \mu\text{l}$ of Clinically Normal Urine. Tentative identification of some components is shown in (b). Seven additional components that elute after glucose in urine are not shown. The gradient was formed from 210 ml of 15% stock buffer and 210 ml of 70% stock buffer.

an unrestricted intake. Chromatograms obtained from the experiment are shown in Fig. 2.

Two experiments have been performed to explore potential pathological applications of the study. In one case, urine from a diabetic patient who used insulin prophylaxis was assayed. In another case, immediate pre- and posttreatment voidings of a patient with Hodgkin's disease were analyzed. In this patient, the malady is being controlled with biweekly injections of vinblastine and chlorambucil. The results of these studies are shown in Figs. 3 and 4.

Results and Discussion

Chromatograms of normal human urine and a standard mixture containing eight components re-

ported to appear in urine are shown in Fig. 1. Although 19 components are indicated, only the neutral forms were eluted. Other analyses show the existence of at least seven additional anionic forms. Examination of the chromatograms in Fig. 4 obtained with samples from a patient with Hodgkin's disease reveals 28 neutral components; however, a different elution gradient was used. It is likely that resolution can be improved further by additional manipulation of elution parameters. The immensity of the task of identifying all the components is evident, and a more fruitful initial endeavor may be a survey approach with priority given to the identification of components that vary with disease.

Chromatograms from two individuals with differing caloric-intake tolerance are shown in Fig. 2.

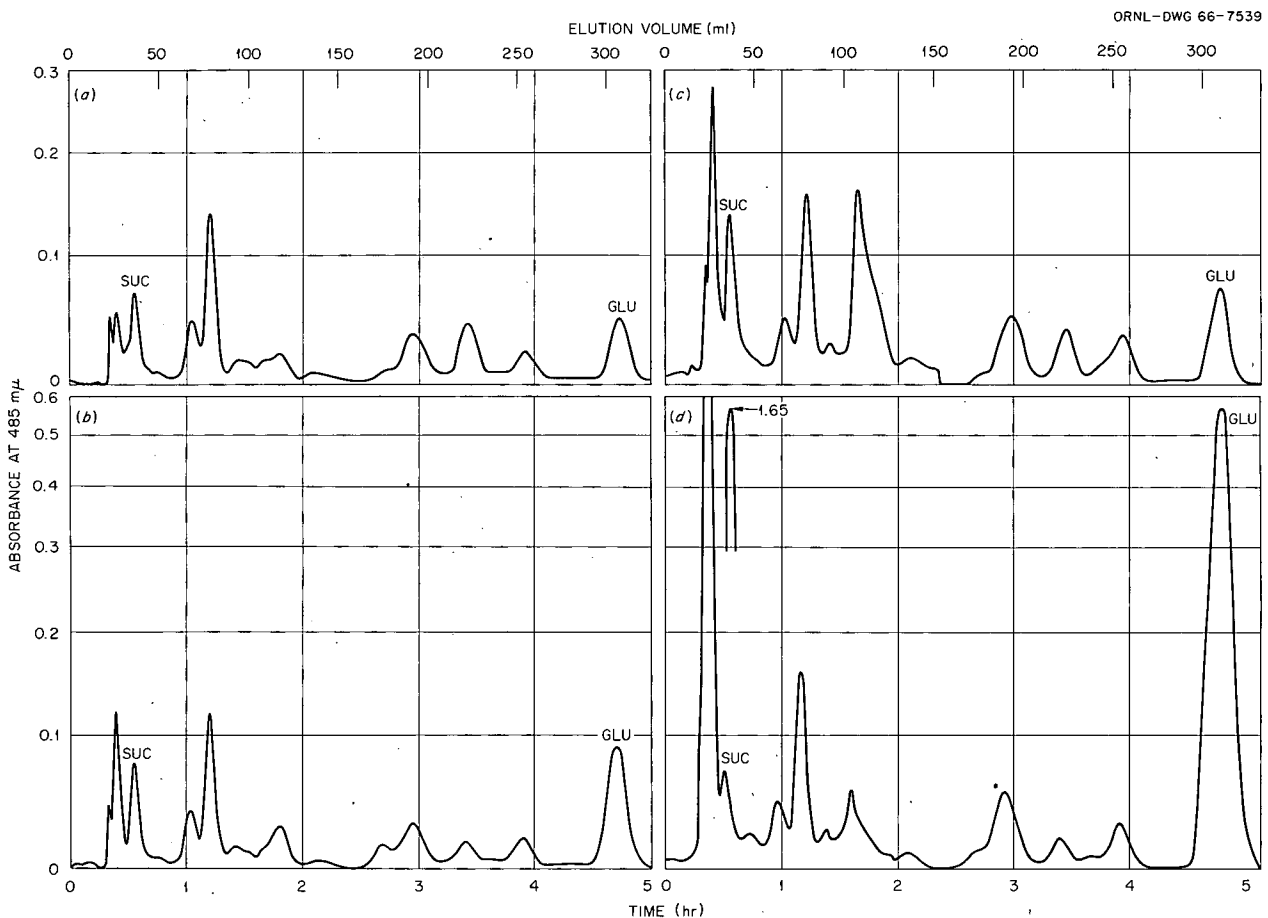


Fig. 2. Effects of Carbohydrate Uptake on Urine Composition. Chromatograms (a) and (b) were obtained from analysis of urine from an individual who must restrict caloric intake as a weight control measure. Chromatograms (c) and (d) were obtained from analysis of urine from an individual with no such dietary restriction. Chromatograms (a) and (c) were obtained with preingestion samples, and (b) and (d) with first postingestion voidings. Elution was performed with a gradient formed from 205 ml of 30% and 205 ml of 70% stock buffer.

Large differences in the magnitudes of certain urinary carbohydrates appear in peak No. 2, which is not yet identified, and in glucose (peak 16). No valid conclusions can be inferred from this single experiment; however, the data suggest the possible role of urinary excretion in dietary response.

In Fig. 3, chromatograms of clinically normal and diabetic (insulin controlled) individuals are shown. No significant differences can be seen. It would be of interest to also examine urine samples obtained from individuals where the malady is controlled by diet or by use of oral medications such as Orinase.

Chromatograms obtained from a patient undergoing treatment for Hodgkin's disease are shown

in Fig. 4. Changes in the magnitude of the peaks obtained from posttreatment voidings appear in the marked components. Insufficient information has been accumulated to warrant any conclusions; however, similar behavior has not been noted in clinically normal samples.

Although the studies reported here are rather cursory, certain conclusions can be made. The carbohydrate constituency of human urine is very complex, and much information may be gained from its definition. Additional attention should be given to sample-preparation techniques as well as to specific-elution procedures. The former can be studied with the prototype system, and elution and characterization should serve as an excellent test of advanced systems.

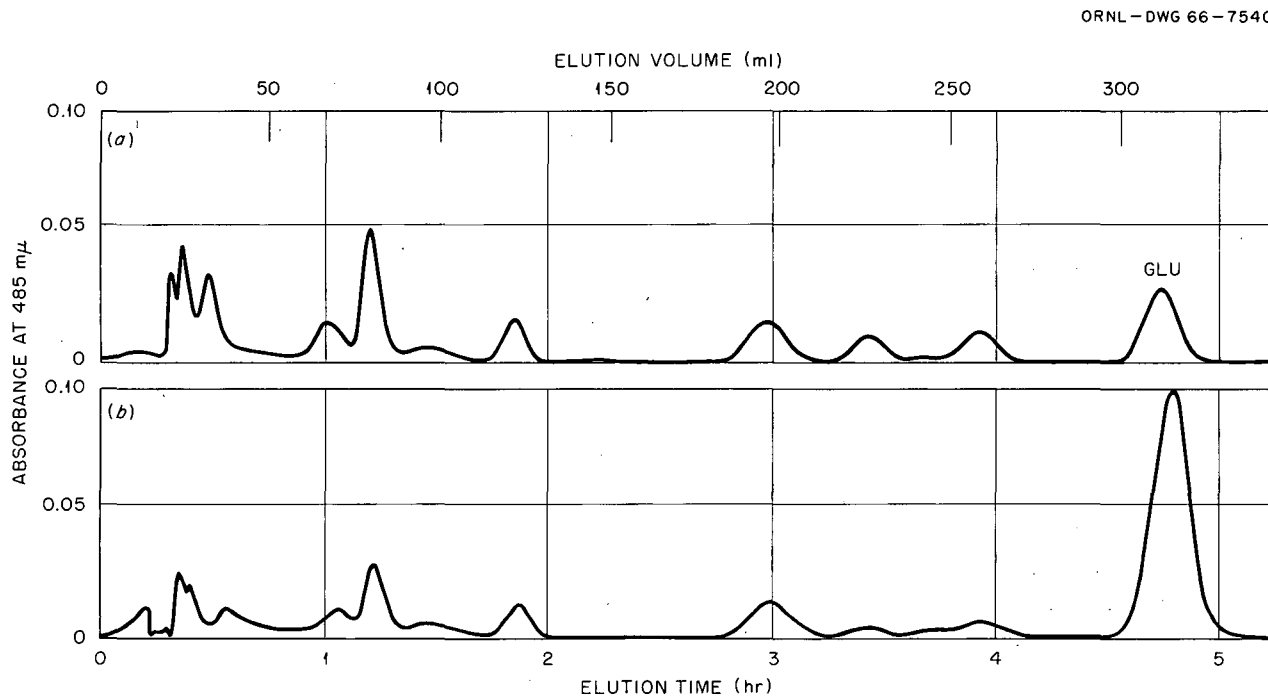


Fig. 3. Chromatograms Obtained from the Analysis of Urine from (a) a Clinically Normal Individual and (b) an Individual with Diabetes Mellitus Which Is Controlled with Insulin. The chromatograms appear to be similar, and the glucose level in chromatogram (b) is higher than observed averages, but not abnormally so. Elution was performed with 200 ml of 30% and 200 ml of 70% stock buffer. The sample size was 150 μ l.

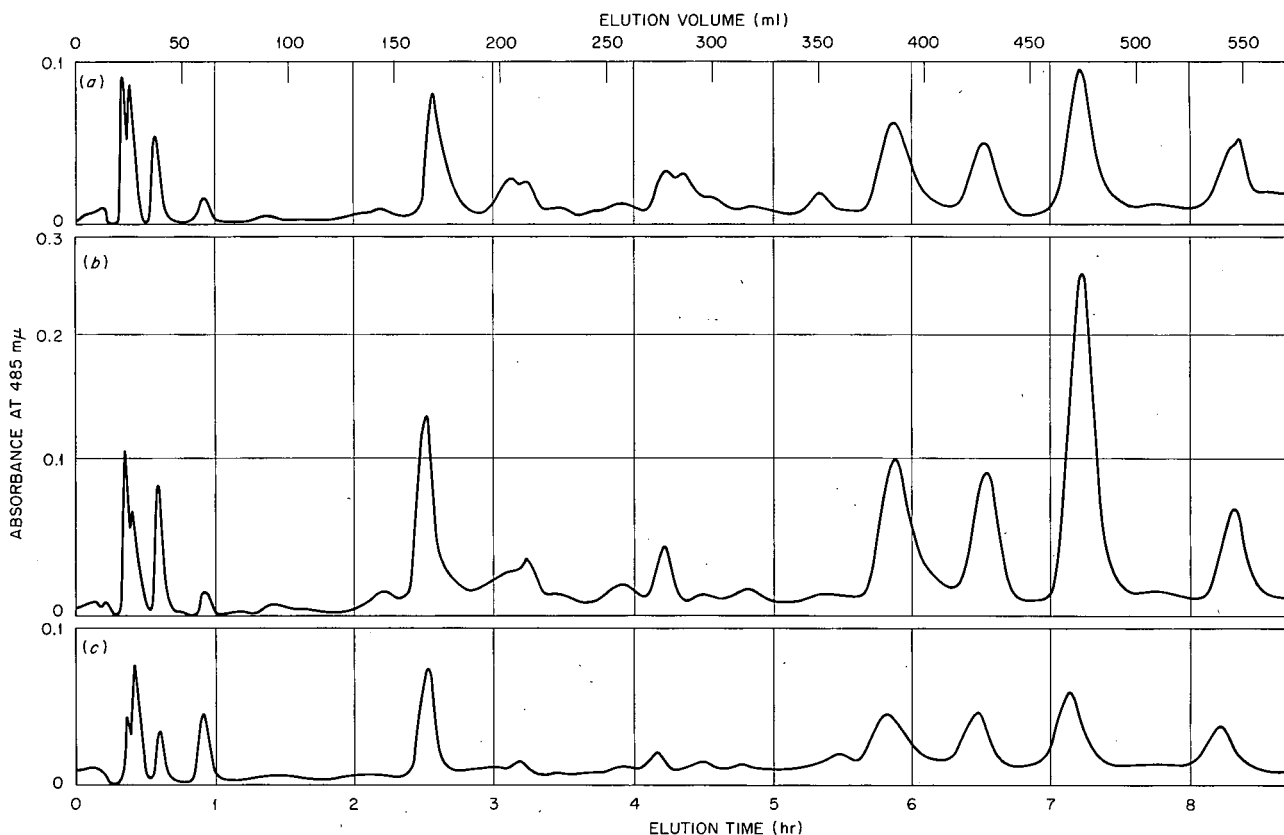


Fig. 4. Chromatograms Obtained from the Analysis of Urine from an Individual Undergoing Therapy for Hodgkin's Disease. The samples were voided at (a) premedication, (b) 3.25 hr after medication, and (c) 7.5 hr after medication. The significance of variation is not known. Elution was performed with a gradient formed from 300 ml of 15% and 300 ml of 60% stock buffer. Sample volume was 600 μ l.

CHROMATOGRAPHIC SEPARATION OF UV-ABSORBING COMPONENTS OF HUMAN URINE

C. D. Scott

Many of the molecular constituents of urine are known to have pathological significance. An automatic urine analyzer of high resolution would be a valuable clinical tool for use in diagnosis and treatment of many diseases. It would also be useful as a research tool in the study of human biochemistry.

A literature search has been started on the subject of urine analysis and urine constituents, and the experimental program has been directed toward development of a modified nucleotide analyzer for the separation of uv-absorbing constituents of urine. This analyzer gives reproducible results,

and it has separated and detected up to 93 uv-absorbing urine constituents, of which 11 have been tentatively identified.

Literature Search

A search of the literature of the last ten years which deals with urine analysis and the significance of urine constituents is being made with assistance from the MEDLARS computer search system at the National Library of Medicine, Bethesda, Md. More than 100 references have been found, and these are being abstracted in an annotated bibliography. Reference to 54 molecular constituents of human urine with pathological significance has been found, and many of these absorb uv light.

Modified Nucleotide Analyzer

The major experimental effort has been expended to develop a modified, automatic nucleotide analyzer for urine. This has included determining the reproducibility of the device, identifying some separated urine constituents, increasing the sensitivity of the ion-exchange separation column, and developing equipment.

The nucleotide analyzer is an automatic, high-resolution device for separating mixtures of nucleotides, nucleosides, and purine and pyrimidine bases.⁵ Gradient elution of an anion-exchange column (0.6-cm ID by 150 cm with Dowex 1-X8 resin) is used for separation, and a continuous uv spectrophotometer, operating alternately at two different wave lengths, is used for detection (Fig. 5). There are also provisions for temperature control of the column, volumetric measurement or collection of the column effluent, and continuous recording of the spectrophotometer output. A urine chromatogram is developed by placing a 1- to 2-ml urine sample on the anion-exchange column and eluting with an ammonium acetate gradient ranging from 0.015 M to 3 M at pH 4.4. A typical chromatogram takes about 40 hr and gives 60 to 80 different peaks.

Urine chromatograms from different people have many differences, but they also have many similar characteristics such as large uric acid and hippuric acid peaks. Some of these differences can be attributed to diet. Figure 6 shows a comparison between the urine of a normal subject on a high-protein, low-vegetable diet and urine from the same subject on the same diet with the addition of coffee and aspirin. Several new chromatographic peaks appear with the addition of coffee and aspirin.

Twenty-seven urine samples (24-hr composites) from normal subjects have been collected and processed, and a total of 48 tests with urine have been made on the modified nucleotide analyzer. There has been no apparent loss of resolution, and reproducibility is adequate.

Identification of Separated Urine Constituents

Urine constituents indicated by the chromatogram are being tentatively identified by determining the

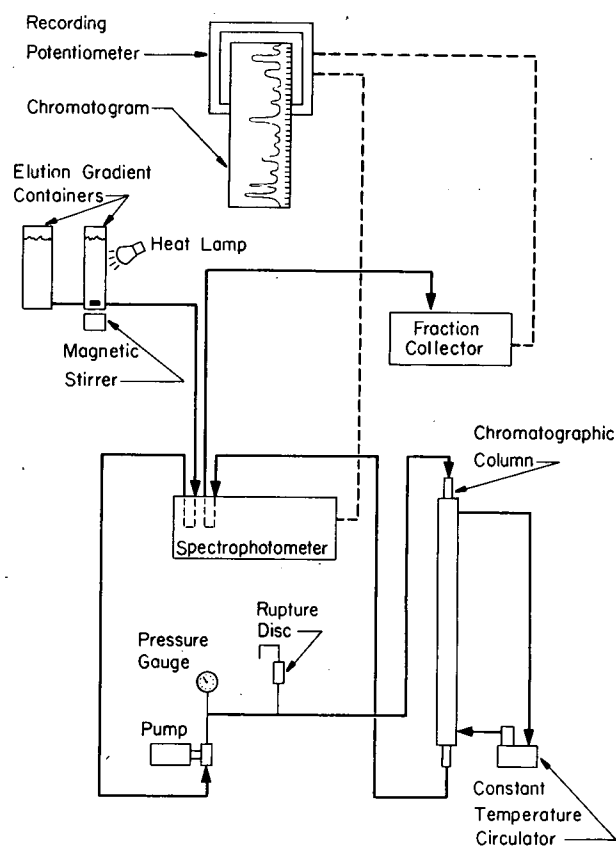


Fig. 5. Schematic Diagram of an Experimental Urine Analyzer.

position and the 280 $m\mu$ /260 $m\mu$ absorbance ratio of known standard peaks in the urine chromatogram and by comparing them with known peaks. This gives two independent means of comparison, both of which should be characteristic of specific constituents. The position of 20 standard peaks has been established, and the following 10 urine peaks have been tentatively identified in urine samples (Fig. 7).

xanthine	<i>p</i> -hydroxy cinnamic acid
hypoxanthine	homovanillic acid
urocanic acid	vanillic acid
uric acid	kynurenic acid
hippuric acid	acetylsalicylic acid

The technique of identification is dependent on isolating essentially pure components in each of the chromatographic peaks. In some tests effluent fractions were collected, and uv-absorption

⁵N. G. Anderson *et al.*, "Analytical Techniques for Cell Fractions. III. Nucleotides and Related Compounds," *Anal Biochem.* 6, 155 (1963).

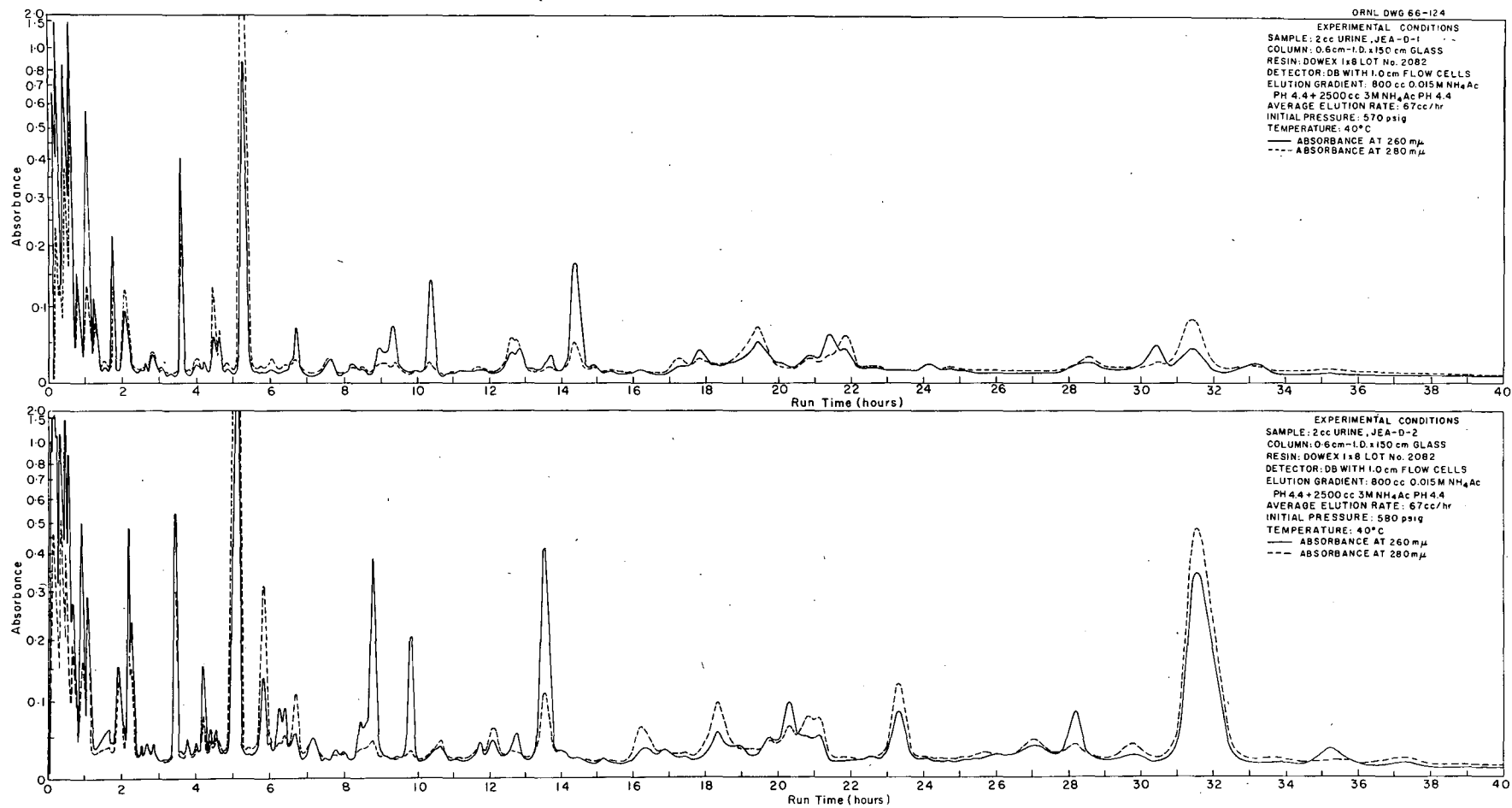


Fig. 6. Typical Urine Chromatograms Showing the Effect of Diet. Top, high-protein diet; bottom, high-protein diet with aspirin and coffee.

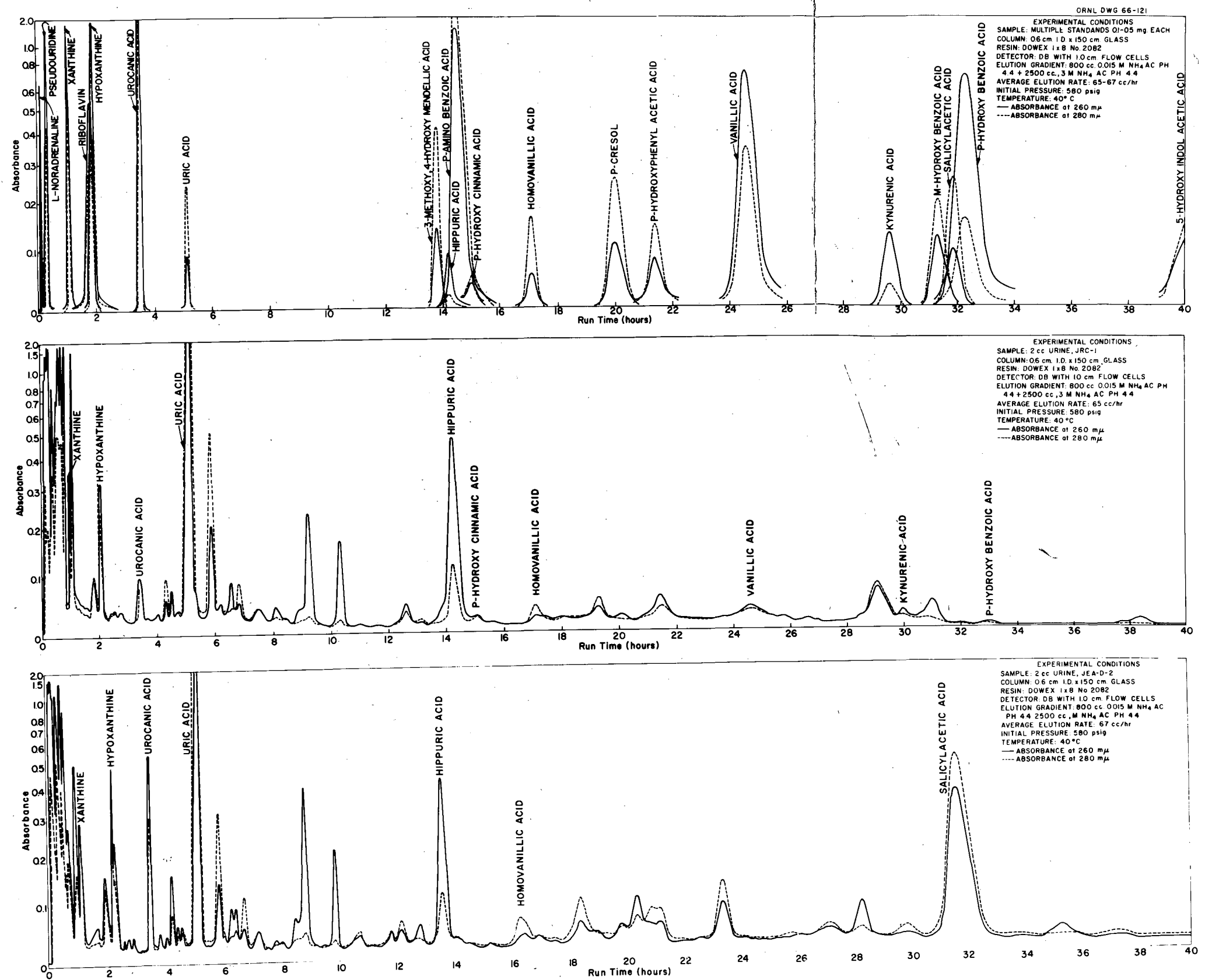


Fig. 7. Chromatographic Positions of 20 Known Standards and Tentative Identification of 10 Urine Chromatographic Peaks.

spectra were made of several such fractions within a few of the single chromatographic peaks. The absorption spectra were different for some of the fractions collected within the same chromatographic peak, thus indicating more than one component in the single peak. Recent tests with ion-exchange columns giving higher resolution also show that some chromatographic peaks are composed of several constituents. For example, the uric acid peak can be resolved into at least six other peaks. This shows the importance of obtaining the greatest possible resolution in the anion-exchange columns before definite identification is made.

Another method for verifying the identity of the chromatographic peaks will be by use of a technique developed by Cohn⁶ and others in which absorbance ratios of the purified unknown at different pH's are used for characterization.

⁶W. E. Cohn, "Pseudouridine, a Carbon-Carbon Linked Ribonucleoside in Ribonucleic Acids: Isolation, Structure and Chemical Characteristics," *J. Biol. Chem.* 235, 1488 (1960).

Ion-Exchange Properties and Column Resolution

The separating power of the ion-exchange column must be increased to circumvent the problem of peak identification and to make it possible to quantify the urine constituents. Anderson *et al.*⁵ found in their earlier work that different batches of the same ion-exchange material (Dowex 1-X8) had different separation powers for the nucleotides and related compounds; however, the reasons for these differences were not determined.

Recent experimental results show that particle size of the ion-exchange resin is very important. A continuous water elutriation system was designed and built for size-separation of the resin. This system is composed of a 4-in.-ID elutriation column, a constant-level water-feed system with flow-rate control, a slurry pump for resin feed, and product receivers for the overhead and bottom fractions (Fig. 8). The elutriation column is composed of a section of constant diameter at the top for feed introduction and particle sizing and

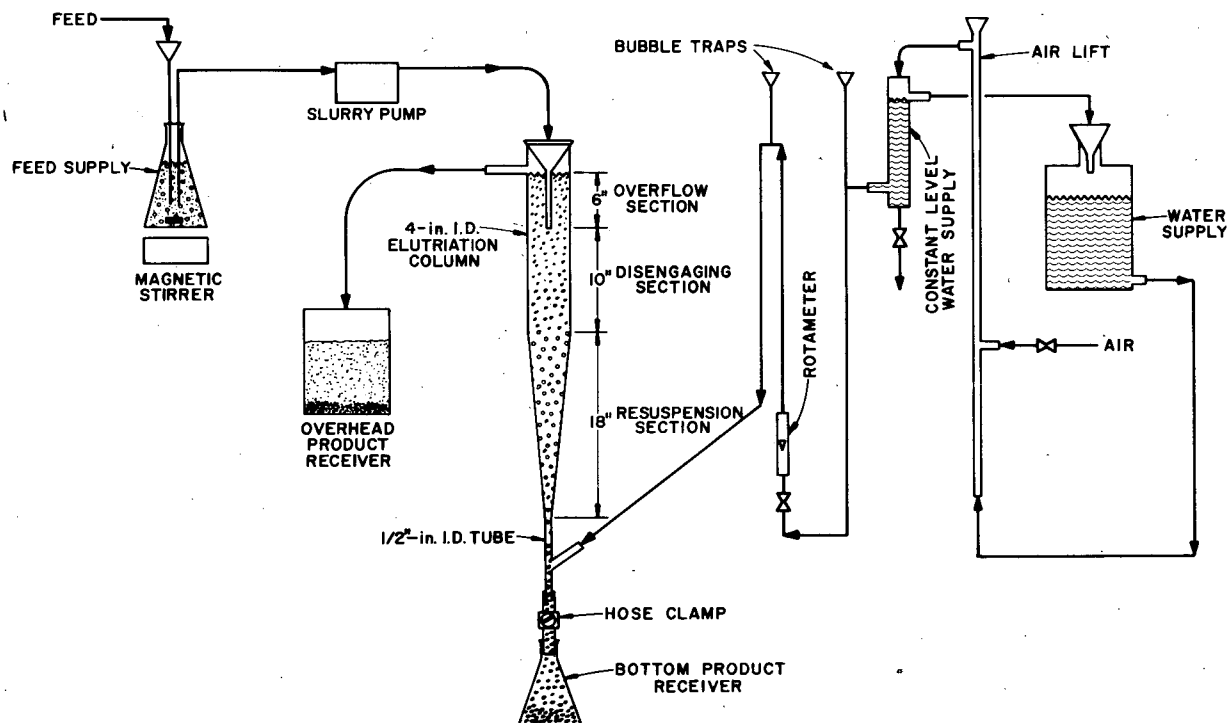


Fig. 8. Automatic Elutriation System for Size Fractionation of Ion-Exchange-Resin Particles.

a lower, tapered section where fine particles are resuspended.

This system is capable of separating resin into different sizes in the range of 5 to 50 μ in diameter. The overhead fraction is closely sized in one pass, but the bottom fraction usually requires two or three passes for removal of all of the small particles.

A batch of anion-exchange resin (Dowex 1-X8), known to be good for nucleotide separation, was separated into three size ranges of 5 to 10 μ , 10 to 20 μ , and >20 μ . These materials were loaded into identical stainless steel columns, 0.45-cm ID by 150 cm, and urine samples were separated on each using the same operating conditions except for pressure. The smaller resin particles gave much better separation. A semiquantitative indication of the separating power was a comparison of the number of chromatographic peaks which were resolved in each case.

Resin Size (μ)	No. of Peaks	Initial Pressure (psig)
5-10	66	1500
10-20	55	580
20	42	350

The best separation has been obtained with a stainless steel column, 0.62-cm ID by 150 cm, filled with 5-to 10- μ resin, and operating at 1500 psig. Ninety-three urine chromatographic peaks were resolved by this system, compared with 60 peaks with the original system.

Other properties of the ion-exchange resin and the effects of different column parameters are also being investigated.

Equipment Development

High-pressure operation is necessary to take advantage of the high resolution of small resin particles. Stainless steel columns were designed and built for operation to 4000 psig. They have proved to be simple to fabricate and operate. A method of sample injection using two three-way valves has also proven satisfactory. With this method, part of the delivery line is used as a sample holder, and the sample is flushed through the line into the columns with the normal delivery of the elution system.

CHANGES IN SOLUBLE CARBOHYDRATES OF SYNCHRONIZED TETRAHYMENA

J. G. Green

G. L. Whitson

Changes in soluble carbohydrates of synchronized *Tetrahymena* are being investigated using a prototype carbohydrate analyzer.⁷ Previous investigations had been restricted to the study of only limited numbers of soluble components.⁸ The availability of large quantities of *Tetrahymena* synchronized by heat shock and the use of this analyzer permits the examination of the total content of soluble sugars in an extract with a single analysis.

Methods

Several liters of log phase cells of *T. pyriformis*, strain GL, were synchronized using the heat-shock method described by Scherbaum and Zeuthen.⁹ About 85% of the cells were in the process of cell division 90 min after the last heat shock. Cells used in this study were sampled at EH (end of last heat shock), at 75 min after EH (just prior to cell division), at 90 min after EH (during peak of cell division), and at 135 min after EH (after cell division had occurred). Cells were pelleted by centrifugation, and 1-ml aliquots of packed cells were lysed with 5 ml of saturated indole solution in water buffered to pH 7.0 with tris (hydroxymethyl) aminomethane. The soluble sugars were then extracted with cold 80% ethanol, and the extract was cleared by centrifugation. The supernatant solution was evaporated under vacuum at room temperature and reconstituted in 2 ml of borate elution buffer; 1 ml of this sample was analyzed for the soluble-sugar content. In addition, 150 ml of medium in which the cells were grown was evaporated to dryness in vacuo and

⁷J. G. Green, "Automated Carbohydrate Analyzer: Experimental Prototype," in *The Development of Zonal Centrifuges and Ancillary Systems for Tissue Fractionation and Analysis*, ed. by N. G. Anderson, Mono. 21, J. Natl. Cancer Inst. Mono. Ser., 1966.

⁸S. C. Chow and O. H. Scherbaum, "Occurrence of Acid Soluble Phosphorylated Deoxysugars in Division Synchronized Cells," *Exptl. Cell Res.* 40, 217-23 (1965).

⁹O. H. Scherbaum and E. Zeuthen, "Induction of Synchronous Cell Division in Mass Cultures of *Tetrahymena pyriformis*," *Exptl. Cell Res.* 6, 221-27 (1954).

reconstituted in 4 ml of borate buffer, and 1 ml of this material was analyzed for sugar content.

To obtain extracts suitable for both the derivation of effective elution gradients and the identification of separated components, log-phase cells were harvested from identical medium, and extracts were prepared. Extracts from such cells would yield the desired information with minimal effort.

Results and Discussion

The first chromatograms obtained from the cell extracts are shown in Fig. 9 and from the medium in Fig. 10. It is obvious that the extracts reflect

changes occurring during the cell cycle, but the significance of these changes remains to be assessed. The identity of a number of the components in an extract from log-phase cells is indicated in Fig. 11. It can be seen that the chromatogram obtained from these cells differs from those obtained from synchronized cells and reflects the averaging tendency of such cultures. Certain components do not give good chromatographs with the known materials that were tested. Additional experimentation is planned (1) to establish suitable sample-preparation procedures, (2) to improve system resolution, (3) to identify unknown varying components, and (4) to assess the significance of the changes. The study of changes in the growth medium during the cell cycle presents an especially challenging problem.

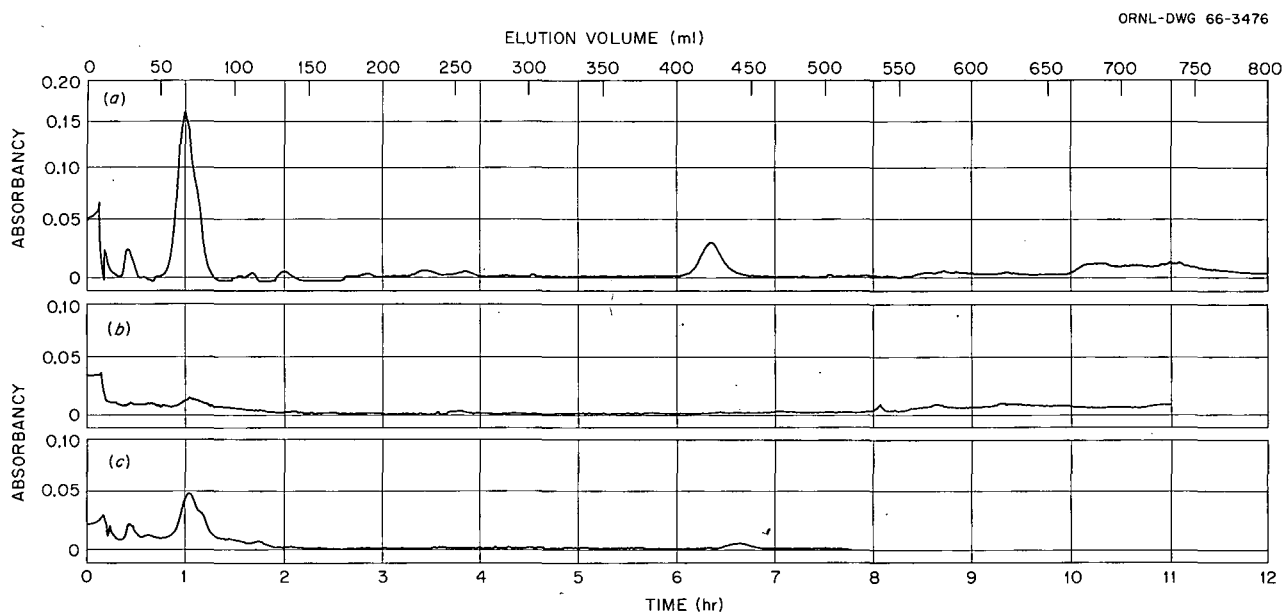


Fig. 9. Soluble Sugars Extracted from Synchronized *Tetrahymena pyriformis*. Samples containing equal numbers of cells were taken at (a) the end of the heat period, (b) 90 min after the heat period, and (c) 135 min after the heat period. See text for details.

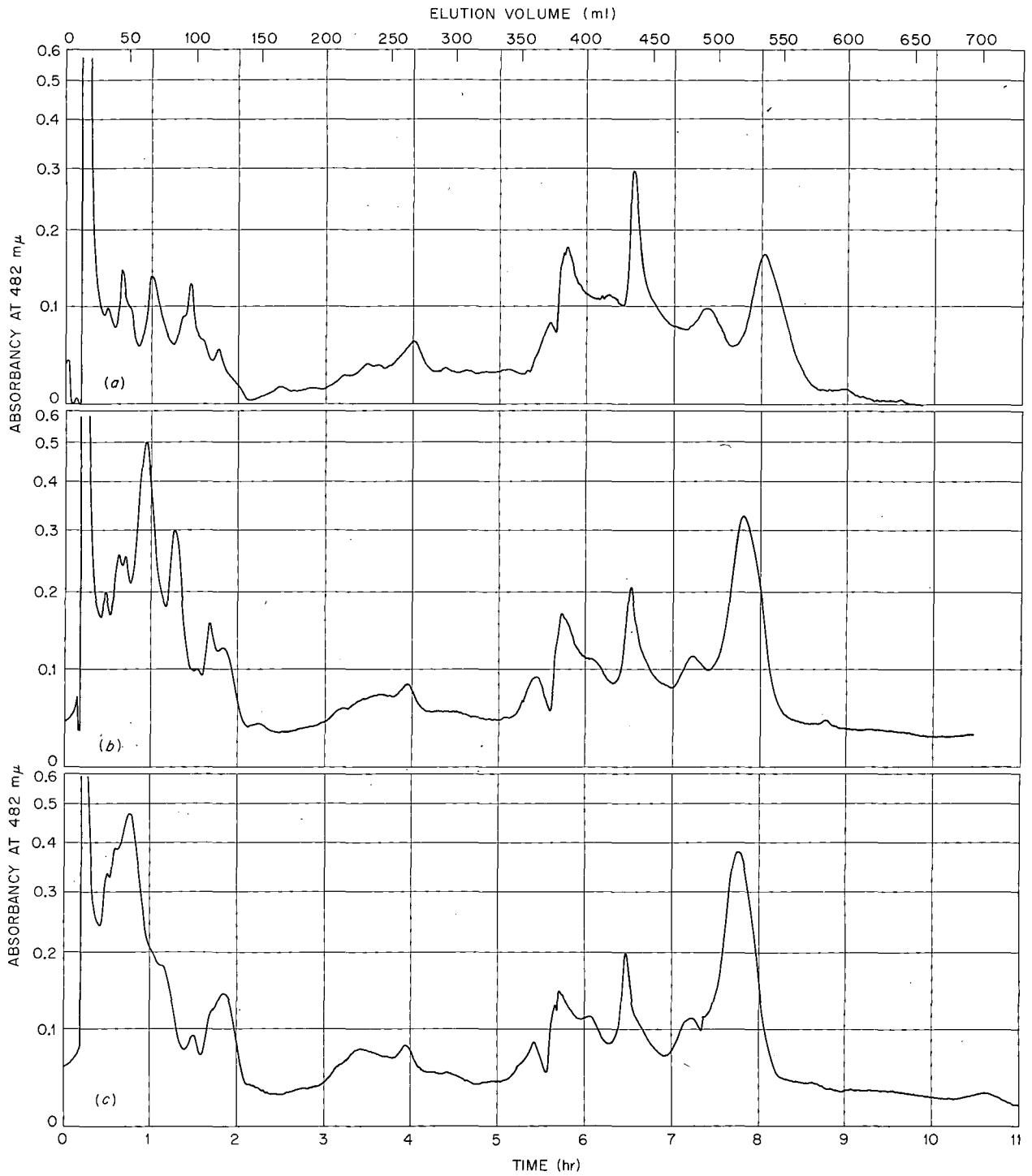


Fig. 10. Chromatograms Obtained from the Analysis of the Growth Medium of Synchronized Cultures of *Tetrahymena pyriformis*. The samples were taken at (a) before the inoculation of the culture vessel, (b) at the end of the heat period, and (c) 135 min after the end of the heat period.

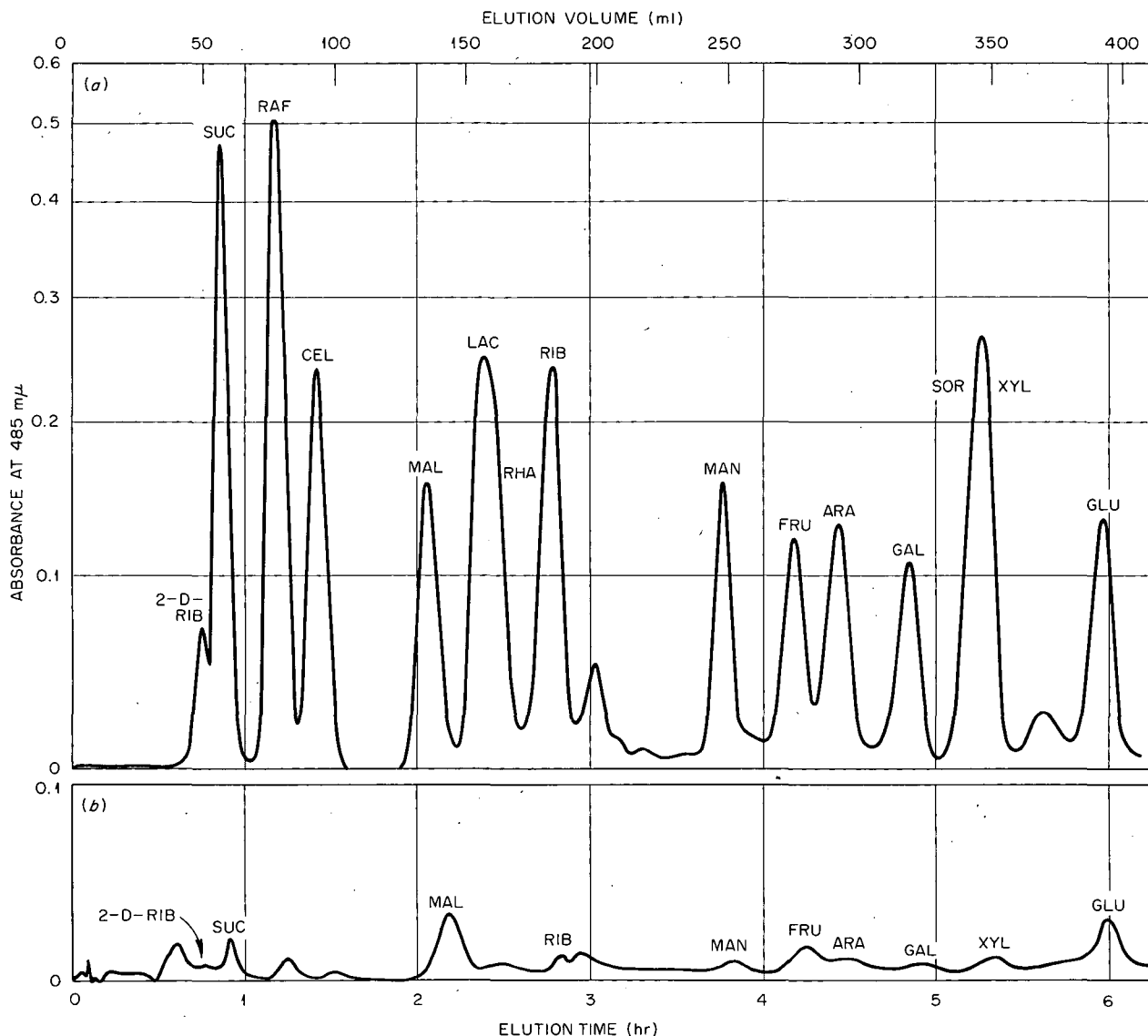


Fig. 11. Chromatograms of Samples of (a) 15-Component Standard Containing 0.5 M of Each Sugar and (b) 1 ml of Extract Obtained from Log-Phase Cells. In the latter case, tentative identification of some components is indicated. The elution gradient consisted of 200 ml of 15% stock buffer and 200 ml of 70% stock buffer.

FLAME-IONIZATION ANALYZER FOR THE DETERMINATION OF CARBON IN LIQUID STREAMS OR SOLID SAMPLES

R. H. Stevens

The determination of the minimum detectable weight of carbon and the sensitivity of the flame-ionization analyzer described in the last two re-

port periods^{10,11} was complicated by the effects of precombustion evaporation of the sample and an apparent nonspecificity to carbon from surface ionization of other elements. These two effects

¹⁰R. H. Stevens, *Joint NIH-AEC Zonal Centrifuge Develop. Program Semiann. Progr. Rept. Jan. 1-June 30, 1964*, ORNL-3752, p. 56.

¹¹R. H. Stevens, *Joint NIH-AEC Zonal Centrifuge Develop. Program Semiann. Progr. Rept. July 1-Dec. 31, 1963*, ORNL-3656.

have been examined further, and the response of the analyzer has been characterized to a degree by use of a new jet design. This design permits the sample-bearing wire and the hydrogen-nitrogen fuel mixture to pass through a common horizontal bore of heavy-walled construction which leads directly into the analyzer flame. The loss of sample by early evaporation or other means is thus precluded, allowing a more quantitative evaluation of carbon specificity in the response of the analyzer, especially in the case of organic samples having a high metal content (e.g., sodium acetate).

The new jet design is shown in an enlarged cross-sectional view in Fig. 12. The wire, moving to the left, bears the sample first into a nitrogen-swept passage at the right end of the assembly to assist in removing any last traces of solvent from dissolved samples. When the sample moves past the nitrogen gas inlet and into the nosepiece, volatile material leaving it by evaporation or pyrolysis is immediately swept into the flame by the nitrogen gas flow in this direction. By this means, none of the sample is lost before reaching the

analyzer flame envelope. The ionization current generated during the sample combustion is collected by a positively charged screen cylinder which surrounds the flame envelope indicated by the dashed lines in Fig. 12. Using this jet and collector assembly, we obtained reproducible signals from replicate samples containing from 10^{-6} g to as little as 2×10^{-9} g of carbon. Figure 13 is a log plot of the average pulse charge obtained from samples of pure hydrocarbons over this weight range. The sensitivity demonstrated by this data varied from about 0.004 to 0.0085 coulomb per gram of carbon, depending upon sample size. This variation resulted from an "air-starvation" problem in the flame, presumably caused by poor air circulation through the fine-wire-screen collector surrounding the flame envelope. This was noted especially at the higher sample weights and will be corrected in future work by replacing the screen with a polarized single-wire collector.

The above results were shown to be valid for several different hydrocarbons, and the highest sensitivity value obtained, 0.0085 coulomb per

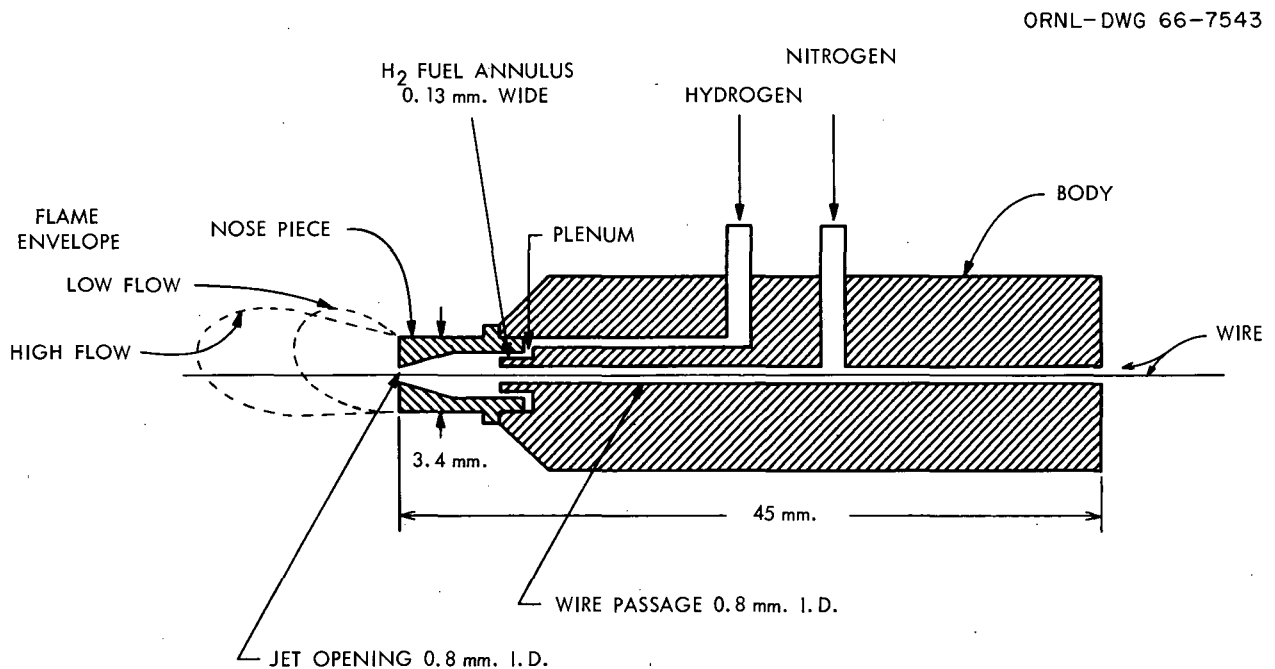


Fig. 12. Cross-Sectional Schematic View of Coaxial-Jet Assembly Showing Hydrogen, Nitrogen, and Wire Passages.

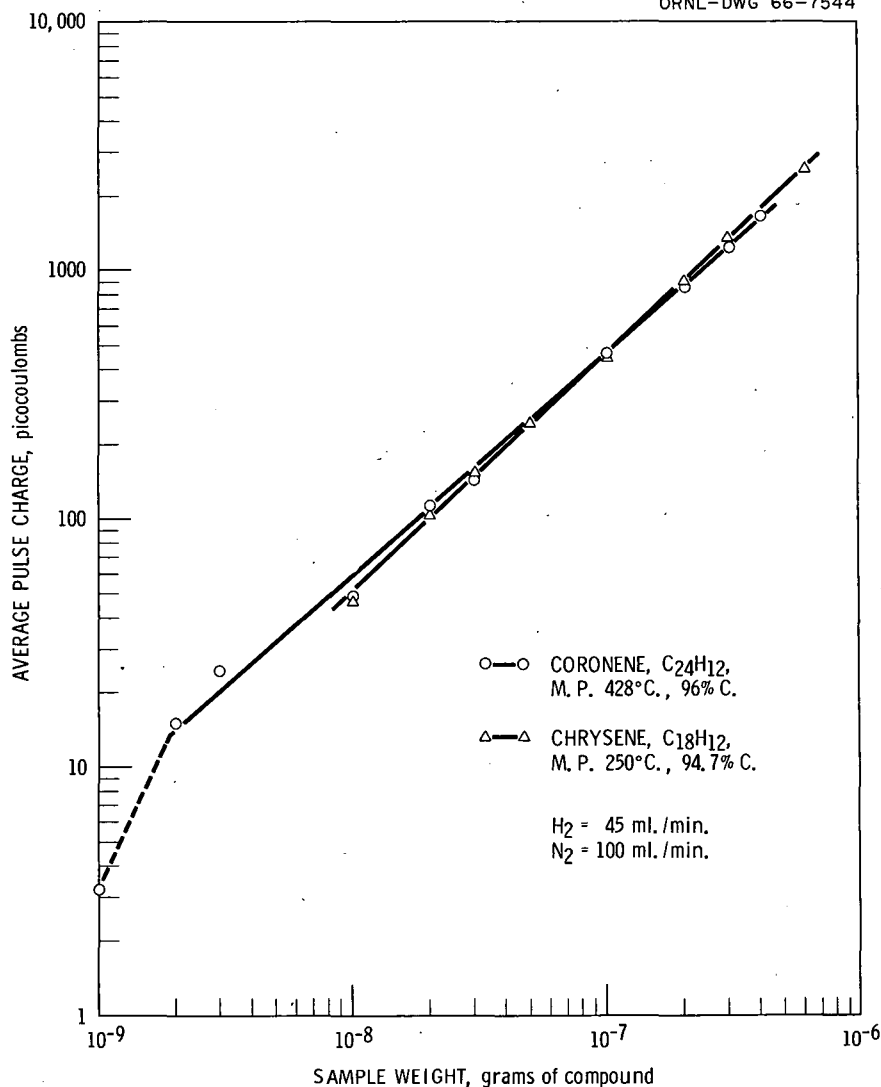


Fig. 13. Analyzer Response to Increasing Weights of Discrete Hydrocarbon Samples.

gram of carbon, was comparable to that reported for other commercial flame detectors using gaseous samples.

The response of the analyzer to organic materials having a relatively high metal content was also examined to determine whether the presence of the metal in the flame interfered with carbon specificity. Samples of sodium acetate were used, since sodium is a common constituent of natural products and is known to ionize in a flame. The signals collected from the combustion of samples containing 10^{-5} and 10^{-6} g of sodium acetate were about six times greater than expected on the

basis of sample carbon content in the case of negative-ion and electron collection from the flame. This was about 100 times greater than anticipated when positive ions were collected. These anomalies might be explained for negative-charge collection by the fact that sodium oxide is a good thermionic emitter at red heat on the surface of a metal wire; the well-substantiated observation that sodium salts emit positive ions readily under the same conditions could explain the large positive-current collection. The fact that many other metals act in the same manner as sodium suggests that the response of this analyzer will not be

specific for carbon when the sample contains a metals content near, and probably much less than, that of sodium acetate (28%), even for negative-charge collection. The lack of specificity for carbon, however, does not alter its applicability as a detector for flowing streams, such as liquid chromatographic column effluents, since the detection of the presence of the passing fraction is of interest in many instances.

The areas of primary application of the analyzer now appear to be as a liquid-chromatography column monitor and for analyzing the carbon content of individual biological cells. The latter leads to the assumption that signals from many discrete cells could be used to determine the population and carbon-content distribution of such particulates in a liquid suspension through the use of pulse-integrating and pulse-height-analyzing techniques.

AUTOMATED CARBOHYDRATE ANALYZER: STATUS OF A LABORATORY MODEL

J. G. Green R. H. Stevens
N. G. Anderson

The design and performance of a prototype automated carbohydrate analyzer have been discussed elsewhere.^{12,13} When the system appeared to be relatively trouble free and separations were acceptable, development was started on a routine-laboratory-use model that would incorporate the latest techniques for high resolution, such as high-pressure elution,¹⁴ in systems employing fine-particle ion exchangers. Photographs of the nearly completed analyzer are shown in Figs. 14 and 15, and a flow diagram showing the relationship of various components is shown in Fig. 16. Final testing of the system will begin after a sealing problem involving reagent pumps is solved.

¹²J. G. Green and N. G. Anderson, "Prototype Automatic Carbohydrate Analyzer," *Federation Proc.* **24**, 606 (1965).

¹³J. G. Green, "Automated Carbohydrate Analyzer: Experimental Prototype," in *The Development of Zonal Centrifuges and Ancillary Systems for Tissue Fractionation and Analysis*, ed. by N. G. Anderson, Mono. 21, J. Natl. Cancer Inst. Mono. Ser., 1966.

¹⁴J. G. Green, C. E. Nunley, and N. G. Anderson, "High Pressure Column Chromatography I. Separation of Bases, Nucleosides, and Nucleotides," in *The Development of Zonal Centrifuges and Ancillary Systems for Tissue Fractionation and Analysis*, ed. by N. G. Anderson, Mono. 21, J. Natl. Cancer Inst. Mono. Ser. 1966.

In this report, the specifications guiding the overall design and the mechanical aspects of the system are described, with emphasis placed on unique features.

Design Specification and Implementation

Three major concepts, high-resolution chromatography, easy maintenance, and good flexibility, guided the design of the analyzer. These concepts, their implementation, and their implications are described in the following paragraphs.

The analytical system should incorporate the latest findings in high-resolution chromatography. The greatest gain in overall resolution arises from the use of spherical ion-exchange resins in the size range of 5 to 10 μ or less. However, the use of such exchangers results in high back pressure from columns, and the problem is further complicated by the fact that higher resolution permits faster flow as well as shorter columns. In the new analyzer, all-steel (316SS) columns are used in two lengths. All fittings will withstand pressures over 1800 psi when only hand tightened; however, pressures in the system are limited to 1250 psi (25% over the rated pump capability) by pressure-relief valves. The high-pressure capability is carried through the system to the vented diffuser column.

Since it was impractical to place samples on opaque columns by conventional procedures, a sample-injection valve was incorporated into the elution system. By the simple exchange of sample loops, it is possible to inject samples varying from 0.1 to 1.5 ml. To prevent transfer to the column of the torque required to operate the sample-injection valve, it is operated by a rotary actuator controlled by the programming system. Very little modification will be required to adapt the system to automatic stream sampling. When in use, the sample injector becomes an integral part of the top of the column; therefore, the sample moves directly to the resin when introduced into the elution system.

All operations involved with an analysis, except filling of liquid containers and the sample loop, are fully programmed, but may be operated independently or switched out of the program. In addition, auxiliary receptacles for the various program functions may be used to operate other systems. When sample injection and programming



Fig. 14. Front View of Improved Carbohydrate Analyzer.

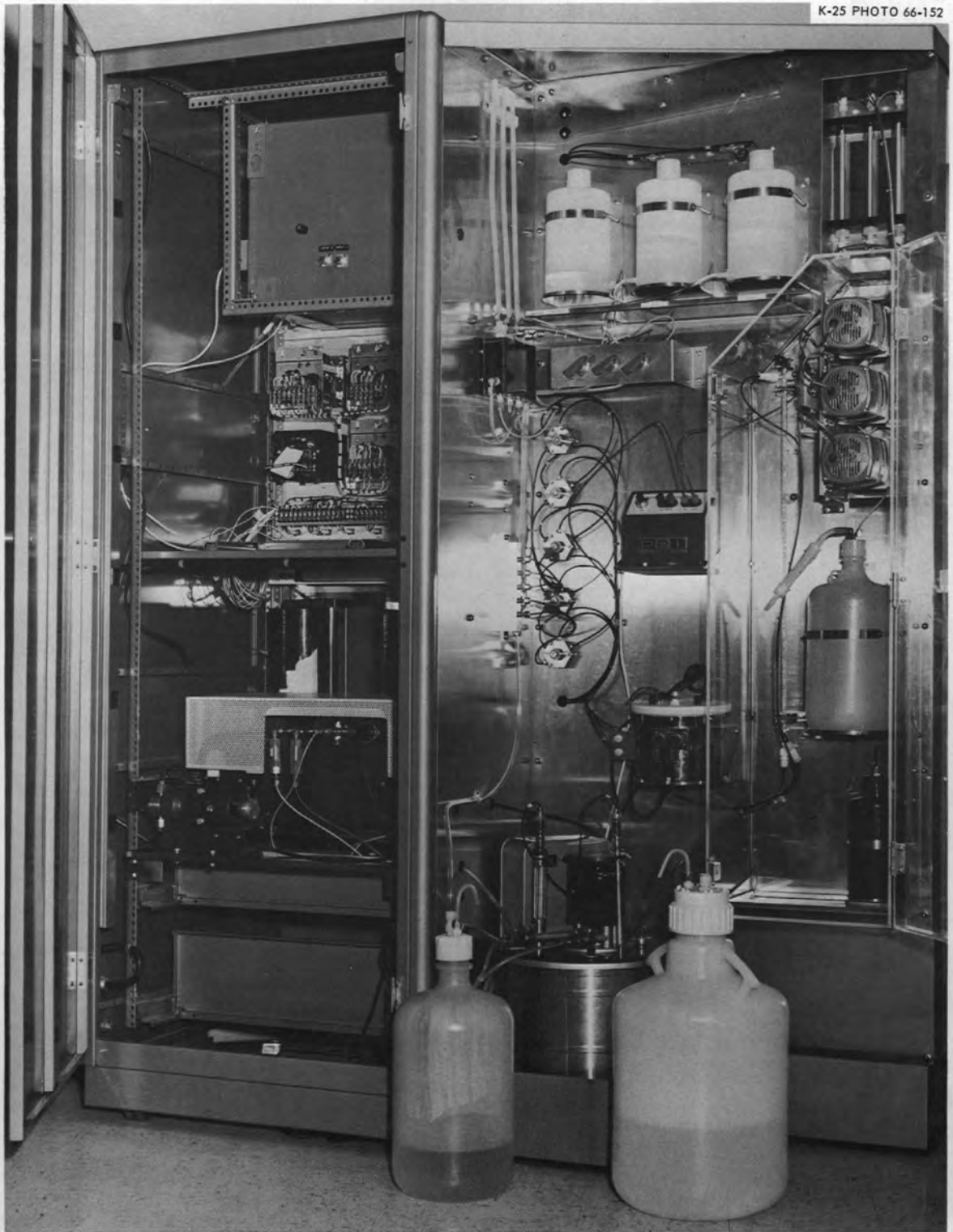


Fig. 15. Rear View of Improved Carbohydrate Analyzer.

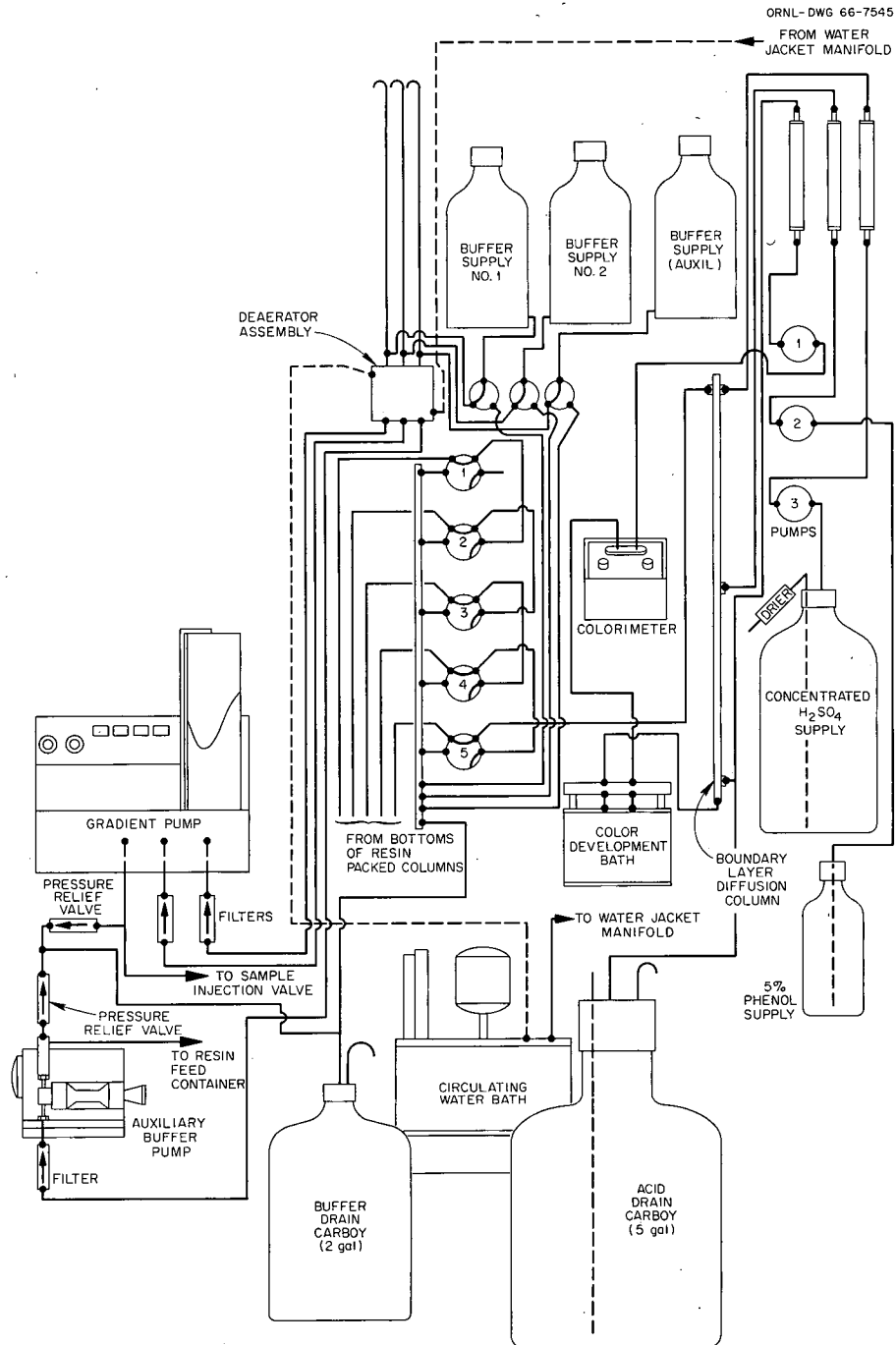


Fig. 16. Diagram of the Liquid-Flow Systems of the Improved Carbohydrate Analyzer. The locations of the various components on the diagram correspond to their placement in (a) Fig. 14 and (b) Fig. 15.

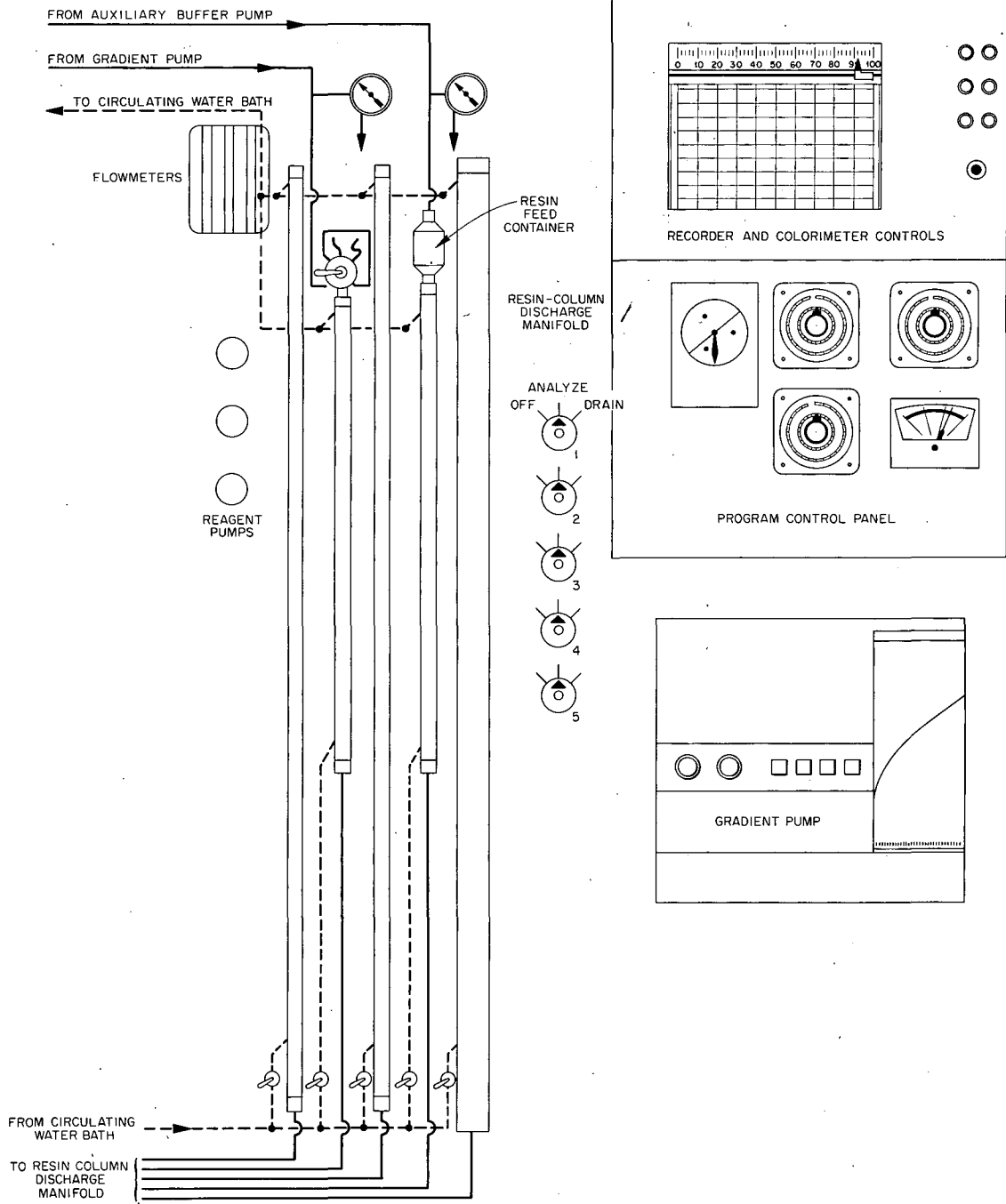


Fig. 16. Continued.

are combined, the analyzer can be operated by personnel with little training, and analyses can be performed easily.

Although basically complex, the analyzer should be trouble-free and easy to maintain. Several measures were taken to minimize potential damage from leakage. As far as possible, electrical and wet-chemical systems were compartmentalized. Electrical components in the stream-processing area were protected by shields, and all corrosive liquids were stored and dispensed within a transparent enclosure. Where electronic and liquid-flow components were in close proximity, care was taken to minimize opening one in the presence of the other during servicing. For example, in the colorimeter the flow cell can be removed from the electrical and optical unit without disengaging any fluid connectors. To further minimize the possibility of leakage of corrosive material, the stream from the diffuser column was drawn through the color development bath and the colorimeter by a pump; therefore, any leaks would allow air to enter the system rather than liquid to be forced out of it. Should the colorimeter pump fail, the stream would be diverted to waste through the diffuser overflow. This adaptation has been extensively tested on the prototype analyzer and found to be quite satisfactory.

To minimize constriction in the line from the diffuser to the colorimeter pump, only a single flow cell is used; however, the stream is monitored at 480 and 490 $m\mu$. Autoranging has been built into the recorder to permit accurate assay of absorbancy to 2.0, and scale expansion permits reading absorbancy to 0.1 full-scale deflection for high-sensitivity applications.

To ease inspection, maintenance, and repair, all fluid and electrical lines are open to view, carefully routed, and color coded.

The analyzer should be as flexible as possible. To permit elution-gradient programming, a variable

gradient pump has been adapted to the system and should offer considerably more flexibility than the two parallel cylinders used in the prototype. In addition, the system has been designed to be open ended; that is, modifications can be made easily, and additional systems for separation and monitoring of amino acids or uv-absorbing compounds can be added with minimal effort. The analyzer is movable, serviceable, modular, and fairly attractive. The monitoring-signal output has been brought to the front panel to allow easy utilization of data-processing equipment later.

Discussion

During the development of this analyzer, we have formulated certain principles that will guide additional activity in the field.

1. In nearly all cases, it is better to design a specific component for a specific system rather than to attempt to adapt existing components. Virtually all components, such as pumps, which have been ordered from external sources have required extensive reworking before they were acceptable. Admittedly, some items were experimental, but they had been openly announced as available. Components that we have designed and fabricated have proven acceptable without extensive redesign.

2. As far as possible, cooperative development should be conducted with large, well-established firms. In this program, such firms have been very useful, have demonstrated a high degree of capability, and have released products to us only after they met performance specifications. Generally, this has not been true of small suppliers.

3. In the general area of liquid proportioning and monitoring, the problem should be approached on the basis of first principles such as the fundamental properties of the fluids to be dispensed.

7. Supporting Studies

PHYSICAL PROPERTIES OF POTASSIUM CITRATE SOLUTIONS

E. J. Barber P. F. Shorten
L. L. McCauley J. F. Simmons

The use of potassium citrate as a gradient material in zonal centrifuges is advantageous in some instances where densities higher than those obtainable with sucrose are required and where cesium chloride produces deleterious effects. Potas-

sium citrate solutions are chemically more complex than sucrose solutions because potassium citrate is a uni-trivalent electrolyte of a strong base and a weak tribasic acid that has relatively small differences in the ionization constants for the three hydrogen ions. Consequently, the hydrolysis of the pure salt in water produces solutions that are too basic for virus stability, the pH approaching 9.4 at saturation as shown in Fig. 1. The addition of citric acid will lower the pH into the range considered satisfactory for virus isolations,

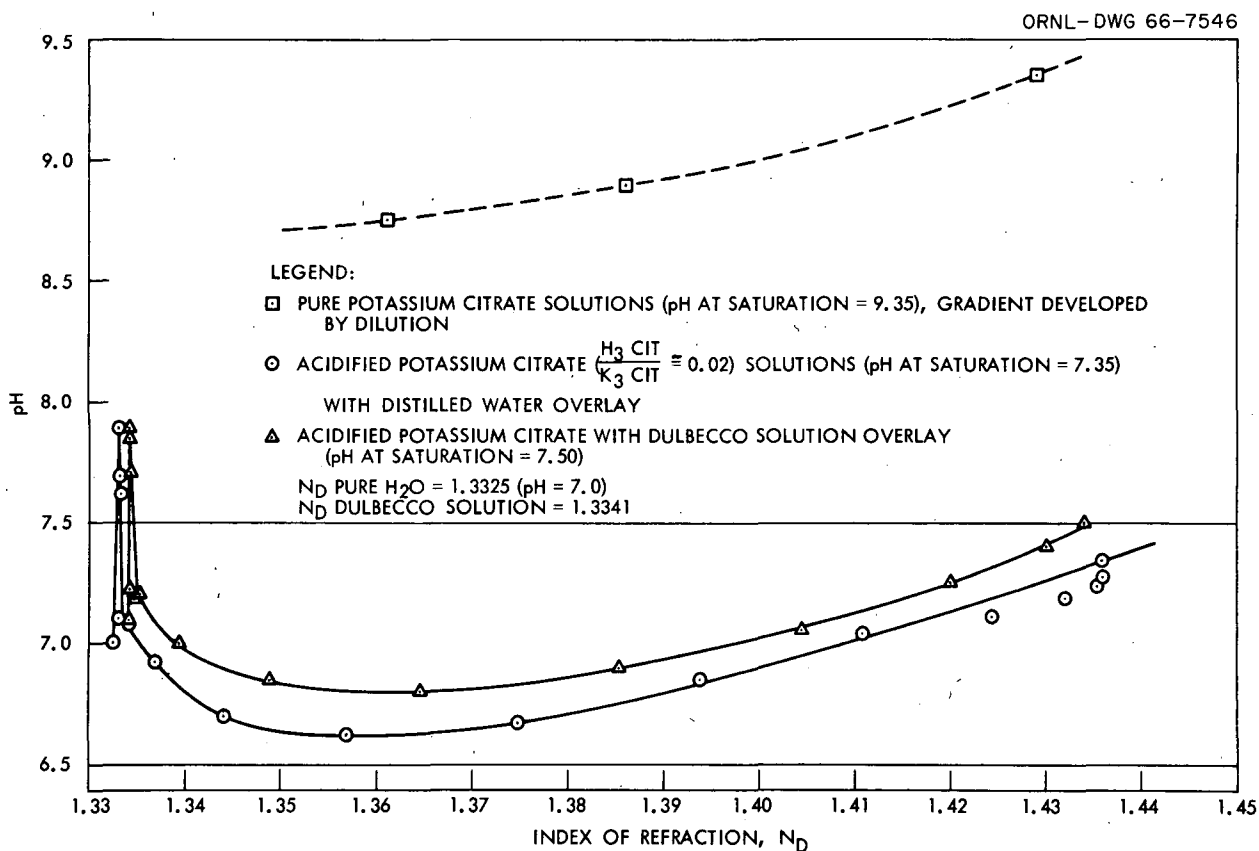


Fig. 1. Relation Between pH of Potassium Citrate Solutions and Index of Refraction (Concentration) at 25°C for Gradient Developed in the B-X Rotor.

but the amount of citric acid required to obtain a given pH changes with the potassium citrate concentration. As a result, centrifugation of a saturated potassium citrate-citric acid solution in a zonal rotor using distilled water as an overlay develops a pH gradient as well as a density gradient, as illustrated in Fig. 1. At low citrate concentrations the pH of the solutions are still excessively high. The use of Dulbecco's solution as the overlay also failed to provide effective buffering in the very dilute concentrations of gradient material.

Buffered overlay solutions can be used to help solve the pH problem when the buffer is included through the gradient, as illustrated in Fig. 2. In this case Dulbecco's solution was used instead of distilled water in the preparation of the saturated potassium citrate-citric acid solution, and Dulbecco's solution was used as the overlay in

a zonal centrifuge. The variations in pH are not eliminated, but they are reduced to an acceptable range for virus stability. A change in the temperature also produces a small change in the pH, as illustrated in Fig. 2, but when compared to the pH change produced by variation in concentration, this change in pH is unimportant. A second approach to the problem of pH control can be the use of overlay solutions containing 0.06 *m* or higher citrate concentrations in which the salt-to-acid molar ratio is about 50. Such solutions have a minimum density at 25°C of about 1.007 g/cm³.

In obtaining the two physical properties of the gradient solutions necessary for the determination of the sedimentation coefficient, namely the density and viscosity, it is customary to relate the measured parameters of temperature and index of refraction to the composition and to obtain the

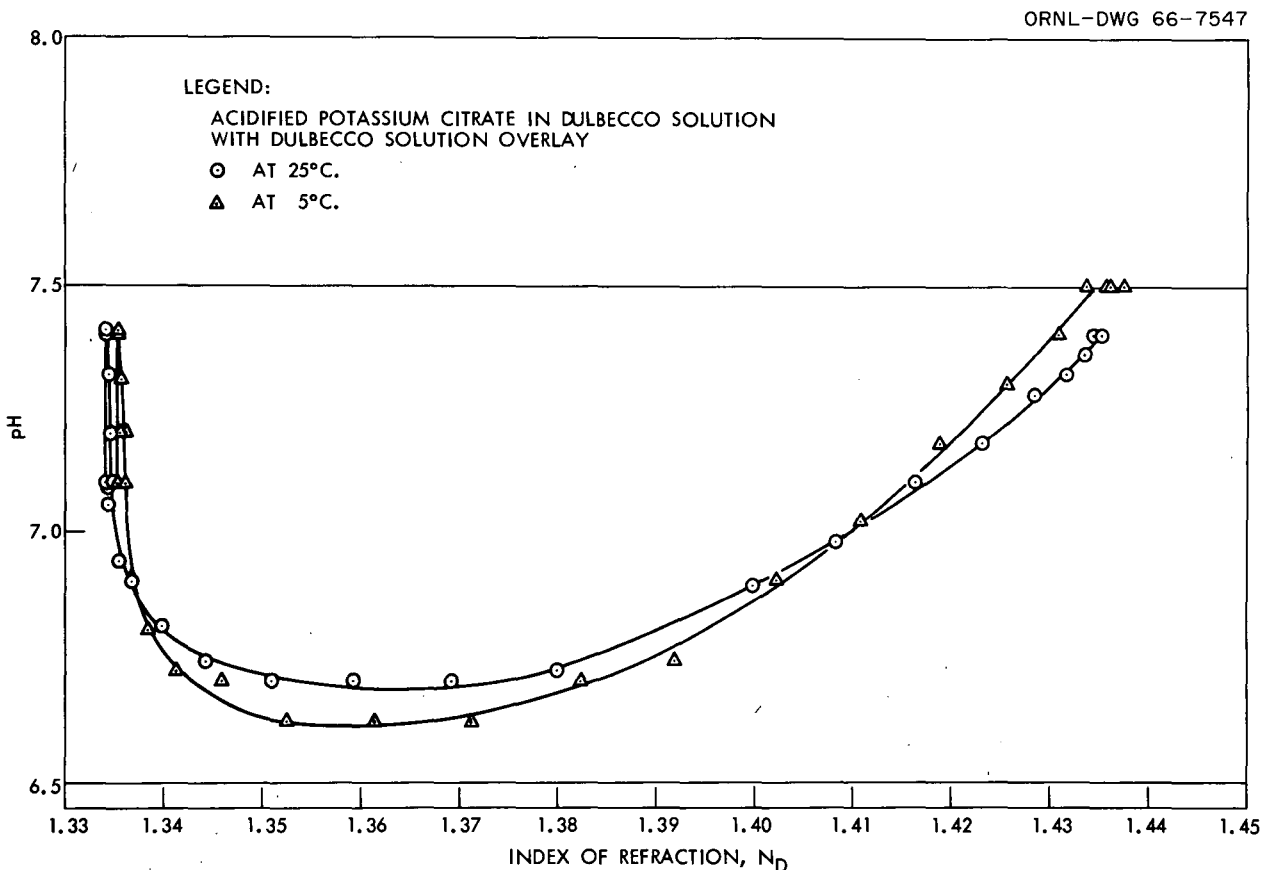


Fig. 2. Relation of pH of Modified Potassium Citrate Solutions and Index of Refraction (Concentration) for Gradient Developed in the B-X Rotor.

values of the density and viscosity from equations relating these intensive properties to the composition. However, the introduction of the citric acid and the use of the overlay solution required for pH control cause difficulties because a given index of refraction at a given temperature is no longer uniquely related to the concentration as it is with sucrose solutions. Since both index of refraction and density are properties related to the number and kinds of particles per unit volume, it is possible that the density can be related to the index of refraction directly without correction for compositional changes or temperature provided the change in either variable is small. Examination of density data on pure potassium citrate solutions and on potassium citrate solutions containing less than about 0.02 mole ratio of citric acid to potassium citrate at temperatures between 0 and 30°C indicates that the density can be calculated from the index of refraction with an average error less than 0.4%. However, with this approach, the density values for the potassium citrate-citric acid mixture made up in Dulbecco's solution are in error by about 1%, the calculated values being low. A method is being developed to account properly for the effect of both the temperature of the solution and the choice of overlay solution on the density used in the gradient preparation.

The viscosity of a solution is its intrinsic resistance to flow. The correspondence of the viscosity to the numbers and kinds of particles per unit volume, while unique at any given temperature, is not as simply related to these factors as is the density or the index of refraction. Thus, the viscosity may prove much more difficult to correlate with the measured parameters than is the density. Preliminary work indicates that a successful correlation can be developed.

DIALYSIS STUDIES

L. L. McCauley R. H. Stevens
W. M. Swartout

The purpose of this work is to provide the laboratory worker with low-cost or disposable items of equipment that will reduce the amount of handling and simplify the dialysis of the numerous small liquid fractions collected from zonal centrifuges.

Two types of equipment are presently undergoing tests, a dialyzer board containing compartments for the simultaneous dialysis of up to twelve 3-ml fractions and a plastic floater head, with serum cap and storage cover, used at one end of prepared cellulose tubing for the pressure dialysis of individual pathogenic fractions up to 5 ml in volume. The dialyzer board, Fig. 3, consists of a 12-hole plastic base into which the fractions are collected or placed prior to dialysis, a sheet of fibrous cellulose dialysis membrane, and a clamped-on cover plate to seal the membrane around the lip of each $\frac{3}{4}$ -in.-diam hole. After assembly, the board is placed in a circulating-water bath and inverted to rest on the four plastic legs. In this position, the fraction is supported by the membrane and desalting proceeds as the fresh water is circulated underneath each dialysis "window." After the dialysis is completed, the board is removed from the bath and placed in the filling position. The dialyzates can then be removed with a syringe by piercing each window with a needle. The bottoms of the holes are coned to permit removal of all material.

The membrane is cut from flattened cellulose tubing made of fibrous cellulose casing No. 2 $\frac{1}{2}$, manufactured by Food Products Division, Union Carbide Corporation, Chicago, Ill. This is similar to standard dialysis tubing, except that a fibrous cellulosic web is embedded in the tubing for strength. The web is only exposed on one side of the membrane sheet, and this "rough side" is turned away from the base containing the fractions during assembly to assure a seal to the holes. This type of membrane is used solely because of its increased tensile strength, and is necessary for safety since the osmotic pressure developed within the fraction compartments is frequently sufficient to rupture conventional membranes when dialyzing concentrated solutions (e.g., 5 M potassium citrate). The relatively small membrane area exposed to the solution in this method results in a considerably longer dialysis period than experienced with $\frac{1}{4}$ -in.-diam tubing for a given fraction volume; however, this is desirable in certain cases, such as in the dialysis of fractions containing osmotically active particles, since too-rapid changes in salt concentration may result in inactivation or damage. Figure 4 is a graph of dialysis times required for 1.5-ml volumes of 5 M potassium citrate using both $\frac{1}{4}$ -in. (No. 8 size)

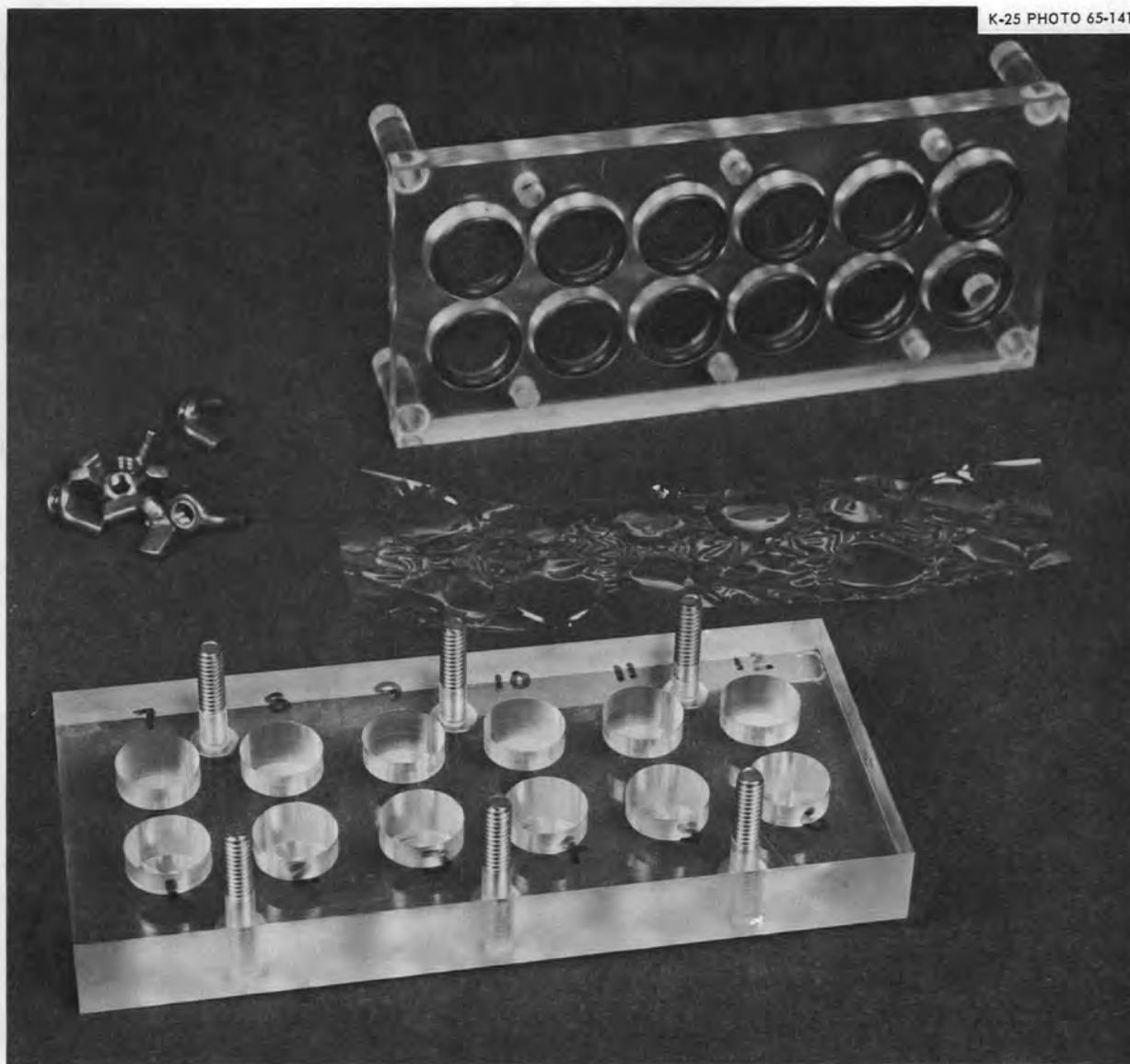


Fig. 3. Dialyzer Board for Simultaneous Dialysis of Twelve 3-ml Fractions. In the upper section O-rings seal the cellulose membrane sheet around the lip of each hole.

standard dialysis tubing in the conventional manner and the dialysis board with sheet membranes of both standard and fibrous materials. Note that the tubing contents reached a refractive index of 1.348 in 1 hr and that the board fractions reached the same point in 5.25 and 7 hr for the standard and fibrous membranes respectively. The difference in the latter two time periods is attributable to differences in initial membrane thicknesses and excessive bulging and stretching of the standard sheet, with a resultant increase in its pore size. The thickness measurement of the fibrous

membrane includes fiber mat contribution; the effective dialyzing layer thickness is therefore unknown, but is somewhat less than the total value. The three single points plotted vertically along the 5.25-hr ordinate represent the refractive indices attained by this time in the dialysis of 2-, 2.5-, and 3-ml samples with a fibrous membrane in the same board. Standard membrane can be used to reduce the dialysis time required for these larger volumes if the initial salt concentration of the fraction is considerably less than 5 M. It cannot be safely used with over 1.5 ml

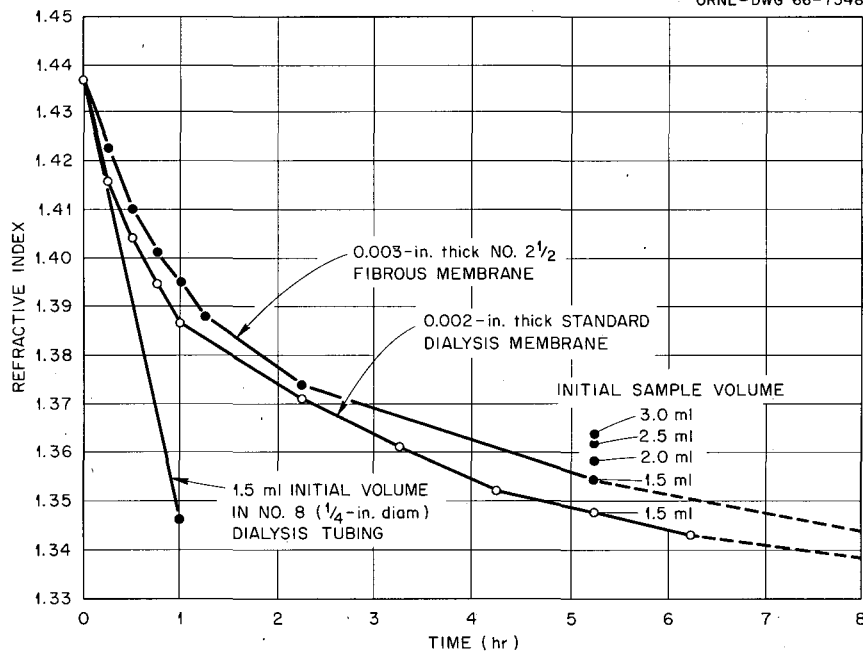


Fig. 4. Dialysis Times Required for 1.5-ml Fractions of 5 M Potassium Citrate to Reach a Refractive Index of 1.348 in $\frac{1}{4}$ -in. Tubing and with Standard and Fibrous Membranes Using the 12-fraction Dialysis Board.

of 5 M potassium citrate solutions because of the pressure developed within the fraction compartment.

The design of the dialyzing board simplifies the handling problems associated with the processing of up to 12 fractions in a glove box, since its rigid parts and the large cellulose sheet are considerably easier to handle through rubber gloves than wet dialysis tubing. If the demand for this type of board is sufficient, a separate, thin polypropylene or polycarbonate fraction-collecting tray with 12 cups could be molded as a disposable item to nest on top of the present, reusable plastic base. In this way, only the trays and dialysis sheets would require sterilization, and could be assembled in the same manner as described above.

The floating plastic head shown in Figs. 5 and 6 is used as a means to simplify handling, containment, and storage in the dialysis of individual fractions whose volumes are up to about $\frac{2}{3}$ the volume of the attached tubing. A hollow float, having a serum-cap septum access on the upper end and an O-ring to clamp the standard $\frac{1}{4}$ -in.-diam dialysis tubing on the lower end, is intended for prior assembly and gas sterilization in the dry state. When needed, the assembly can be floated in a deep container of water to remove

the glycerin from the tubing and the sample is then introduced through the septum. Additional air can also be injected into the float through the septum to prepressurize the system and reduce the sample volume after the dialysis by forcing some of the water back through the tubing membrane. The floater head had received only initial tests at the end of this report period; however, the results of the dialysis of a 3-ml fraction of 5 M potassium citrate pressurized to 10 psig is shown in Fig. 7. In this case, the air volume contained in the head and tubing was about 12 ml at the start of the run. A smaller head volume of 5 ml is planned, and this modification should reduce the postdialysis time required to reach the original volume by reducing the air cushion above the liquid and raising the air pressure during the operation.

The tubing used below the floater heads has thus far been standard $\frac{1}{4}$ -in.-diam dialysis tubing, supplied on an experimental basis by the Food Products Division, Union Carbide Corp., Chicago. This is clipped at 24-in. intervals by an aluminum wire crimp identical to that used for closing large cellulose tubing in the meat packing industry (e.g., on cylindrical sausage and bologna casings). A pair of clips placed $\frac{3}{4}$ in. apart and spaced at

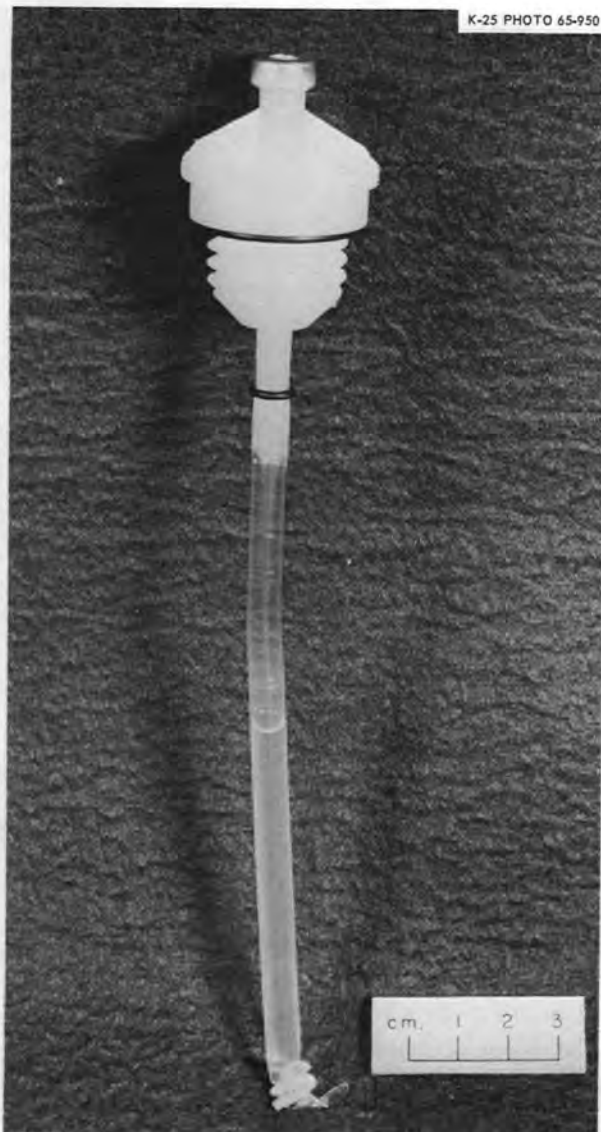


Fig. 5. Plastic Floater Head for Use with Clipped Dialysis Tubing for the Dialysis, Containment, and Storage of Pathogenic Fractions. The assembly may be assembled, gas sterilized, and stored in a dry state prior to filling through the cap septum.

using Buna-N rings. Other O-ring materials and seal designs are being evaluated to increase the holding power of the tubing seal to about 18 psig; the burst pressure of standard dialysis tubing is about 23 psig. An improved seal will allow a higher air pressure in the head and will reduce the dialysis time required to return to the original fraction volume.

The present floater heads were machined from polyethylene and heat sealed. The heads and caps also may be blow-molded of polycarbonate at low cost. Disposable assemblies would then be practical, and the chance of cross contamination in reused components eliminated.

In addition to the advantages of assembly and dry sterilization afforded by this design, the injection of liquid fractions into the tubing by a syringe provides better contamination control and allows a partial withdrawal of the dialyzate during the desalting period. Another advantage is that after the dialysis is completed, the liquid can be drained back into the floater head, the tubing rolled up, and the cap (shown in Fig. 6) screwed on for sealing and storage of the fraction in a refrigerator.

24-in. intervals provide two 12-in.-long dialysis tubes when cut midway between adjacent clips and eliminate the need for wetting and tying one end before use. No leakage past the clip has been observed. A stainless steel wire clip may be available in the future. The present O-ring seal for the tubing at the base of the float will hold without wet-tubing slippage to about 13 psig

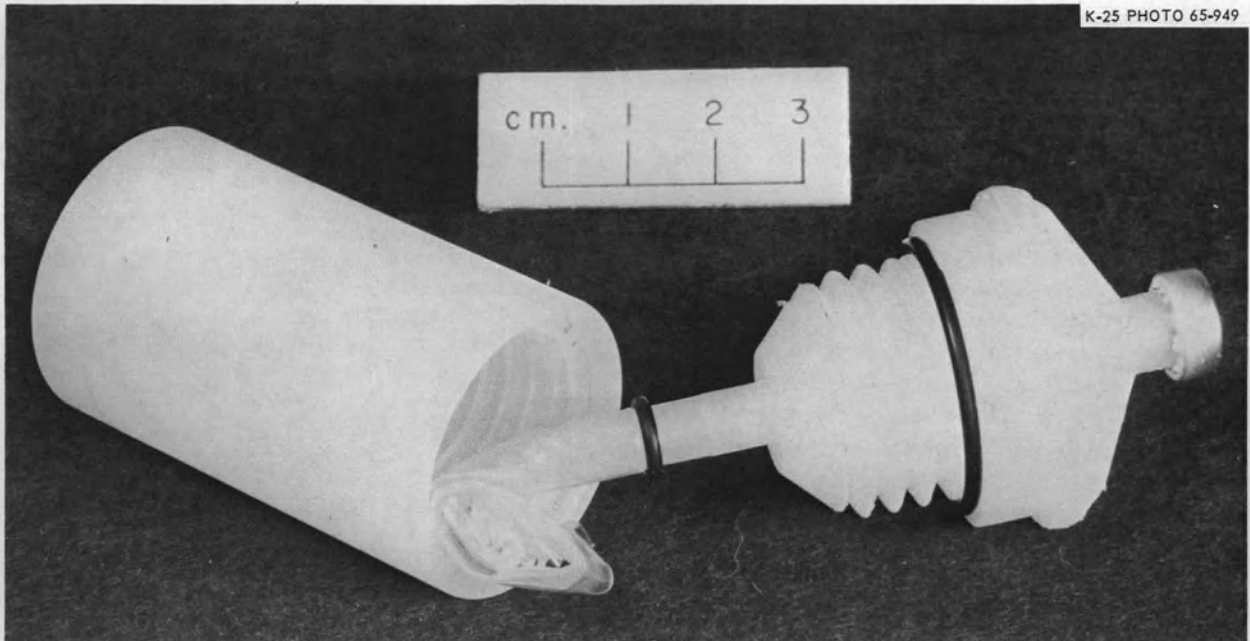


Fig. 6. Plastic Floater Head Showing the Method of Coiling the Dialysis Tubing and Use of the Self-Sealing Cover for Storing Fractions That Have Been Drained from the Tubing into the Hollow Head Section.

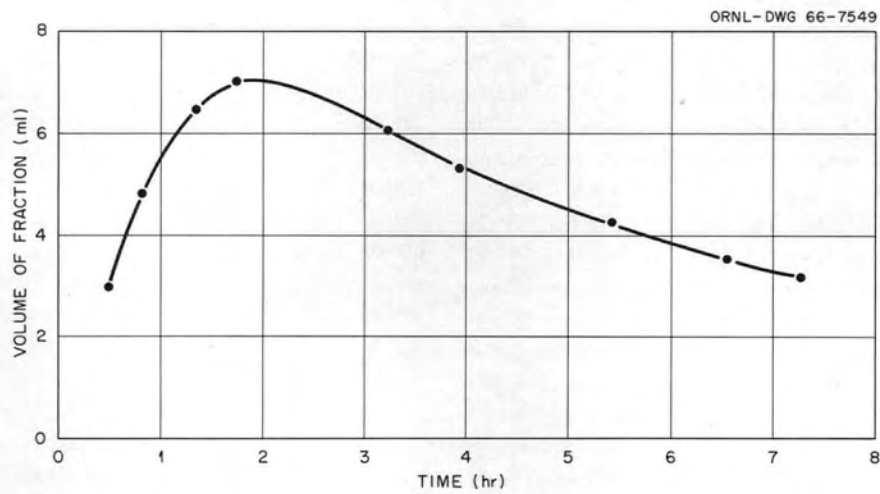


Fig. 7. Volume of Dialyzate with Time During the Dialysis of a 3-ml Sample of 5 M Potassium Citrate at 10 psig Initial Pressure in the Floating Plastic Head.

DENSITY-INDICATING BEADS

N. G. Anderson

N. Cho

The development of plastic beads as density indicators is one phase of this laboratory's effort to develop simplified virus-isolation systems. As mentioned in a previous report,¹ one feature of this simplified system was the fabrication of a series of color-coded density-indicating beads. During centrifugation, these density-indicating beads are suspended in the gradient at their isopycnic positions, just as are viruses or any other particles present in the sample. The beads indicate the buoyant density of the virus at its isopycnic position with minimum chance for contamination of the observer or his surroundings.

The basic requirements were low cost and homogeneity. Attempts to vary the density of a polymer, such as polystyrene, by blending with a filler met with limited success due to nonhomogeneities caused by incomplete mixing and/or entrapped air. The percent of water uptake and surface condition also presented problems.

Development of new techniques of compounding and molding or extruding plastics having selected and unique properties was too costly.

By use of resins already commercially available from Eastman Kodak Co., plastic beads of four different densities were processed at a cost of slightly less than 3¢ each. A controlled process yielded a nonporous mix, the plastic was extruded in continuous strands, and these strands after being cooled were chopped into short rods. These were reduced to $\frac{1}{16}$ -in.-diam beads in a ball mill.

Determination of the homogeneity of the beads was performed at the Biophysical Separations Laboratory. Density variations in each of four batches of beads were established by banding samples isopycnicly in both shallow and steep density gradients. Sample populations ranging from 24 to 60 beads were used for each determination.

Sixty beads from each of the four batches were isopycnicly banded in a very shallow density gradient. Density distributions to within ± 0.005 g/cm³ were established from these data. The results are shown in Table 1.

¹N. Cho *et al.*, "Problems in Biocontainment," in *The Development of Zonal Centrifuges and Ancillary Systems for Tissue Fractionation and Analysis*, ed. by N. G. Anderson, Mono. 21, J. Natl. Cancer Inst. Mono. Ser., 1966.

Table 1. Classification of Density-Indicating Plastic Beads

Batch Color and Range of Densities (g/cm ³)	Density Distribution	
	Density (± 0.005 g/cm ³)	% of Total Sample
Yellow, 1.065 to 1.105	1.070	3.4
	1.080	43.3
	1.090	43.3
	1.100	10.0
Green, 1.272 to 1.278	1.275	100
Tan, 1.361 to 1.369	1.365	100
Gray, 1.518 to 1.534	1.520	10
	1.530	90

Large-scale separation of tan and gray beads was done on subcontract by Udy Analyzer Company, Boulder, Colo. The beads were annealed at 120°C for 40 hr. The densities of the main fractions separated were 1.366 ± 0.001 g/cm³ and 1.528 ± 0.001 g/cm³ at 20°C. Both sets of beads gained 0.003 g/cm³ in density when the temperature was lowered to 5°C. Also, there was a gain of 0.001 to 0.002 g/cm³ in density when the particles were submersed in ZnCl₂ for a day. No further increase in density occurred after five days.

Other beads were studied: metal-coated plastic beads and plastic beads overcoated first with metal and then with a plastic layer. Addition of metal and other materials may allow beads with a wide variety of densities to be prepared.

STRESS-CORROSION TESTS IN SODIUM PERCHLORATE

W. S. Dritt

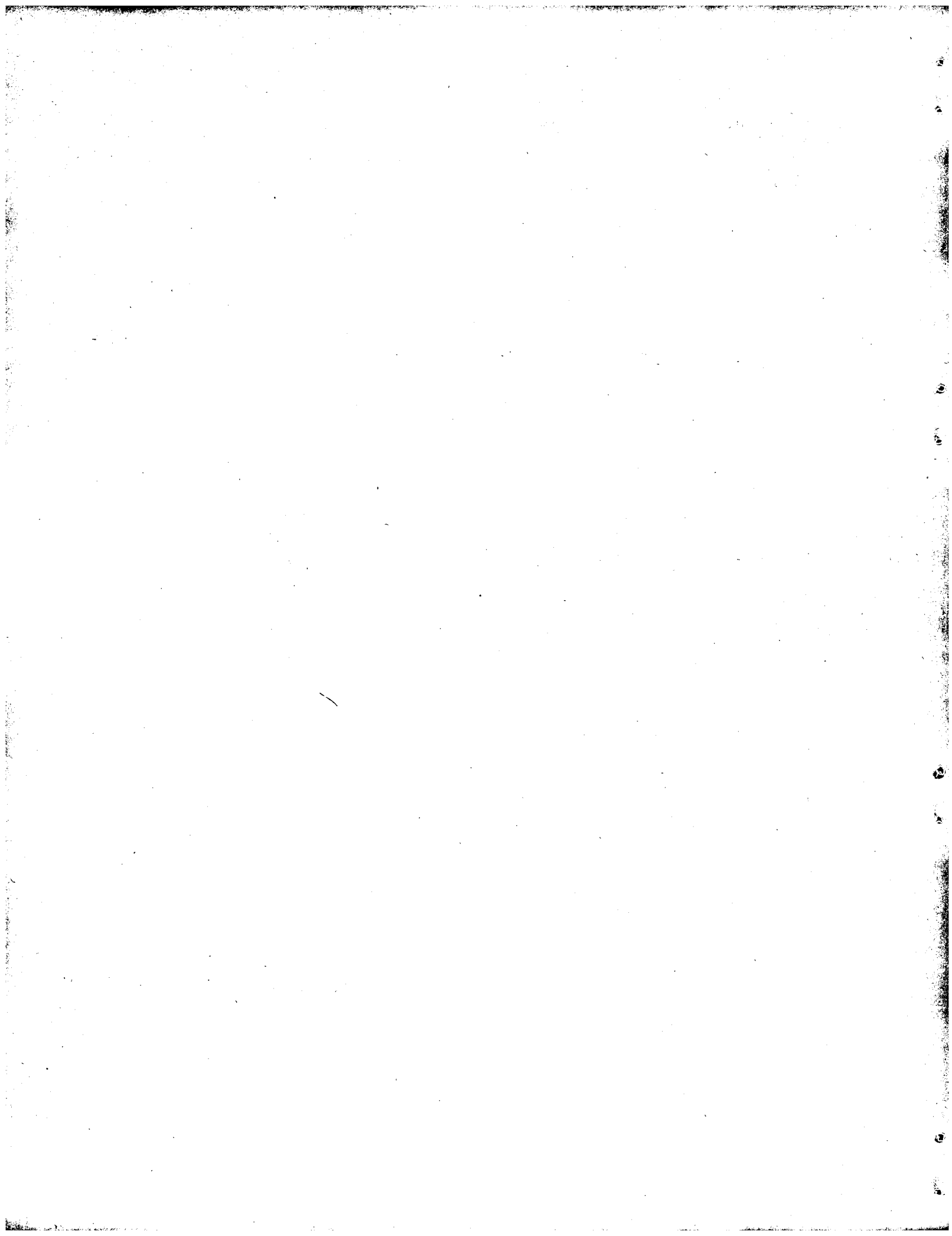
Sodium perchlorate has been proposed for use as a biological centrifuge fluid. Stress-corrosion failures have been identified in operation of biological centrifuge units with water (Maraging steel) and with cesium chloride (7075 aluminum). A group of materials has therefore been tested for

susceptibility to stress-corrosion cracking in a saturated solution of sodium perchlorate in water.

Materials tested included Kanigen-plated Maraging steel, anodized 7075 aluminum, and the β -titanium alloy B120VCA. Coupons were stressed in four-

point loading fixtures to 90% of their yield strength and submerged in the sodium perchlorate solution.

No susceptibility to cracking was observed in any of the materials tested for exposure times up to 2000 hr.



INTERNAL DISTRIBUTION

1. S. I. Auerbach
2. R. Baldock
3. R. E. Biggers
4. A. L. Boch
5. D. S. Billington
6. C. J. Borkowski
7. G. E. Boyd
- 8-9. Clark E. Center (ORGDP)
- 10-11. D. D. Cowen
12. C. J. Collins
13. F. L. Culler
14. P. B. Dunaway
15. J. L. Fowler
16. J. H. Frye, Jr.
17. R. F. Hibbs (Y-12)
18. A. S. Householder
19. J. S. Johnson
20. W. H. Jordan
21. K. A. Kraus
22. M. T. Kelley
23. J. A. Lane
- 24-25. C. E. Larson
26. T. A. Lincoln
27. R. S. Livingston
28. K. Z. Morgan
29. D. J. Nelson
30. M. L. Nelson
31. J. S. Olson
- 32-33. R. B. Parker
34. M. E. Ramsey
35. R. M. Rush
36. M. J. Skinner
37. E. H. Taylor
38. A. M. Weinberg
39. G. C. Williams
40. H. I. Adler
- 41-60. N. G. Anderson
61. W. A. Arnold
62. M. A. Bender
63. S. F. Carson
64. E. H. Y. Chu
65. G. B. Cline
66. W. E. Cohn
67. C. C. Congdon
68. F. J. de Serres
69. D. G. Doherty
70. W. D. Fisher
- 71-73. C. J. Whitmire, Jr.
74. A. H. Haber
75. A. Hollaender
76. M. A. Kastenbaum
77. R. F. Kimball
78. S. P. Leibo
79. D. L. Lindsley, Jr.
80. T. Makinodan
81. P. Mazur
82. G. D. Novelli
83. T. T. Odell, Jr.
84. A. P. Pfuderer
85. M. L. Randolph
86. W. L. Russell
87. R. B. Setlow
88. G. E. Stapleton
89. A. C. Upton
90. E. Volkin
91. R. C. von Borstel
92. T. Yamada
93. E. F. Babelay
94. E. J. Barber
95. J. C. Barton
96. A. S. Berman
97. H. A. Bernhardt
98. Barbara S. Bishop
99. H. D. Culpepper
100. J. T. Dalton
- 101-115. E. C. Evans
116. J. Farquharson
117. R. L. Farrar, Jr.
118. W. W. Harris
- 119-121. W. L. Harwell
122. E. T. Henson
123. A. P. Huber
124. J. L. Liverman
125. J. G. Green
126. H. G. MacPherson
127. G. R. Jamieson
128. E. C. Johnson
129. T. J. Lewis
130. C. E. Nunley
131. P. R. Vanstrum
132. D. A. Waters
133. C. W. Weber
134. S. J. Wheatley
135. R. H. Stevens

- | | |
|-----------------------------------|--|
| 136. W. J. Wilcox, Jr. | 148. Curt Stern (consultant) |
| 137. A. A. Barber | 149. C. E. Carter (consultant) |
| 138. R. E. Canning | 150. Henry S. Kaplan (consultant) |
| 139. E. L. Candler | 151-152. Biology Library |
| 140. L. H. Elrod, Jr. | 153. Reactor Division Library |
| 141. R. M. Jamison | 154-156. Central Research Library |
| 142. C. T. Rankin, Jr. | 157-158. ORNL - Y-12 Technical Library |
| 143. Elizabeth L. Rutenberg | Document Reference Section |
| 144. W. T. Lammers | 159-202. Laboratory Records Department |
| 145. R. D. Hotchkiss (consultant) | 203. Laboratory Records, ORNL R.C. |
| 146. E. R. Stadtman (consultant) | 204. Laboratory Shift Supervisor |
| 147. Herschel Roman (consultant) | |

EXTERNAL DISTRIBUTION

205. D. J. Davis, NIAID (Director), Bethesda, Maryland
206. G. A. Andrews, ORINS, ORAU
207. C. Baker, National Cancer Institute, Bethesda, Maryland
208. F. Baronowski, AEC Production Division, Washington, D.C.
209. N. F. Barr, Atomic Energy Commission, Washington, D.C.
210. N. Berlin, National Cancer Institute, Bethesda, Maryland
211. H. E. Bond, National Cancer Institute, Bethesda, Maryland
212. Myron Drakke, U.S. Department of Agriculture, Agriculture Research Service, Plant Physiol. Department, University of Nebraska, Lincoln 3, Nebraska
213. H. D. Bruner, Atomic Energy Commission, Washington, D.C.
214. W. R. Bryan, National Cancer Institute, Bethesda, Maryland
215. J. C. Bugher, Puerto Rico Nuclear Center, Rio Piedras, P.R.
216. W. W. Burr, Jr., Atomic Energy Commission, Washington, D.C.
217. R. M. Chanock, National Institute of Allergy and Infectious Diseases, Bethesda, Maryland
218. R. A. Charpie, Union Carbide Corporation, New York
219. M. A. Churchill, Chief, Stream Sanitation Staff, Edney Bldg., TVA, Chattanooga, Tennessee
220. W. D. Claus, Atomic Energy Commission, Washington, D.C.
221. Peter Dans, National Institute of Allergy and Infectious Diseases, Bethesda, Maryland
222. B. T. Cole, Department of Zoology, University of South Carolina, Columbia, S.C.
223. E. Dapper, U.S. Army Chemical Corps, Fort Detrick, Maryland
224. C. M. Davidson, Environmental Hygiene Branch, Edney Bldg., TVA, Chattanooga, Tennessee
225. Irving S. Johnson, Eli Lilly Co., Indianapolis, Indiana
226. O. M. Derryberry, Director of Health and Safety, Edney Bldg., TVA, Chattanooga, Tennessee
227. Harold S. Diehl, Sr., Vice President for Research in Medical Affairs, American Cancer Society, 521 W. 57th St., New York 19, New York
228. C. L. Dunham, Atomic Energy Commission, Washington, D.C.
229. K. M. Endicott, National Cancer Institute, Washington, D.C.
230. S. G. English, Assistant General Manager for Research and Development, AEC, Washington, D.C.
231. J. L. Fahey, National Cancer Institute, Bethesda, Maryland
232. E. Frei, National Cancer Institute, Bethesda, Maryland
233. F. E. Gartrell, Assistant Director of Health and Safety, Edney Bldg., TVA, Chattanooga, Tennessee
234. H. Bentley Glass, State University of New York, Stony Brook, L.I., N.Y.
235. Donald A. Glaser, Virus Lab., U. of Calif., Berkeley 4, Calif.
236. H. N. Glassman, U.S. Army Chemical Corps, Fort Detrick, Maryland
237. E. Grabowski, AEC Production Division, Washington, D.C.

238. S. T. Grey, Food and Drug Administration, Washington, D.C.
239. N. S. Hall, University of Tennessee, Knoxville
240. John Harris, AEC Public Relations Division, ORO
241. Fred J. Hodges, University of Michigan, Medical Center, Ann Arbor
242. E. C. Horn, Department of Zoology, Duke University, Durham, N.C.
243. J. G. Horsfall, Connecticut Agricultural Experimental Station, New Haven
244. R. D. Housewright, U.S. Army Chemical Corps, Fort Detrick, Maryland
245. R. J. Huebner, National Cancer Institute, Bethesda, Maryland
246. J. S. Kirby-Smith, Atomic Energy Commission, Washington, D.C.
247. R. M. Kniseley, ORINS Medical Division, ORAU
248. K. W. Kohn, National Cancer Institute, Bethesda, Maryland
249. P. Kotin, National Cancer Institute, Bethesda, Maryland
250. E. L. Kuff, National Cancer Institute, Bethesda, Maryland
251. A. D. Langmuir, Chief, Epidemiology Branch, Communicable Disease Center, Atlanta, Georgia
252. R. E. Learmouth, National Cancer Institute, Bethesda, Maryland
253. R. F. Loeb, College of Physicians and Surgeons, Columbia University, New York
254. W. H. Magruder, National Cancer Institute, Bethesda, Maryland
255. W. E. McMahon, Atomic Energy Commission, ORO
256. R. G. Meader, National Cancer Institute, Bethesda, Maryland
257. J. L. Melnick, Department of Virology and Epidemiology, Baylor University, College of Medicine, Houston, Texas
258. G. R. Mider, National Cancer Institute, Bethesda, Maryland
259. Carl V. Moore, Washington University, St. Louis, Missouri
260. P. T. Mora, National Cancer Institute, Bethesda, Maryland
261. J. E. Moynahan, National Institutes of Health, Bethesda, Maryland
262. W. G. Pollard, ORINS, ORAU
263. C. A. Price, Department of Plant Physiol., Rutgers - The State University, New Brunswick, N.J.
264. H. M. Roth, Research and Development Division, AEC, ORO
265. W. P. Rowe, National Institute of Allergy and Infectious Diseases, Bethesda, Maryland
266. D. G. Sharp, University of North Carolina, Department of Biophysics, Chapel Hill
267. Byron T. Shaw, Administrator, Agricultural Research Service, U.S. Department of Agriculture, Washington, D.C.
268. C. S. Shoup, Atomic Energy Commission, Oak Ridge
269. R. G. Smith, Food and Drug Administration, Washington, D.C.
270. H. A. Sober, National Cancer Institute, Bethesda, Maryland
271. W. M. Stanley, Virus Laboratory, University of California, Berkeley
272. S. R. Tipton, Department of Zoology, University of Tennessee, Knoxville
273. John Totter, Atomic Energy Commission, Washington, D.C.
274. Rodes Trautman, Plum Island Lab., USDA, Greenport, L.I., New York
275. Shields Warren, New England Deaconess Hospital, Boston, Massachusetts
276. A. G. Wedum, U.S. Army Chemical Corps, Fort Detrick, Maryland
277. J. White, National Cancer Institute, Bethesda, Maryland
278. H. G. Wood, Western Reserve University, Cleveland, Ohio
279. M. Zelle, Argonne National Laboratory, Argonne, Illinois
- 280-290. R. E. Stevenson, National Cancer Institute, Bethesda, Maryland
291. A. B. Sabin, Children's Hospital Research Foundation, Cincinnati, Ohio
292. C. G. Zubrod, National Cancer Institute, Bethesda, Maryland
293. Atomic Energy Commission, Washington, D.C.
294. General Electric Company, Richland, Washington
295. New York Operations Office
296. AEC Patent Branch, Washington, D.C.
- 297-301. Division of Technical Information Extension, Oak Ridge

302. UCLA Medical Research Laboratory
303. Arne Tiselius, University of Uppsala, Uppsala, Sweden
304. Peter Alexander, Chester Beatty Cancer Institute, London, England
305. Wayne Rundles, Medical School, Duke University
306. J. A. Swartout, Union Carbide Corporation, New York, N.Y.
307. Biomedical Library, University of California, Center for the Health Sciences, Los Angeles, California
- 308-382. Daniel I. Mullally, Chief, Vaccine Development Branch, National Institute of Allergy and Infectious Diseases, Bethesda, Maryland
383. James A. Shannon, Director, National Institutes of Health, Bethesda, Maryland
384. F. L. Stone, Director, National Institutes of General Medical Sciences, National Institutes of Health, Bethesda, Maryland
385. H. P. Jenerick, National Institute of General Medical Sciences, Bethesda, Maryland
386. Robert Melville, National Institute of General Medical Sciences, Bethesda, Maryland
387. L. E. Slater, BAC, American Institute of Biological Sciences, Washington, D.C.
388. H. P. Barringer, Stellite Division, Union Carbide Corporation, Kokoma, Indiana
389. S. P. Spragg, Department of Chemistry, The University, Birmingham 15, England
390. W. G. Marley, UKAEA, Health and Safety Branch, Radiology Protection Division, Harwell, Didcott, Berks., England